Curriculum Vitae

Heather VerValin Buck
University of Maryland Baltimore

Date: April 15, 2025

Contact Information:

Business Address: 660 W Redwood St
Howard Hall, Room HH560
Baltimore, MD 21201
Email Address: hbuck@som.umaryland.edu
vervalin@gmail.com

Education:

2001-2005	B.A., Religious Studies, The University of South Florida, Tampa, FL
2017-2020	B.S., Molecular Biology, Biochemistry and Bioinformatics, Towson University, Townson, MD
2020-2025	Ph.D. Candidate, Graduate Program in Life Sciences, Molecular Medicine, University of Maryland Baltimore, Baltimore, MD Advisor: Joseph Stains, Ph.D. Degree Conferral: May 2025

Training:

2018-2018	Research Volunteer, Molecular Ecology Laboratory, Towson University, Towson, MD Advisor: Brian Masters, Ph.D.
2018-2020	Research Assistant, Diet and Cancer Laboratory, Towson University, Towson, MD Advisor: Petra Tsuji, Ph.D.
2019-2019	Summer Intern, Nathan Schnaper Intern Program in Translational Cancer Research, University of Maryland Baltimore, Baltimore, MD Advisor: Paul Shapiro, Ph.D.
2020-2020	Teaching Assistant, Molecular Biology Lab, Towson University, Towson, MD. Assisting: Cheryl Warren, Ph.D.
2020-2025	Graduate Research Assistant, Graduate Program in Life Sciences, Molecular Medicine, University of Maryland Baltimore, Baltimore, MD Advisor: Joseph Stains, Ph.D.

Publications:

Original Research:

Martinez R III, Huang W, **Buck H**, Rea S, Defnet AE, Kane MA, Shapiro P. *Proteomic Changes in the Monolayer and Spheroid Melanoma Cell Models of Acquired Resistance to BRAF and MEK1/2 Inhibitors.* ACS Omega. 2022;7(4):3293-3311. Published 2022 Jan 18. doi:10.1021/acsomega.1c05361

Leser JM, Torre OM, Gould NR, Guo Q, **Buck HV**, Kodama J, Otsuru S, Stains JP. *Osteoblast-lineage calcium/calmodulin-dependent kinase 2 delta and gamma regulates bone mass and quality*. Proc Natl Acad Sci U S A. 2023;120(47):e2304492120. doi:10.1073/pnas.2304492120

Buck HV, Torre OM, Leser JM, Gould NR, Ward CW, Stains JP. *Nitric oxide contributes to rapid sclerostin protein loss following mechanical load*. Biochem Biophys Res Commun. 2024;727:150315. doi:10.1016/j.bbrc.2024.150315

(In preparation) **Buck HV**, Leser JM, Murray PJ, Chatree S, Stains JP. *Single-Gene CaMKIIγ or CaMKIIδ Conditional Deletion in Osteoblast-Lineage Cells Does Not Recapitulate Severe Skeletal Phenotype of CaMKIIγ/δ Double Conditional Deletion*.

Review Articles:

Leser JM, Harriot A, **Buck HV**, Ward CW, Stains JP. *Aging, Osteo-Sarcopenia, and Musculoskeletal Mechano-Transduction*. Front Rehabil Sci. 2021;2:782848. doi:10.3389/fresc.2021.782848

Buck HV, Stains, JP. *Osteocyte-Mediated Mechanical Response Controls Osteoblast Differentiation and Function*. Front Physiol. 2024:15. https://doi.org/10.3389/fphys.2024.1364694

Funding:

2021-2022 T32 Training Program in Membrane Biology "Osteocytic Osteolysis and Perilacunar Remodeling in Bone."

Seminar Presentations:

February 2020. Towson University Chapter, American Society for Biochemistry and Molecular Biology Student Seminar. "Impact of Sorghum Polyphenols on Expression of Carcinogen Metabolizing Enzymes in Human Colon Cancer Cells."

December 2022. University of Maryland Baltimore Student Seminar Series. "Nitric Oxide's Role in Mechanically-Stimulated Sclerostin Degradation."

April 2024. University of Maryland Baltimore Graduate Research Conference. "CaMKIIδ and CaMKIIγ May Regulate Bone Mass and Quality Through Differing Mechanisms."

October 2024. University of Maryland Baltimore Molecular Medicine Program Student Seminar. "CaMKIIδ and CaMKIIγ Compensate to Prevent Severe Bone Loss and Skeletal Fragility Caused by Dual Conditional Deletion of Both Isoforms."

Poster Presentations:

1. **Buck HV**, Singh A, Reynolds K, Smolensky D, Tsuji P. (2019) Impact of Sorghum Polyphenols on Expression of Carcinogen-Metabolizing Enzymes in Human Colon Cancer Cells. American Society for Nutrition, Baltimore, MD.
2. **Buck HV**, Martinez R, Shapiro P. (2019) Restoring Sensitivity of Resistant Melanoma Cells to Kinase Inhibitors. UMBC Undergraduate Research Symposium in the Chemical and Biological Sciences, Baltimore, MD
3. **Buck HV,** Torre O, Gould N, Ward C, Stains JP. (2022) Nitric Oxide's Role in Mechanically-Stimulated Sclerostin Degradation. ASBMR Annual Meeting, Austin, TX, USA.

4. **Buck HV,** Torre O, Leser J, Gould N, Ward C, Stains JP. (2023) Nitric Oxide's Role in Mechanically-Stimulated Sclerostin Degradation. University of Maryland Baltimore Graduate Research Conference. Baltimore, MD, USA.
5. **Buck HV,** Torre O, Leser J, Gould N, Ward C, Stains JP. (2023) Nitric Oxide's Role in Mechanically-Stimulated Sclerostin Degradation. ASBMR Annual Meeting, Vancouver, Canada.
6. **Buck HV,** Torre O, Leser J, Gould N, Ward C, Stains JP. (2024) eNOS-Derived Nitric Oxide Directly Participates in Sclerostin Expression Control After Mechanical Stimulation. Symposium on Metabolic Bone Disease, Odense, Denmark.
7. **Buck HV,** Leser J, Chatree S, Murray PJ, Stains JP. (2024) Osteocytic CaMKIIδ and CaMKIIγ May Regulate Bone Mass and Quality Through Similar Mechanisms. ASBMR Annual Meeting, Toronto, Canada.

Service and Teaching:

Summer 2022: Basic skills training and supervision of high school student Lily Baharlou
Summer 2022: Training of rotating graduate student Shanaliz Natta, Molecular Medicine Program
Fall 2022: Training of rotating graduate student Philippa Rogers, Molecular Medicine Program
Fall 2022: Training of rotating graduate student Sushrut Pathy, Molecular Medicine Program
Oct 2022: Served as peer reviewer for the Molecular Medicine Student Seminar Series
Summer 2023: Basic skills training and supervision of high school student Luke Caldwell
Oct 2023: Served as the student representative on the committee for the selection of the new Molecular Medicine Program Director
Feb 2024: Served as peer reviewer for the Molecular Medicine Program Student Seminar Series
Mar 2024: Presented poster at recruitment research event and acted as new student host
June 2024 – Present: Training of Postdoctoral Fellow Saimai Chatree
Sep 2024: Scored GPILS/OPS award packets and reviewed with committee for student and mentorship award consideration
Jan 2025 – Present: Training of Laboratory Technician Maddy Arena
Feb 2025 – Present: Training of rotating graduate student Jessica Oswald, Molecular Medicine Program

Professional Society Memberships:

2019-present	American Society for Biochemistry and Molecular Biology
2021-present	American Society for Bone and Mineral Research
2024	American Society for Bone and Mineral Research Student Cohort Training Program

Abstract

Title: Osteocytic Nitric Oxide and CaMKII Mediate Bone Mass and Quality

Heather VerValin Buck, Doctor of Philosophy, 2025

Dissertation Directed by: Joseph Stains, Ph.D., Professor, Orthopaedics

Bone mass peaks in early adulthood before declining with age and is influenced by many factors, such as activity, reproduction, nutrition, and disease. In the post-developmental skeleton, changes in bone mass are due to the activity of osteoclasts, which secrete proteases and hydrogen protons to demineralize and remove existing bone, and osteoblasts, which deposit organic matrix and facilitate its mineralization in order to produce new bone. In the healthy adult, these two processes, resorption and deposition, continually occur to maintain the skeleton and adapt it to changing needs. The cycle of removal and replacement of bone by osteoclasts and osteoblasts is coordinated by osteocytes, which form a tightly-interconnected system of local and systemic signaling. Osteocytes act to receive, incorporate, and transmit anabolic and catabolic signals down to bone-resident cells and their progenitors to tune the balance of bone removal and replacement.

When osteocytes are mechanically stimulated, as by fluid shear stress, several anabolic pathways are activated. We have recently defined one such pathway in which mechanical strain deforms the microtubule network, leading to the production of reactive oxygen species (ROS) by NOX2. ROS induces TRPV4 calcium channels to open, leading to calcium influx and an elevation in intercellular calcium. This causes activation of calcium/calmodulin-dependent protein kinase II (CaMKII), which leads to lysosomal

degradation of sclerostin protein, a powerful catabolic signal. As a consequence of this mechanically-sensitive pathway activation, reduced sclerostin abundance unleashes osteoblast differentiation and new bone deposition.

Osteocytes have long been known to produce nitric oxide during mechanical stimulation, however the biological effect of this elevation has been uncertain. Our recent work demonstrated that exogenous nitric oxide is sufficient to suppress sclerostin abundance. Here, we demonstrate that nitric oxide production participates directly in the above-mentioned pathway to suppress sclerostin expression and that nitric oxide production is necessary for the loss of sclerostin abundance. We will also show that the endothelial (eNOS, *NOS1*) and inducible (iNOS, *NOS2*) isoforms of nitric oxide synthase are most relevant to this process.

We will also discuss CaMKII, another osteocytic mediator of anabolic signaling. We have previously demonstrated that two isoforms of CaMKII, *CaMKIIδ* and *CaMKIIγ,* are expressed in primary osteocytes. We conditionally deleted both isoforms from osteoblast-lineage cells using the Osteocalcin Cre driver. Camk2delta/gamma double cKO mice express a profound reduction in bone mass and quality, which appears to be mediated through FGF23 overexpression and hypophosphatemia. Here, we will characterize independent models of *CaMKIIδ* or *CaMKIIγ* conditional deletion to determine whether these isoforms may fulfil redundant or separate roles and to better understand CaMK2's function in post-developmental bone maintenance.

Osteocytic Expression of Nitric Oxide and CaMKII Mediate Bone Mass and Quality

by
Heather VerValin Buck

Dissertation submitted to the faculty of the Graduate School of the
University of Maryland, Baltimore in partial fulfillment
of the requirements for the degree of
Doctor of Philosophy
2025

Acknowledgements

I would first and foremost like to thank my husband, Arthur, for his unwavering support of my return to school. We've had lots of late dinners and working weekends and I can't express to you how impossible this would have all been without you beside me. Growing up together and sharing my life with you is an unmitigated privilege. You are the best person I know and I try very hard to be the person you see in me.

To my son, Demetri, I find so much joy in your silliness and humor. Thank you for being exactly who you are. Thank you for your hugs when I have a hard day. Thank you for making stupid jokes with me. Thank you for being a funny, old soul. I hope that I set a good example for you, and that you see that you can do anything if you're stubborn enough.

To my mentor, Joe, thank you for always expecting me to do better and to know more. You've given me the room to grow at my own pace and I've felt supported and challenged but not rushed. Thank you for always having an open door and for making the time to talk both about science and nonsense. When I've had major life events you've shown me a level of kindness and consideration that has made the big problems easier. Earning my PhD has been in turns both joyful and soul-crushing and it would have been so much harder without your guidance and comradery.

To Chris Ward and Ramzi Khairallah, thank you for always meeting my stupid questions with practical answers. Chris, your untethered enthusiasm for science is contagious, and you seem to have an insight into any random thing I bring up. Ramzi, thank you for asking pointed questions, for being a patient teacher, and for being unflappable. Thank you for making me a better researcher. I would be a worse off person without your and Joe's triune guidance.

To my current and former lab mates Olivia, Nicole, Jenna, Qiaoyue, Pippa, Sush, and Saimai, thank you eternally for troubleshooting with me, for providing feedback and ideas, and most of all, for knowing what it's like. Thank you for talking me down when I was sure that everything was terrible and thank you for being there to chat and goof off when I needed a friend. To Jenna especially, thank you for being such a practical and patient teacher when I was so afraid, and most of all, thank you for being my partner in crime.

To my thesis committee, thank you for your valuable help and direction. Thank you for asking hard and pragmatic questions about the work, timelines, practicality, and my career.

Table of Contents

List of Tables

List of Figures

List of Abbreviations

ROS	Reactive oxygen species
TRPV4	Transient receptor potential vanilloid 4
CaMKII	Calcium/calmodulin-dependent protein kinase II
eNOS	Endothelial nitric oxide synthase
iNOS	Inducible nitric oxide synthase
nNOD	Neuronal nitric oxide synthase
FGF23	Fibroblast growth factor 23
BMP	Bone morphogenetic protein
RANKL	Receptor activator of nuclear factor- κB
RGD	Arginine-glycine-aspartic acid
TRAP	Tartrate-resistant acid phosphatase
CTX	Cleaved cross-linked C-telopeptide of type I collagen
ALP/ALPL	Alkaline phosphatase
PTH	Parathyroid hormone
PTHrP	Parathyroid hormone-related protein
LCS	Lacunar canalicular system
PTM	Post-translational modification
BMD	Bone mineral density
FDA	U.S. Food and Drug Administration
GSK-3β	Glycogen synthase kinase 3
APC	Adenomatous polyposis coli
CK1a	Casein kinase 1

LRP5/6	Low-density lipoprotein receptor-related protein 5/6
OPG	Osteoprotegrin
PPR	Parathyroid hormone/parathyroid hormone-related protein receptor
NONOate	Diethylamine NONOate sodium salt hydrate
ECL	Enhanced Chemiluminescence
HRP	Horseradish peroxidase
μCt	Micro-computed Tomography
ROI	Region of interest
ASBMR	American Society for Bone and Mineral Research
DMP1	Dentin matrix protein 1
NF-κB	Nuclear factor kappa-B
PGE2	Prostaglandin E2
IGF1	Insulin-like growth factor 1
DKK1	Dickkopf 1
RT-qPCR	Reverse transcription quantitative polymerase chain reaction
FSS	Fluid shear stress
siRNA	Small interfering RNA
NO/NO•	Nitric oxide
OCN	Osteocalcin
BV/TV	Bone volume fraction of tissue volume
NOX2	NADPH oxidase enzyme

Chapter 1. Introduction

1.1 Composition

1.1.1 Material

Bone is a heterogenous tissues comprised of an organic fraction (~25%), an inorganic fraction (~65%), and water (~10%)[1]. The organic component, also called osteoid, is principally comprised of type-I collagen, which is organized in rope-like trimers. Each trimer is arranged offset to its neighbor, like bricks, forming small voids between the trimers in which the inorganic hydroxyapatite is initially formed. These trimers are arranged into fibrils, which are further arranged into the lamellar bone that comprises almost all of the mature skeleton (Figure 1)[2]. While the osteoid is chiefly type-I collagen, cells are found within the bone matrix, as well as growth factors, BMPs, fibronectin and other proteins which support differentiation, repair, and maintenance of the bone and its resident cells[3].

The inorganic fraction is primarily comprised of hydroxyapatite ($Ca_{10}(PO_4)_6(OH)_2$)[4] (Figure 2)[5]. Other inorganic components may also be found in bone, like a small proportion of ions like magnesium, zinc, and sodium[6].

Bone is replete with calcium and phosphate, and bone formation and resorption are used to reduce or increase circulating calcium on demand. Furthermore, during periods of malnutrition or starvation, or during periods of increased need, like gestation and lactation, mineralized bone can be aggressively resorbed to liberate the minerals from preexisting bone, freeing them for use.

The organic and inorganic components of bone are often likened to rebar in concrete. The hydroxyapatite provides compressive strength while the collagen allows for

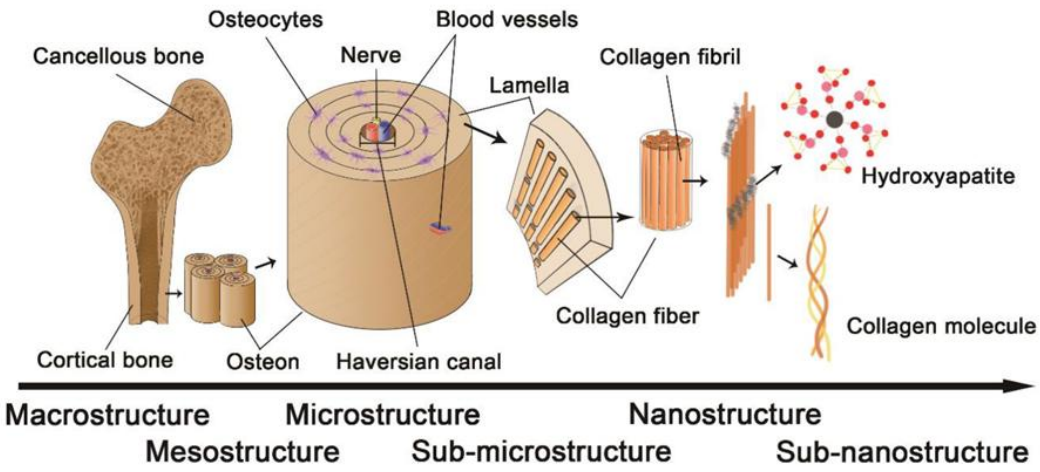

Figure 1. Hierarchical Structure of Bone

Bone is a complex, heterogeneous tissue. Type-I collagen trimers are formed into stacks, between which hydroxyapatite crystals can be found. These stacks are arranged into fibrils, which form the lamellar sheets that make up bone. In larger mammals, these lamellar sheets are organized around Haversian canals, which allow the penetration of blood vessels and nerves into the bone.

Taken from: Fan J, Abedi-Dorcheh K, Sadat Vaziri A, et al. A Review of Recent Advances in Natural Polymer-Based Scaffolds for Musculoskeletal Tissue Engineering. *Polymers (Basel).* 2022;14(10):2097.

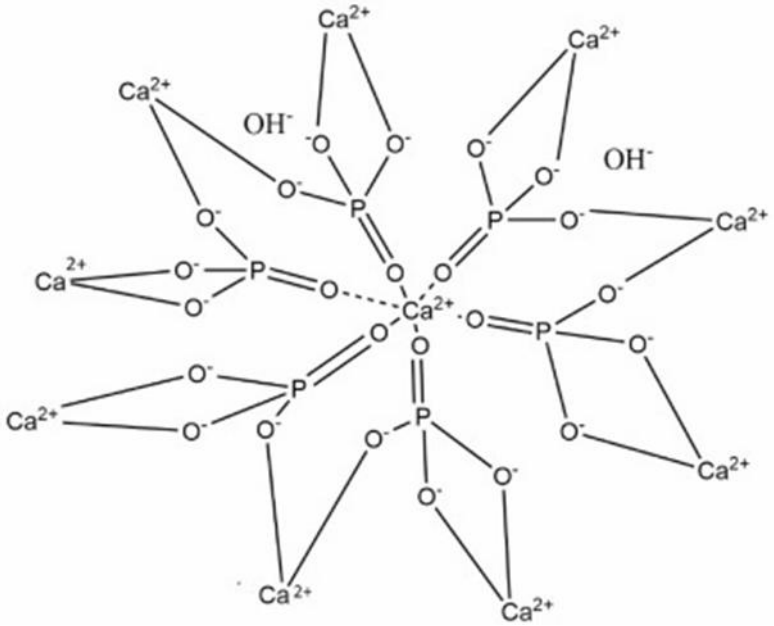

Figure 2. Chemical Structure of Hydroxyapatite

The inorganic component of bone is almost entirely comprised of hydroxyapatite, which contains the vital minerals calcium and phosphate.

Taken from: Panda S, Biswas CK, Paul S. A comprehensive review on the preparation and application of calcium hydroxyapatite: A special focus on atomic doping methods for bone tissue engineering. *Ceram Int.* 2021;47(20):28122.

flexibility. Water content in bone is vital for maintaining its mechanical properties and quality as well[7].

1.1.2 Bone-Resident Cells

Bone is a complex tissue that contains many types of cells. Some of which, like endothelial cells in blood vessels and immune cells, are also found in other tissues, but bone-resident cells, like osteoclasts, osteoblasts, and osteocytes, are specific to the skeleton.

Osteoclasts

Osteoclasts are multinucleated cells of the monocyte/macrophage lineage and are the cell type primarily responsible for the resorption of existing mineralized matrix. These cells form "on demand" where calcium is found on bony surfaces. Production of Receptor Activator of Nuclear Factor-κB Ligand (RANKL) by other bone cells, like osteocytes[8] and osteoblasts[9], supports osteoclast precursor differentiation and maturation, and increases the resorptive activity of osteoclasts. Osteoclastic αvβ3 integrin binds to RGD elements in the extracellular matrix proteins on the bone surface, like osteopontin and bone sialoprotein, to help osteoclasts adhere[10]. Upon activation, osteoclasts pump H+ protons and secrete lysosomal elements, like tartrate-resistant acid phosphatase (TRAP), cathepsin K, and other proteolytic enzymes, through the ruffled border at their apical face[11]. This acidic environment supports the degradation of the existing bone, creating a resorption pit (Figure 3)[11], which allows liberation of calcium and other minerals. Secreted proteolytic enzymes digest the primary collagenous osteoid, producing cleaved cross-linked C-telopeptide of

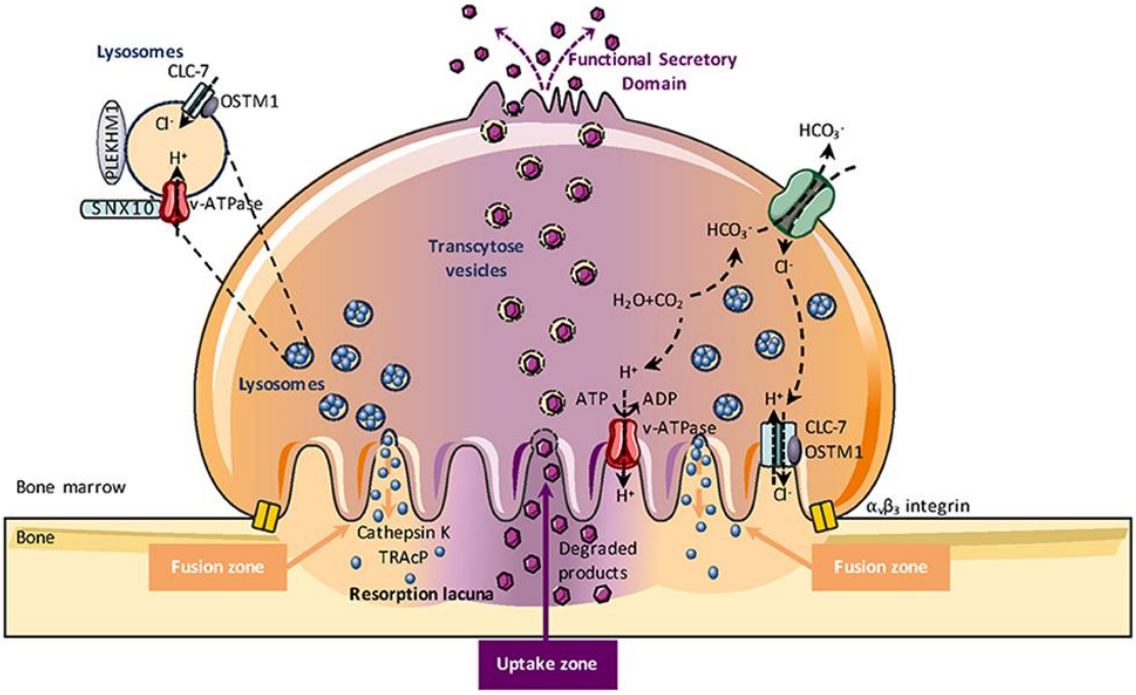

Figure 3. Osteoclasts

Osteoclasts are the cell type responsible for most bone resorption. Activated osteoclasts adhere to the bone's surface. They excavate a resorption pit under their apical surface through the secretion of H+ protons and proteolytic enzymes like cathepsin K, freeing vital minerals and embedded factors from existing bone.

Taken from: Madel MB, Ibáñez L, Wakkach A, et al. Immune Function and Diversity of Osteoclasts in Normal and Pathological Conditions. *Front Immunol.* 2019;10:1408.

type I collagen (CTX) as a byproduct of resorption. The circulating concentration of CTX may be measured as a pre-clinical and clinical marker for bone loss or turnover[12].

Osteoblasts

Osteoblasts are the cell type primarily responsible for the deposition of new bone matrix in the mature skeleton. They are found on bony surfaces and are able to perform various functions as they mature through stages of differentiation (Figure 4)[13]. Early osteoblasts express high levels of the gene Col1a1[14], which produces type-I collagen. As they secrete large amounts of collagen at their apical face, they create a layer of unmineralized osteoid on top of the existing mineralized bone.

As osteoblasts mature, they begin to express proteins that support mineralization of the new osteoid as well. Alkaline phosphatase (ALP or ALPL) is one such. When mature osteoblasts begin to support mineralization, they express ALPL, which converts pyrophosphate into organic phosphate. While pyrophosphate is a mineralization inhibitor, organic phosphate combines with calcium, and allows hydroxyapatite crystal nucleation in the osteoid[15]. ALPL may be detected in serum and is another important clinical marker of bone turnover. Mature osteoblasts also express other mineralization-associated proteins, like osteocalcin, which is believed to help control mineral deposition[16], and bone sialoprotein, which may facilitate collagen binding and mineral attraction[17].

Osteoblasts will generally follow one of three trajectories after mineralization. They may differentiate into quiescent bone lining cells, which may later re-differentiate into osteoblasts when stimulated by anabolic signals, like parathyroid hormone (PTH) or

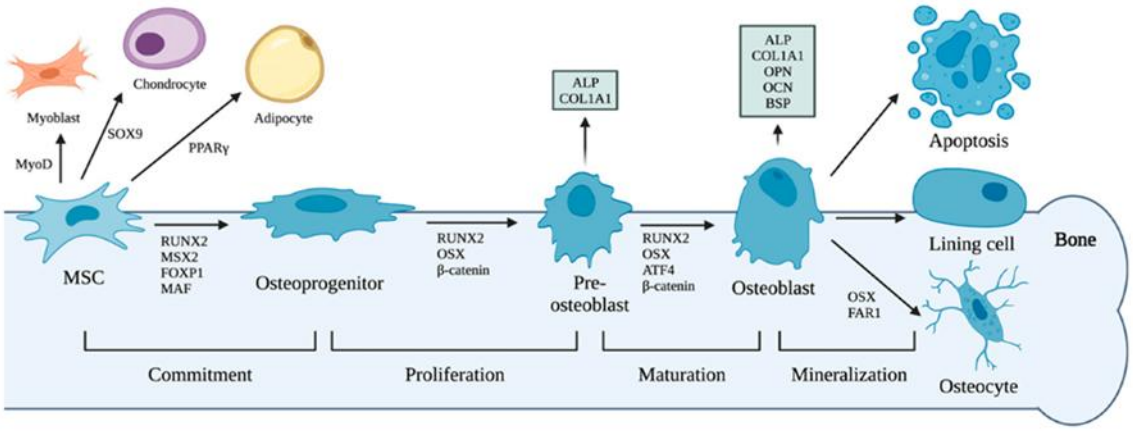

Figure 4. Osteoblasts

Osteoblasts support the deposition of nascent bone matrix and its mineralization as they mature. They respond to a range of signals to drive their differentiation and are able to express a range of proteins associated with osteoid production and mineralization before ultimately undergoing apoptosis or further differentiation.

Taken from: Liu Z, Wang Q, Zhang J, Qi S, Duan Y, Li C. The Mechanotransduction Signaling Pathways in the Regulation of Osteogenesis. *Int J Mol Sci.* 2023;24(18):14326.

mechanical stimulation[18]. They may also become entrapped in the newly deposited matrix where they may differentiate into osteocytes, or they may undergo apoptosis.

Osteocytes

While osteoclasts and osteoblasts are found on the surface of bone, osteocytes are found within the bone itself, where they serve diverse functions (Figure 5)[19]. Osteocytes are not primarily responsible for depositing or resorbing bone, but instead coordinate these processes by receiving, incorporating, and transducing signals to bone-resident cells and their precursors.

Osteocytes are found within a complex three-dimensional series of chambers and tunnels called the lacunar canalicular system (Figure 6)[20], where their ovular cellular bodies are found in chambers called lacunae, and their long, thin dendritic processes are found in tunnels called canaliculi. Their cell bodies are around 20-30μm apart[21], which is generally consistent among land-dwelling animals, and they have around 50 processes[22], which may be several cell-bodies in length. While individual structures are quite small, the totality of the lacunar canalicular system is vast, with a calculated surface area of 215m^2[23]. The presence of osteocytes is necessary for healthy bone. While some percentage of lacunae is found empty in bone sections, loss of local osteocyte populations can result in collapse, or necrosis of the bone.

Osteocytes are able to respond to systemic signals, like parathyroid hormone, signals from other osteocytes, like Wnt ligands and sclerostin, and local mechanical signals, as experienced during load. Osteocytes respond to stimuli either directly, or by converting these incoming signals to target bone-resident cells and their progenitors.

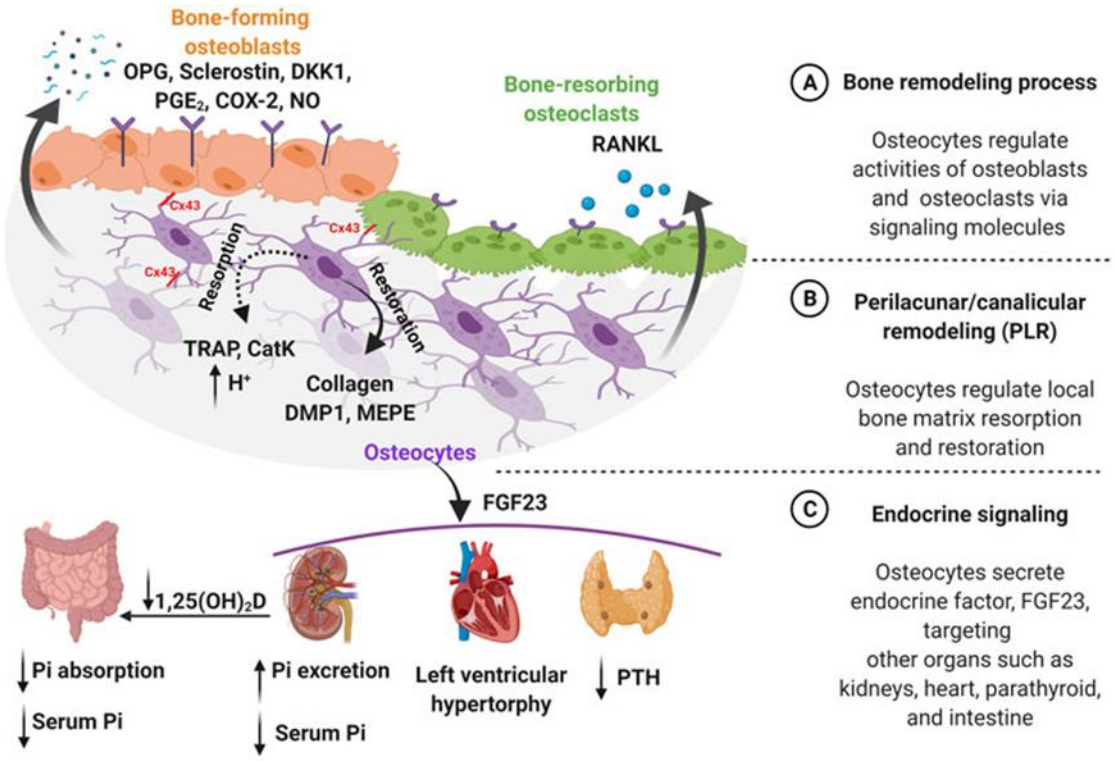

Figure 5. Osteocyte Signaling

Osteocytes are able to receive and transduce a range of signals to influence bone mass both locally and systemically.

Taken from: Choi JUA, Kijas AW, Lauko J, Rowan AE. The Mechanosensory Role of Osteocytes and Implications for Bone Health and Disease States. *Front Cell Dev Biol.* 2022;9:770143.

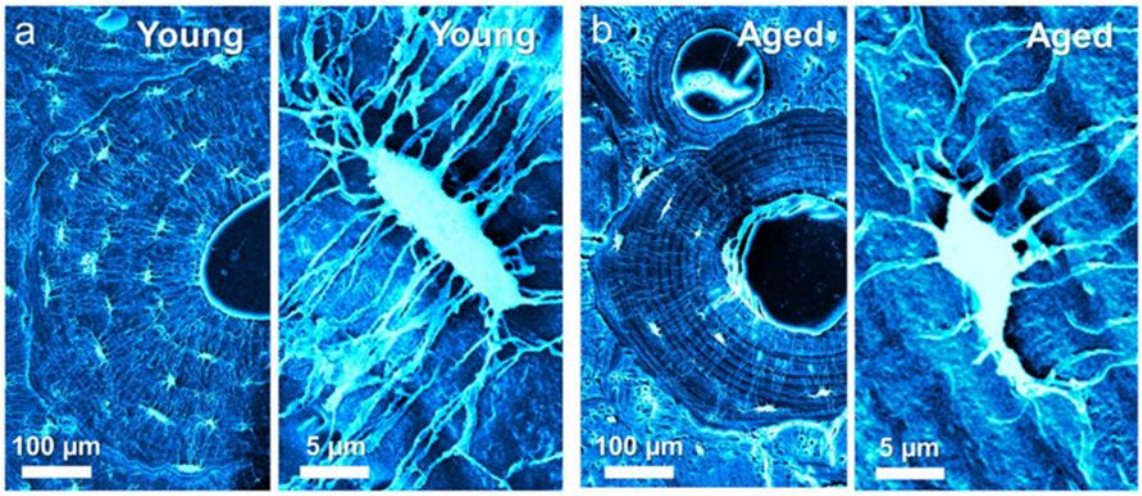

Figure 6. Osteocytes Within Their Lacunar Canalicular System

Osteocytes reside within a complex series of chambers and canals called the lacunar canalicular system (LCS). The LCS is dynamic and changes in response to aging as well as the needs of the organism.

Taken from: Tiede-Lewis LM, Dallas SL. Changes in the osteocyte lacunocanalicular network with aging. *Bone.* 2019;122:101-113.

Osteocytic signaling, especially in response to mechanical stimulation, will be covered below.

1.1.3 Cellular Level

Bone-resident cells possess the same basic structural composition as other types of cells; the elements more relevant to bone-cell function and our work in mechano-transduction will be discussed.

Cytoskeleton

Like all cells, osteocytes rely on their cytoskeletal systems for their structure, motility, and internal trafficking, but they are also necessary for mechanical response, which is a prominent feature of osteocyte function. The cytoskeleton is comprised of three types of fibers, microtubules, intermediate filaments, and the actin (microfilaments) network.

Microtubules are dense in the perinuclear space, but may also be found throughout osteocytes' long, thin dendritic processes (Figure 7), where they are believed to support functions such as mechanical response[24], and may also support trafficking of elements like organelles and protein cargo to the relatively-distant tips, though this has not yet been firmly established. Many post-translational modifications (PTMs) of the microtubules are implicated in changes to the stability and stiffness of the microtubules[25].

One such post-translational modification, detyrosination, is the cleavage of the terminal tyrosine from the alpha dimer. In cardiomyocytes it has been demonstrated that

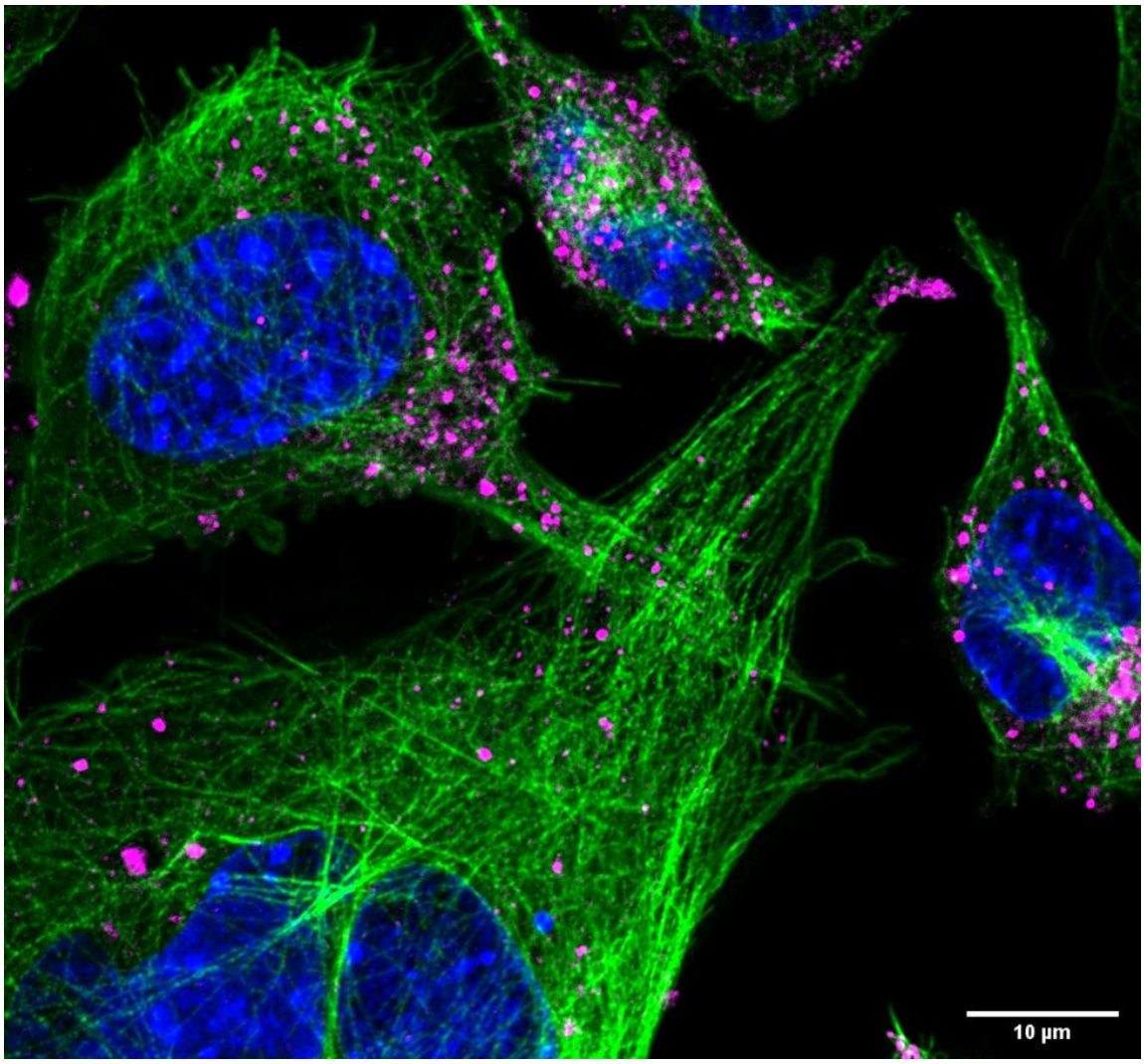

Figure 7. Microtubules and Lysosomes in the Osteocyte

Microtubules and lysosomes can be found throughout osteocyte cell bodies and dendrites. Fixed OCY454 osteocyte-like cell line. Blue = DAPI (nuclear stain), green = alpha tubulin (conjugated 488 antibody), magenta = lysosomes (SiR-Lysosome). Unpublished image taken by the author.

detyrosinated tubulin is more likely to be anchored to the sarcomere than tyrosinated tubulin. During contraction, detyrosinated microtubules transiently bend or buckle, rather than sliding past the sarcomere, allowing them to transduce force generated by sarcomere contraction[26].

Detyrosination has also been shown to greatly increase the likelihood of a lysosome's association with the microtubule network[27], suggesting that detyrosination may increase a cell's ability to traffic lysosomes.

Lysosomes

Lysosomes are membrane-bound organelles that are canonically known for their ability to degrade internal cargo through acidification and enzymatic action. They are also well-studied in their ability to fuse with endosomes to degrade larger cargo through autophagy[28]. Recently, we reported a new role for the lysosome in anabolic bone signaling through the osteocyte[29].

Sclerostin is produced by osteocytes and is a potent signal to prevent new bone deposition. Sclerostin is continually expressed and secreted, but after osteocytes receive a sufficient anabolic signal sclerostin protein expression is quickly, transiently, and robustly decreased[29–33]. It has been demonstrated that sclerostin and the lysosome colocalize within the unstimulated osteocyte[29]. It has also been shown that following anabolic signaling, lysosomal markers like cathepsin B activity, p62 expression, and LC3II/I ratio increase, indicating increased lysosomal activity, and that treatment *in vitro* with bafilomycin A, a lysosomal inhibitor, prevents the loss of sclerostin protein abundance following mechanical stimulation or treatment with parathyroid hormone[29]. Importantly, blocking the

lysosome or pathways upstream of lysosomal activation *in vivo* also prevents load-induced bone formation and the mechanically-induced loss of sclerostin protein in bone[29]. These data together indicate that sclerostin may be stored in the inactive lysosome or associated precursor in preparation for secretion or degradation, and that following anabolic cue, the lysosome acidifies, degrading sclerostin, rather than fusing with the membrane to release the sclerostin.

1.1.4 Tissue level

Organization

Bone is not comprised of a uniform block of material, but instead contains many highly-organized subunits (Figure 8)[34]. Penetrating blood vessels and nerves can be found within the bone in dynamic structures called Haversian canals. These canals run parallel to the bone's orientation and are critical for nutrient delivery and fracture healing in relatively large animals, like rats, while smaller animals, like mice, do not form these structures. Cells must be within 100-200μm of a blood vessel[35], so organisms with smaller, thinner bones do not need to form Haversian canals to provide cells with nutrients.

Haversian canals are excavated by osteoclasts, which form a cutting cone through existing bone. These osteoclasts create a new tunnel through the bone and are followed by extending blood vessels. Matrix is subsequently deposited into concentric layers called lamellae as osteoblasts are recruited to fill the newly-created void, together forming a new unit of bone called an osteon. Other structures, called Volkmann's canals, run perpendicular to the bone and connect Haversian canals.

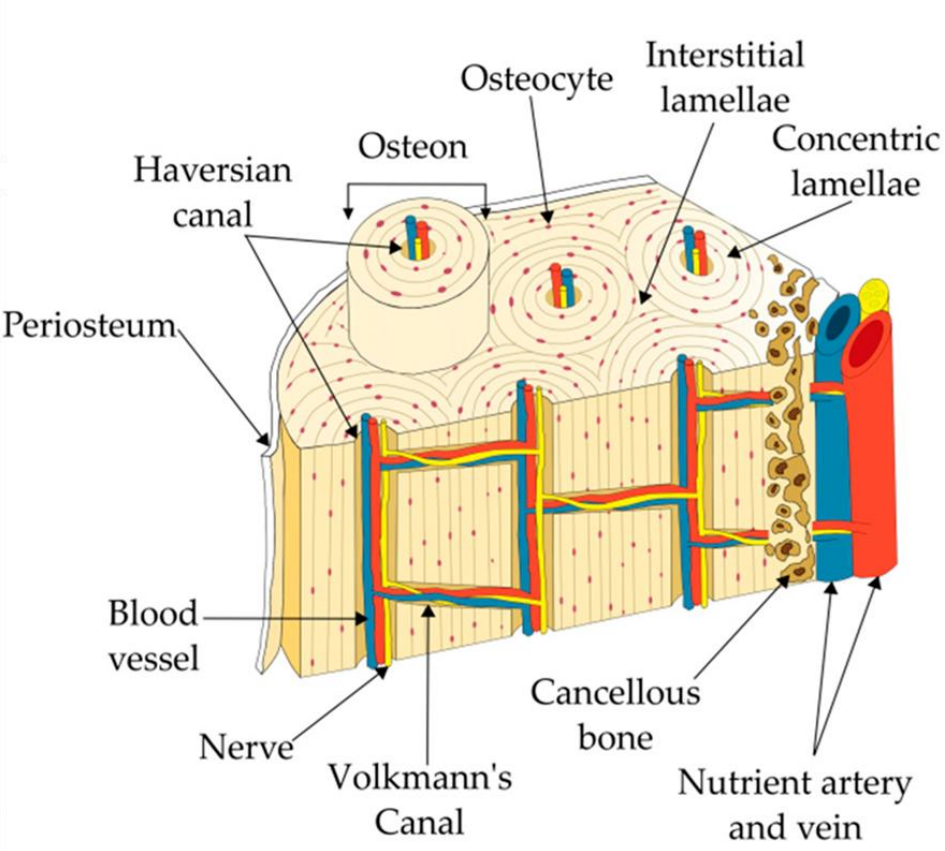

Figure 8. Haversian Canals

In larger animals, blood vessels and nerves penetrate the bone through Haversian canals. Concentric layers of matrix are deposited in the newly-excavated Haversian canals to form layers of lamellae, both of which together make up the osteon.

Taken from: Robles-Linares JA, Ramírez-Cedillo E, Siller HR, Rodríguez CA, Martínez-López JI. Parametric Modeling of Biomimetic Cortical Bone Microstructure for Additive Manufacturing. *Materials (Basel).* 2019;12(6):913.

Bone Marrow Cavity

Within most bones there is an inner chamber, called the bone marrow cavity. This niche is distinct from other regions of the bone in that it is the primary source of hematopoiesis, an important site for immune cell development, and an adipocyte depot[36]. The bone marrow cavity is also central to the health of the bone itself, as it houses a significant population of osteoblast progenitors[37], as well as the lipids that may fuel bone cell activity[38]. These cell populations change throughout life and can affect the health of the organism as well as local bone density.

1.1.5 System level

Connective Tissues

Bone works with other tissues, like tendons, ligaments, and cartilage to provide structure to vertebrate animals. Ligaments are bands of collagenous tissue that connect bones to each other to provide stability and support joints[39]. Tendons are fibrous bands that connect muscle to bone which are able to transduce large amounts of force[40]. Cartilage a is connective tissue that is found between bones, as in the knee, which allows for smooth operation of the joint and protects the ends of the bones from each other during movement[41]. In concert with bone, these systems protect organs and allow for mobility.

1.2 Bone in Health

1.2.1 Phases of Life

Development

Bone growth in the developing embryo is not primarily achieved by osteoblasts, but rather by chondrocytes. These chondrocytes deposit cartilage that will be replaced by bone through a process called endochondral ossification[42]. As fetal development progresses, longitudinal bone growth continues at the ends of bones, in areas called growth plates, where chondrocytes mature and new bone is produced. These processes continue through development until the growth plates close around or after puberty in humans[43].

While rodents do not close their growth plates, their rapid growth of long bones tends to slow around 12-16 weeks of age, after which they are generally referred to as "skeletally mature". The net accumulation of bone mass uncoupled from bone resorption is refred to as bone modeling and is the predominant means of bone accretion during developmental bone growth.

Adult Tissue

Peak bone mass is achieved around 30 years of age in humans, and continues to decrease gradually over time, outside of the onset of menopause or certain disorders where loss may be accelerated (Figure 9)[44]. In mice, this process of bone loss typically occurs after 6 months of age and progresses through the life span. Female mice do not experience a menopause but rather a peri-menopause-like state that has milder impacts on mouse bone mass than does human menopause.

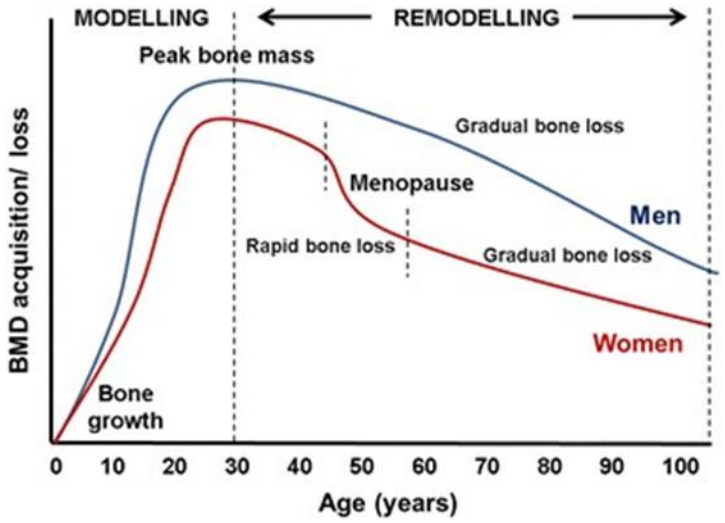

Figure 9. Bone Mass Changes with Age

Bone mass changes throughout the normal course of life, peaking around 30 years of age in humans.

Taken from: Kruger MJ, Nell TA. Bone mineral density in people living with HIV: a narrative review of the literature. *AIDS Res Ther.* 2017;14(1):35.

Throughout this stage of life, the healthy skeleton is continually renewed through a process called remodeling. During remodeling small amounts of bone are resorbed by osteoclasts. Growth factors embedded in the resorbed matrix, as well as other signals, recruit osteoblasts to the site to replace the lost bone with new osteoid[45]. The activity of osteoclasts and osteoblasts in the process is related through a relationship called coupling and does not result in a net change in bone mass. This cycle of renewal maintains the integrity of the bone and is necessary to deal with mineral demands as well as everyday wear and tear, which can produce microscopic cracks called microdamage.

With few exceptions, mature bone does not continue to grow, though it is still capable of robust response to stimuli or changes in the organism. In the healthy adult, bone mass is adaptive and may respond to sufficient changes in loading, be it either increased exercise or disuse. Osteocytes are able to detect strain, or the lack thereof, and signal to other bone-resident cells to tune bone mass to attempt to balance fracture risk with the energy required to maintain skeletal tissue. For example, a new exercise routine of sufficient intensity can stimulate new bone deposition in areas experiencing increased strain, while immobilization can result in a sudden loss of bone mass either locally, as in a casted fracture, or systemically, as during bedrest.

Reproduction

During gestation and lactation there is a significant maternal need for minerals like calcium, as well as nutrients like fat and energy. A human fetus contains about 30g of calcium at birth and around 280-400mg of maternal calcium is lost daily to milk production [46]. This extra calcium may come from the maternal diet, but if insufficient quantities are

ingested or absorbed, calcium will be liberated from the maternal skeleton. This is accomplished largely through an increased osteoclast population, which work to remove existing mineralized bone, freeing calcium and phosphate for use[47].

While osteoclasts are the primary driver of bone resorption, emerging data indicates that osteocytes may be able to resorb bone adjacent to them within the lacuna-canalicular system[48]. During lactation, lacunar area increases, osteocytic tartrate-resistant acid phosphatase (TRAP) activity increases, and the fluid within the lacunar-canalicular system becomes more acidic, all suggesting that osteocytes may be utilizing a process similar to osteoclastic resorption[49]. This process has not been fully described, however, and there is some debate as to the full capacity of osteocytes to remove or replace matrix and bone.

Aging

Some loss of bone mass with aging is unavoidable, but other age-related changes or disorders can increase this loss. During and around menopause women may experience a period of intense bone resorption due to a drop in estrogen, which is protective against osteoclastic resorption[50].

Over the course of a lifetime, damage can accrue to the point that systems can no longer compensate. Degradation of processes like oxidative stress management, autophagy, or immune response can lead to chronic inflammation, also known as ‘inflammaging,’ which can exacerbate bone loss[51].

Additionally, a fear of falling can discourage activity in the elderly, leading to a progressive cycle of disuse, weakening, and frailty.

Fracture

Despite bone's robust ability to resist shock and strain, fractures can still occur. Low-energy fractures, or falls from height, typically affect the elderly, who are more likely to have reduced mobility and bone mass, and to a lesser extent, adolescents, who are more active and are more likely to be participating in physical forms of play.

When a fracture occurs, blood vessels at the site of the break are ruptured, causing an influx of blood and allowing circulating immune cells to enter the injured tissue. This creates a hematoma, or blood clot at the fracture, which acts as a template for the soft callus[52]. Chondrocytes deposit cartilaginous fibers, stabilizing the fracture via formation of the soft callus, while osteoblasts quickly form disorganized woven bone. Endochondral ossification also acts to replace the cartilage with bone. Over time, the woven bone is remodeled into lamellar bone[52] (Figure 10)[53].

Disease

Bone is capable of self-maintenance and healing, but is also subject to disorders, like osteoporosis, osteomalacia, and sclerosteosis, which can greatly affect the quality of life or mortality of an individual.

Osteoporosis, the significant loss of bone mass, is determined by comparing an individual's bone mineral density (BMD) to BMDs of young, healthy adults that are sex- and race-matched to the individual. If the individual's BMD is 2.5 standard deviations below the mean healthy adults' BMD, then they are diagnosed with osteoporosis[54]. Osteoporosis is estimated to affect around 20% of the global population[55], and puts individuals at risk for fracture, loss of independence, and mortality. Fracture risk is greatly

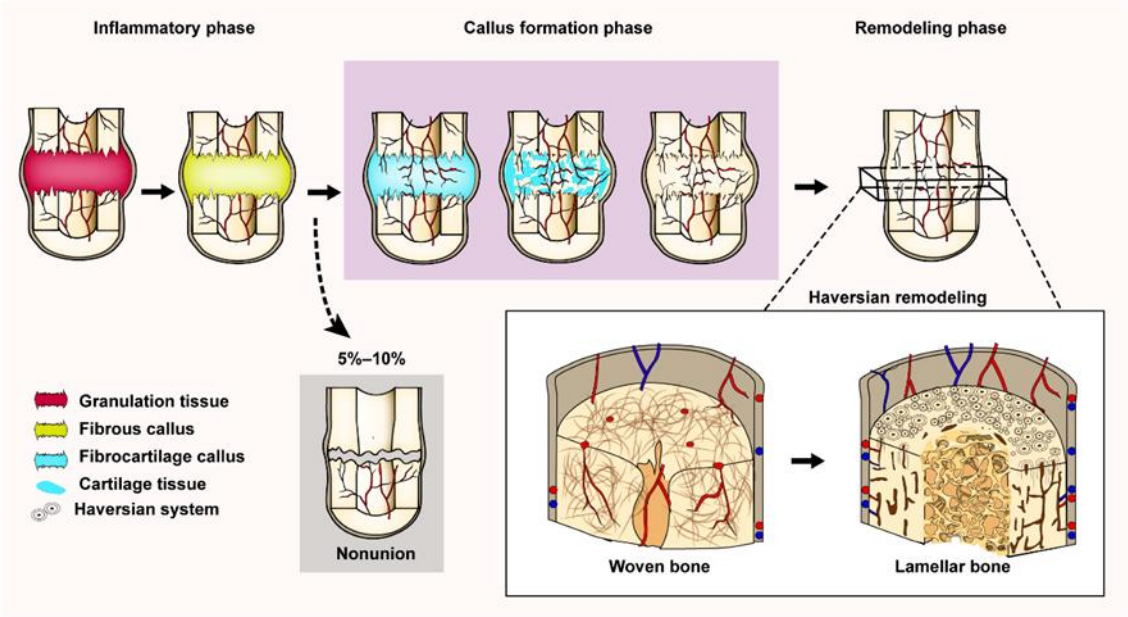

Figure 10. Fracture Healing

Following fracture, bone goes through several phases of healing. Hematoma and inflammation start soon after injury. The soft callus forms next, and is a fibrous structure that surrounds the break. Woven bone is deposited to stabilize the break and the hard callus forms. Over time, woven bone is remodeled and replaced with healthy, well-organized lamellar bone.

Taken from: Gao H, Huang J, Wei Q, He C. Advances in Animal Models for Studying Bone Fracture Healing. *Bioengineering (Basel).* 2023;10(2):201.

increased for those with osteoporosis, with an estimated 50% of women and 20% of those over 50 years of age experiencing an osteoporotic fracture[56]. Mortality rates vary by fracture site and comorbidities, but have been shown to reach 33% in the year following an osteoporotic fracture[57]. Non-pharmacological bone mass improvement following an osteoporosis diagnosis can be challenging due to the reduced mechanical response capacity in the elderly, but several clinically available treatments are available to support bone mass.

Unlike osteoporosis, which is a disorder of low bone mass, deficits in minerals like phosphate or calcium that can occur due to vitamin D deficiency can induce a weakened mineral state and softening of the bones leading to deformation, like outward bowing of the femurs or tibiae[58]. This can occur during development and acquisition, called rickets, or during adulthood, called osteomalacia. Other similar disorders of mineral metabolism can be due to insufficient dietary intake, gene mutation (e.g. PHEX), or kidney dysfunction leading to decreased absorption or retention of these vital minerals[59].

Sclerosteosis, on the other hand, is a disease of increased bone mass, which is causes be a mutation in gene, *SOST*, that produces sclerostin. Sclerostin is an important negative regulator of bone mass, and its absence results in thickened cortices and trabeculae, as well as overgrowth and malformation of the skull, fingers, and other structures.

Therapeutics

Bisphosphonates are one of the older classes of medications still prescribed to prevent bone loss. Modern bisphosphonates closely resemble pyrophosphate and have

nitrogen-containing moieties. They are highly attracted to bone and can still be found in the bone after long periods of disuse. When bisphosphonate-containing bone is resorbed by osteoclasts the bisphosphonates act on the osteoclasts, reducing their activity or causing apoptosis to prevent further resorption[60]. While bisphosphonates do prevent bone loss, they may also impair bone remodeling, which can allow microdamage to accumulate until an atypical fracture occurs. Because of this, drug holidays are recommended, during which the patient is either given an adjuvant treatment, or is monitored for extensive bone loss before medication is resumed.

Romosozumab, an anti-sclerostin antibody, is also a potent protector of bone mass. It effectively "removes" sclerostin and allows for greater osteoblast differentiation and activity, thereby increasing bone mass[61]. Despite producing robust BMD increase in the femoral neck[62], romosozumab is not ideal for all patients. Since its FDA approval in 2019 it has carried a black box warning against administration to persons who have had myocardial infarctions or stroke, and warns that it may increase the risk of serious cardiac events[63]. Because of FDA recommendation, it is generally prescribed to those with lower risk for cardiac events, and may not significantly increase risk in this population[64].

Denosumab is an anti-RANKL antibody that reduces osteoclast differentiation, number, and activity to prevent bone resorption[65]. However, due to its robust ability to prevent resorption within days of administration it can induce hypocalcemia, especially in those with chronic kidney disease[66]. The cessation of denosumab also results in a sudden loss or rebound in bone mass, which can significantly increase fracture risk[67].

The parathyroid gland was first identified in the 1800s, and while its full mechanism of action was not yet uncovered, the parathyroid gland was understood to

contribute meaningfully to bone mass in the early 1900s[68]. Teriparatide, or a 1-34 amino acid fragment of the hormone secreted by the parathyroid gland, PTH, is administered intermittently and has the capacity to greatly increase osteoblast activity and BMD, especially in the spine[69]. Abaloparatide, which is an analog to parathyroid hormone-related protein (PTHrP), functions similarly to teriparatide, though it has been shown to produce a slightly smaller effect[70]. Like romosozumab, teriparatide and abaloparatide both carried an FDA black box warning, which was removed in 2020 and 2021, respectively, but a maximal administration of two years is still recommended due to potential risk of osteosarcoma[71,72].

1.3 Molecular Signaling

1.3.1 Parathyroid Hormone

As mentioned in the previous section, parathyroid hormone (PTH) can induce anabolic reactions in bone-resident cells and their precursors, but it can also activate resorption. Physiologically, the parathyroid gland acts to detect circulating calcium, and when insufficient calcium is detected PTH is secreted. When PTH binds to its cognate receptor on osteoblast-lineage cells it induces both RANKL expression to increase osteoclast number and suppresses sclerostin abundance to increase osteoblast number (Figure 11)[73]. In the short term, increased osteoclastic activity quickly acts to remove small amounts of mineralized bone, freeing calcium for use. Osteoblastogenesis and deposition of new matrix is slower, however, so over the long term this does not result in a net change of bone mass. Continual exposure to PTH, as in hyperparathyroidism, can cause

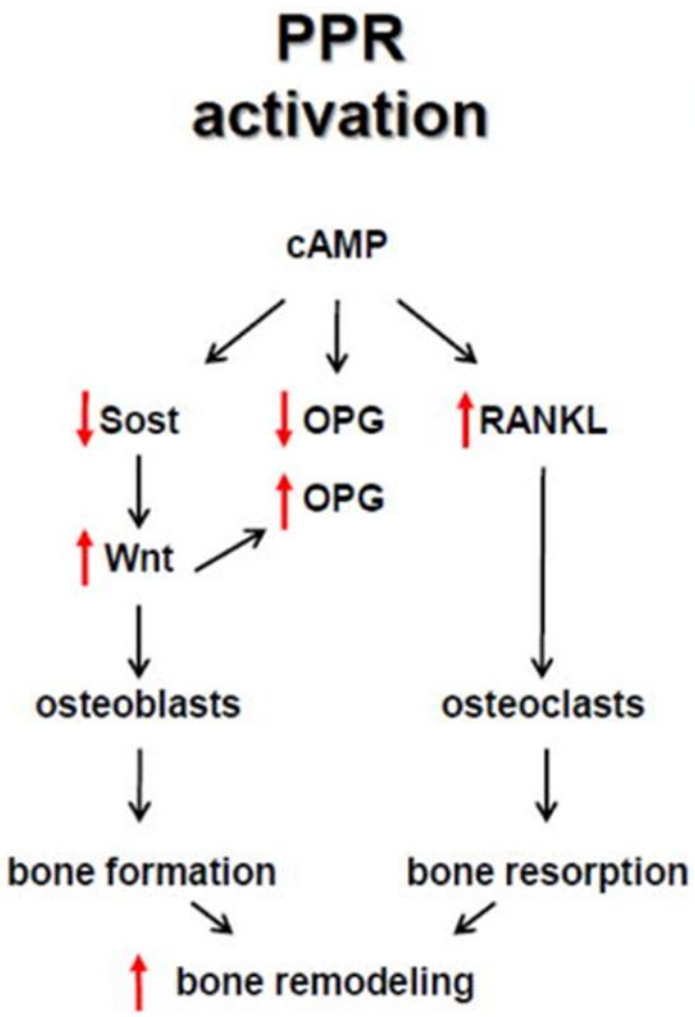

Figure 11. PTH Pathway

Parathyroid hormone (PTH) or parathyroid hormone-related protein (PTHrP) can bind to the PTH receptor (PPR) to initiate a cascade of processes that results in short-term bone resorption and longer-term bone deposition. In the healthy, adult system this results in remodeling, but not a change of overall bone mass.

Taken from: Bellido T, Saini V, Pajevic PD. Effects of PTH on osteocyte function. *Bone.* 2013;54(2):250-257.

hypercalcemia and may result in poorly mineralized bone, increased fracture risk, and even osteoporosis if untreated[74].

1.3.2 WNT Pathway

The WNT family of genes, named for their discovery in drosophila, are important to bone development and maintenance, as well as many other processes. WNTs like WNT1 and WNT3a have been shown to support osteoblast precursor maturation during development[75], while expression of WNT1[76] and WNT10b[77] have been shown to increase following mechanical stimulation. Each of these WNTS may act as ligands in the WNT/β-catenin pathway to increase osteoblast number and bone matrix deposition.

Briefly[75], the receptors for this path way, Frizzled and Low-Density Lipoprotein-Related Receptors 5 and 6 (LRP5/6) are located on the surface of bone-resident cells. In the absence of WNT ligand, these receptors do not interact. β-catenin, which is ubiquitously expressed, is phosphorylated by the destruction complex, comprised of glycogen synthase kinase 3 (GSK-3β), Axin, adenomatous polyposis coli (APC), and casein kinase 1 (CK1a). Once phosphorylated, β-catenin is polyubiquitinated and degraded by the proteosome and unable to affect gene expression.

Alternatively, when WNTs are available, they may form a complex with Frizzled and LRP5/6. Disheveled is then recruited to bind with Frizzled, preventing the destruction complex from phosphorylating β-catenin. β-catenin is no longer targeted for degradation and accumulates in the cytoplasm. β-catenin may then be translocated to the nucleus where it prevents the inhibition of the TCF/LEF transcription factor, allowing for expression of many osteoblastogenesis-related genes (Figure 12)[78].

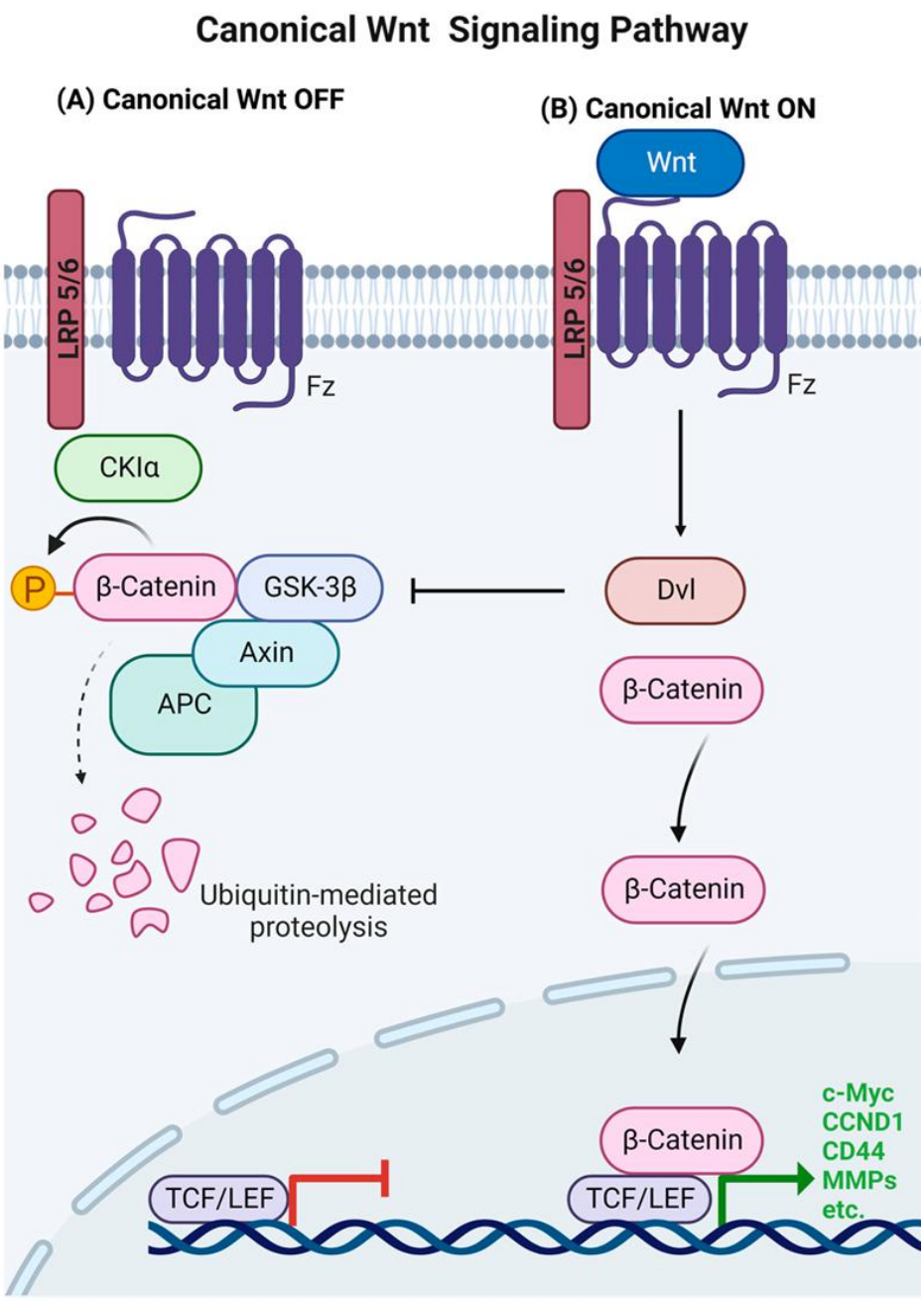

Figure 12. WNT/β-catenin Pathway

The canonical WNT/β-catenin pathway acts to control expression of many osteoblastogenesis-related genes through the TCF/LEF transcription factor.

Taken from: Ben-Ghedalia-Peled N, Vago R. Wnt Signaling in the Development of Bone Metastasis. *Cells.* 2022;11(23):3934.

1.3.3 Sclerostin

Sclerostin is primarily expressed and secreted by osteocytes. It is a powerful catabolic signal that acts to inhibit osteoblast precursor differentiation. Sclerostin competitively inhibits WNT/β-catenin activation by binding to Frizzled/LRP5/6. It prevents activation of the WNT/β-catenin pathway, ensuring the degradation of β-catenin and preventing osteoblastogenic gene expression.

Sclerostin, like RANKL and OPG, is secreted via endosome-related extracellular vesicles, where it can act to signal both systemically and locally[79]. Immediately following sufficient anabolic stimulation, sclerostin protein expression in the osteocyte is decreased, but neither is more sclerostin secreted. Instead, lysosomal acidification and markers of lysosomal activity are increased and sclerostin protein abundance is reduced[29]. Following anabolic stimulation, WNT expression is increased and sclerostin expression is decreased, allowing for osteoblastogenesis and deposition. This process is discussed in greater depth in Chapter 3.

1.3.4 FGF23

FGF23, or fibroblast growth factor 23, is a hormone produced by osteocytes[80] in response to elevated circulating phosphate[81] (Figure 13)[82]. FGF23 signals to the intestine where it reduces the production of 1,25-dihydroxyvitamin D3, or calcitriol, which is needed for absorption of phosphate from the diet. FGF23 also signals to the kidney, where phosphate transporters are downregulated to prevent phosphate reclamation from renal filtrate.

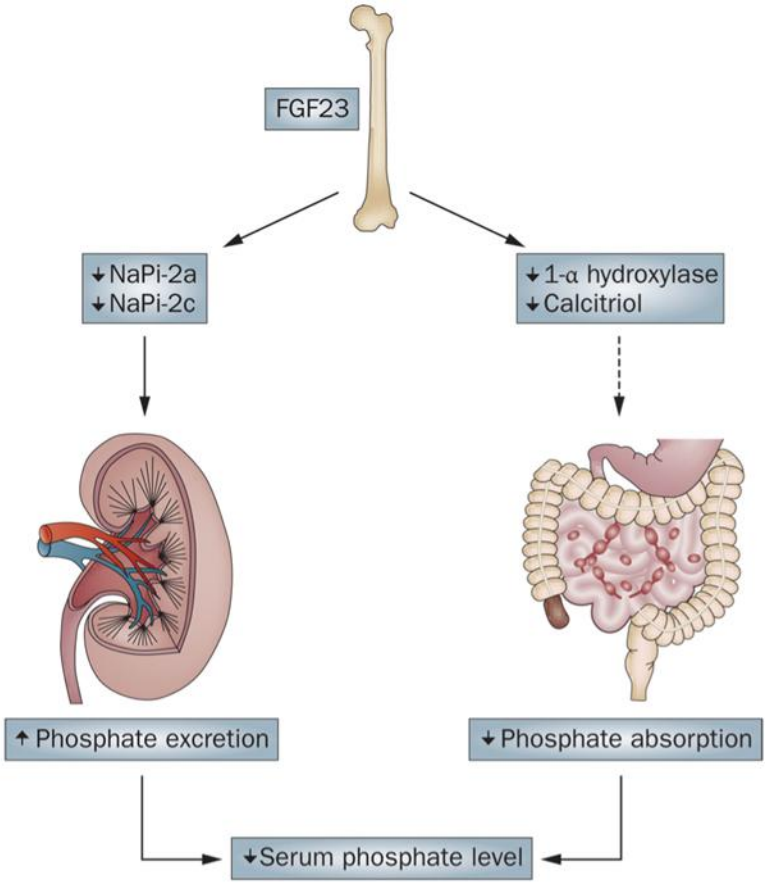

Figure 13. FGF23 Signaling

FGF23 is secreted by osteocytes to reduce reabsorption of phosphate by the kidney and absorption by the intestine, which reduces circulating phosphate.

Taken from: Razzaque MS. The FGF23-Klotho axis: endocrine regulation of phosphate homeostasis. *Nat Rev Endocrinol.* 2009;5(11):611-619.

1.3.5 Mechanical Response

A vital aspect of bone's ability to respond to the needs of the organism is controlled through the magnitude, duration, and frequency of experienced strain. Unlike parameters like circulating calcium, which have a *fixed* homeostatic set point, bone experiences *adaptive* homeostasis, and is able to adjust its set point to the types of loading experienced by the organism[83]. Levels of strain typically experienced by an organism (i.e., accustomed load) fall within the 'lazy zone' and do not result in a net change to bone mass. Amounts of strain just below the lazy zone does not induce much change, while total unloading (i.e., disuse) can result in a significant loss of bone mass. Amounts of strain above the lazy zone induce new deposition, up to the point that the amounts of strain become damaging (Figure 14)[84]. Other aspects of mechanical response are discussed in chapters 3 and 4.

To study mechanical response *in vivo*, axial loading of long bone can be utilized to produced controlled and consistent stimulation. Small rodents, like mice and rats are often selected as models, and the tibia or ulna are common targets for load. First, strain gauging must be performed to normalize strain to differences based on the size or composition of the bone for the control and treatment groups and sexes[29]. The target limb is isolated from a euthanized animal and the bone in the region of expected strain is exposed. Small strain-sensing resistors are applied to the bone and current is measured during a range of known compressive forces. The interaction of the material, bone, with the applied axial load allows the calculation of the amount of load that must be applied to a given group to achieve a specific level of strain. Typically, strains above 1000-1800 microstrain from axial loading generate an anabolic bone response in murine bone[85]. Loads above 2000 microstrain can

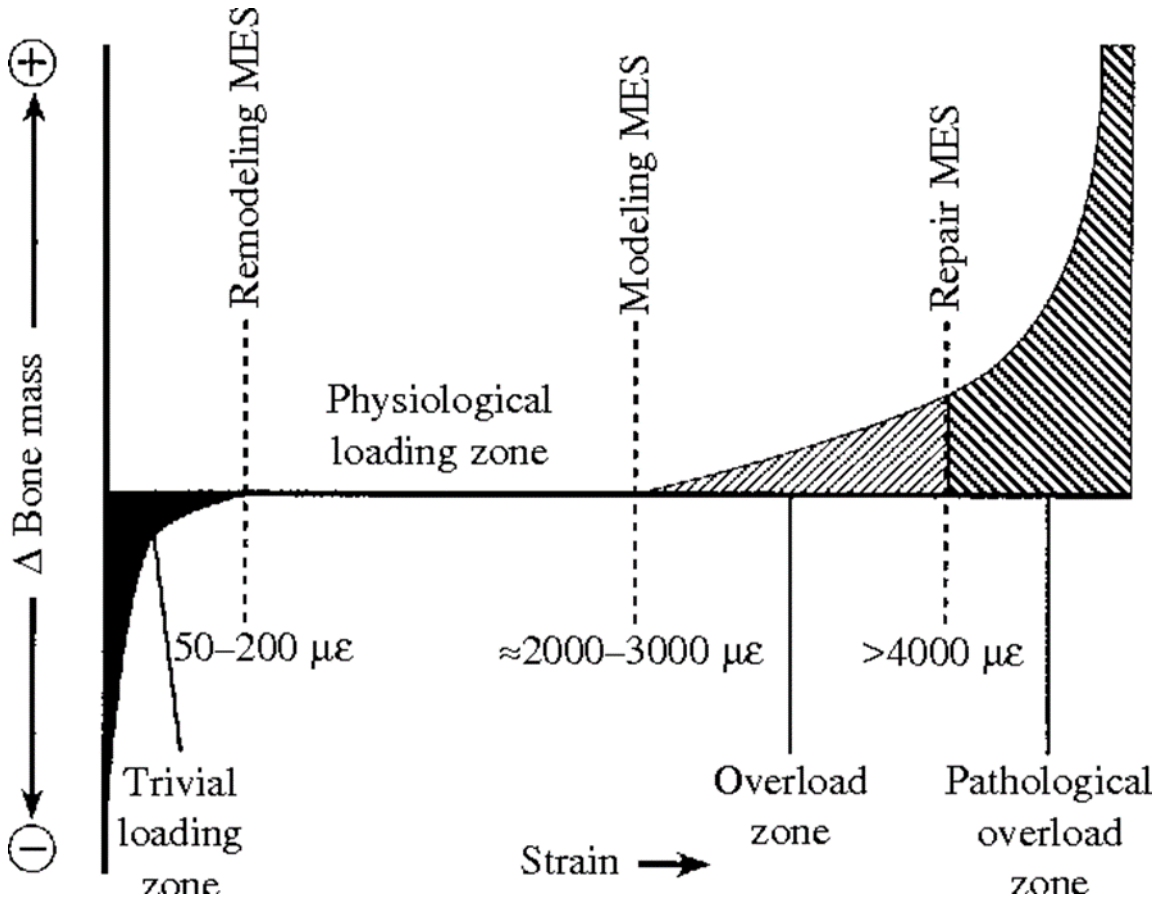

Figure 14. Physiological Outcomes of Strain

Normal, day-to-day activities generally produce strain that falls within the physiological loading zone and do not result in a change of bone mass. Strain far below this range, as experienced during immobilization, results in a drop in bone mass. Strains exceeding the physiological zone can induce new bone formation, while strains beyond that range can damage bone, requiring repair.

Taken from: Su SC, Skedros JG, Bachus KN, Bloebaum RD. Loading conditions and cortical bone construction of an artiodactyl calcaneus. *J Exp Biol.* 1999;202(Pt 22):3239-3254.

induce pathological, woven bone formation, and even damage, while loads below 200 microstrain can mimic disuse and bone loss.

To load a bone *in vivo*, the animal is put under sedation and placed in the loading rig (Figure 15)[86]. For example, for tibial loading, the foot rests in the lower receptacle, and the knee is fit into the upper cup. Cyclical compression is then applied to anesthetized animal, for example, 1800 microstrain at 2Hz for 90 seconds in a sine wave, or rest-inserted loading patter. The contralateral limb is left as an unloaded control. Assays ranging from dynamic histomorphometry, protein analysis, or spatial transcriptomics can be performed downstream.

Many techniques are available to study mechanical loading *in vitro*, one being fluid-shear stress via peristaltic pump[87,88]. In this technique, cells are seeded into 96-well plates at a specified density. A special tip is connected to tubing leading to and from the pump; the tip is fitted firmly onto the top of the well, creating a closed, fluid-filled loop. Once the pump is activated, fluid is jetted onto the adherent cells at a fixed rate of flow to simulate the type and range of mechanical stimulation that osteocytes are believed to experience physiologically. An unstimulated well of identical treatment is used as the control. Many techniques, like transfection or treatment, can be used to modify cells before mechanical stimulation, and most cell culture outcomes can be analyzed, to include live-cell imaging during stimulation.

In addition to loading, the activation of mechanical response pathways can be mimiced pharmacologically *in vitro* using a variety of anabolic signaling molecules, like PTH or nitric oxide, which will be discussed in chapter 4.

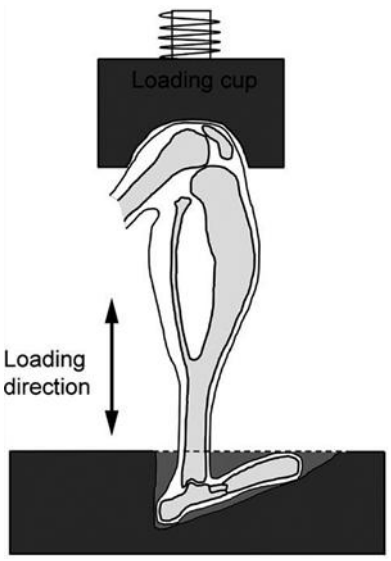

Figure 15. Axial Tibial Load

Axial tibial compression may mechanically stimulate regions of the tibia, based on the bone's geometry. This example shows the way that an anesthetized mouse's foot is placed in the lower receiver and the knee is placed in the upper cup. In this illustration, the upper cup is cyclically compressed to create reproducible load in the tibia.

Taken from: Zhao D, Riquelme MA, Guda T, et al. Connexin hemichannels with prostaglandin release in anabolic function of bone to mechanical loading. *Elife.* 2022;11:e74365.

Chapter 2. Materials and Methods

2.1 Cell culture

Ocy454 osteocyte-like cell line (provided by P. Divieti-Pajevic, Boston University) were cultured as previously reported[29,31,89]. Briefly, Ocy454 cells were cultured in αMEM (Corning) with 10% FBS (Benchmark, GenClone) and 1% penicillin/streptomycin (Corning Cellgro). For cell expansion, cells were plated on rat tail collagen I (BD Biosciences) coated plasticware and maintained at 33°C and 5% CO_2 with media changes every 2 to 3 days. For experiments, cells were maintained at 37°C and 5% CO_2.

2.2 Cell Treatment with Nitric Oxide Donor

The NO• donor, diethylamine NONOate sodium salt hydrate (Sigma-Aldrich), was prepared as 64mM stock and diluted in water just prior to use and administered at a final concentration of 10μM.

2.3 Fluid Shear Stress

Assay was performed as previously reported[88]. Briefly, cells were plated in Stripwell (Costar) 96-well-size vessels at 35,000 or 40,000 cells per well the day before flow. Processively by strip, media was replaced with 37°C, pH 7.4 mouse Ringer's solution (140 mM NaCl, 4 mM KCl, 1 mM $MgSO_4$, 10 mM Hepes, 10 mM glucose, 5 mM $NaHCO_3$, 1.8 mM $CaCl_2$). Strips were allowed to acclimate on a benchtop warming mat (38°C) for 20 minutes. Cells were stimulated at a flow rate of 38ml/min (flow rate modelled at 7 dynes/cm^2, 5min), unless otherwise indicated, in Ringer's solution for 5 minutes by peristaltic pump (Harvard) via custom-printed tips[90]. After completion of fluid shear stress

(FSS) exposure, cells were allowed to incubate on benchtop warming mat from 0-10min, as indicated. Cells were lysed in 1X RIPA buffer supplemented with 2% SDS, 1% HALT protease and phosphatase inhibitor (Thermo) and 1% EDTA (0.5M) or 2x Laemmli buffer with 5% BME, 1% HALT (Thermo Fisher) and 1% EDTA (0.5M).

2.4 Griess Assay

Following exposure of cells to FSS, Ringer's solution from wells and tubing was collected. Additional Ringer's solution was added to no-flow samples collected from wells to volume-match FSS samples. Colorimetric Griess assay (Thermo Fisher) was performed using 280µl each sample/standard. Standards were produced and protocol followed per manufacturer's instructions. Plates were read at 548nm on µQuant (Bio-Tek Instruments) plate reader. Fluorometric Griess assay (Invitrogen) was performed using 20µl each sample/standard. Plates were read at 350/450nm on Tristar 3 (Berthold) plate reader.

2.5 *Ex Vivo* Treatments

Camk2d$^{flox/flox}$/*Camk2g*$^{flox/flox}$ mice were backcrossed into the C57BL/6 background and generously provided by the Oslon group[91]. Mice were then crossed with osteocalcin-cre mice (RRID:IMSR_JAX:019509), which are also in the C57BL/6 background. Mice were maintained with ad libitum access to water and standard rodent chow under Animal Care and Use Committee-approved protocols at the University of Maryland Baltimore, protocol# 00000134. Five male and six female mice between 6-23 weeks of age were utilized and no sexual differences were observed in the data. Briefly, as described[92], following euthanasia, femur or ulna/radius were isolated from surrounding soft tissues,

epiphyses were removed and marrow was flushed. Bones were maintained in 37°C complete αMEM during collection, before transfer to 37°C mouse Ringer's solution for treatment. After treatment, bones were transferred to Laemmli lysis buffer supplemented with protease and phosphatase inhibitors. Bones were homogenized with 1mm metal beads in a Precellys Evolution (Bertin Technologies) homogenizer.

2.6 Western Blot

Western blots were performed as previously reported[32]. Briefly, cell lysates were sonicated and electrophoresed on 10% or 4-20% SDS-Page gels (Bio-Rad) and transferred to PVDF film (Millipore). Total protein stain imaging was taken on Odyssey CLx (LI-COR) following five minutes Revert 700 Total Protein Stain (LI-COR) incubation. Membranes intended for ECL development were blocked in phosphate buffered saline with 0.1% Tween-20 and 5% non-fat dry milk. Membranes intended for goat-derived ECL antibodies were blocked in 3% bovine serum albumen as well. Membranes intended for LI-COR development were blocked in Intercept (LI-COR). Primary and secondary antibody concentrations varied by target (Table 1). ECL membranes were developed with Pierce ECL Western Blotting Substrate (Thermo Scientific) or SuperSignal West Femto Maximum Sensitivity Substrate (Thermo Scientific). Blots were analyzed using ImageLab software (Bio-Rad). Loading controls were probed sequentially on the same membrane as its experimental target for all probes except p-CaMKII. For p-CaMKII, two membranes were produced and processed at the same time, keeping all conditions and handling as identical as possible until p-CaMKII or panCaMKII probing.

Table 1. Western Blot Antibodies

Antibody	Dilution	Manufacturer	Catalog Number
Sclerostin (goat)	1:500	R&D Systems	AF1589
pCaMKII (T286) (rabbit)	1:500	Cell Signaling	12716S
panCaMKII (rabbit)	1:500	Cell Signaling	4436S
Beta Actin (mouse)	1:5000	Sigma	A1978
Alpha Tubulin (mouse)	1:5000	Millipore	T9026
FGF23 (goat)	1:500	R&D Systems	AF2604
ALPL (goat)	1:500	R&D Systems	AF2910
HRP x Goat	1:1000	Jackson ImmunoResearch	805-035-180
HRP x Rabbit	1:1000	Cell Signaling	7074S
HRP x Mouse	1:8000	Cell Signaling	7076S
Donkey x Goat 800	1:20,000	LI-COR	926-32214
Donkey x Mouse 700	1:20,000	LI-COR	926-68072

2.7 RT-qPCR

RT-qPCR was performed as previously reported[93]. Briefly, cells were lysed in TRIzol (Sigma). RNA was isolated using Direct-zol RNA Miniprep kit (Zymo) per manufacturer's instructions and measured for quantity and purity using μQuant plate reader. RNA was converted to cDNA using High-Capacity RNA-to-cDNA kit (Thermo Fisher) on a MyCycler thermocycler (Bio-Rad). Maxima SYBR Green/ROX qPCR Master Mix (Thermo Fisher) was used to prepare samples, which were run on Applied Biosystems 7300 sequence detection system. Commercially available primers were utilized (Table 2).

Relative gene expression for each sample was simultaneously normalized to three housekeeping genes, *Gapdh*, *Hprt*, and *Rpl13*.

Table 2. RT-qPCR Primers

Target	Forward Primer	Reverse Primer
nNOS/*Nos1*	TGTCGACAATCCAAG ATAGATCATATC	GAGTAGGCAGTGTAC AGCTCTCTGAA
iNOS/*Nos2*	CCTGGTACGGGCATTGCT	CATGCGGCCTCCT TTGAG
eNOS/*Nos3*	TCTGCGGCGATGTCACTATG	CCATGCCGCCCTCTGTT
Gapdh	CGTGTTCCTACCCCCAATGT	TGTCATCATACTTGG CAGGTTTCT
Hprt	AGCAGTACAGCCCCA AAATGG	AACAAAGTCTGGCCT GTATCCAA
Rpl13	CGAAACAAGTCCACG GAGTCA	GAGCTTGGAGCGGTA CTCCTT

2.8 Transient Transfection

Transfections of Ocy454 cells were performed using JetPrime transfection kit (Polyplus) per manufacturer's recommendation at the listed concentrations (Table 3).

Table 3. Plasmids

Target	Type	Reference Number	Concentration (pmol/cells)	Manufacturer
Murine myc-tagged-sclerostin	Plasmid	MR222588	0.05µg/40,000	Origene
Scramble	siRNA	D-001810-01-20	4pmol/40,000	Dharmacon
nNOS	siRNA	J-047847-09-0005	4pmol/40,000	Dharmacon
iNos	siRNA	J-042006-05-0005	4pmol/40,000	Dharmacon
eNOS	siRNA	J-040956-05-0005	4pmol/40,000	Dharmacon

2.9 Cell Viability Assay

Cells were passaged and transfected as normal prior to assay (see Section 2. Materials and Methods). Cells were plated in an opaque white 96-well plate at 40,000 cells/well. CellTiter-Glo 2.0 (Promega) kit was used per manufacturer's instructions and luminescence was read on Tristar 3 (Berthold) plate reader.

2.10 Live Calcium Imaging

Cells were seeded onto optically clear-bottom 96-well plates. Media was removed and replaced with 350µl Fluo-4-AM ester (5µM, 30m) in mouse Ringer's solution, as described[32]. Mechanical stimulation via pulsatile pump was performed as above. Images were recorded using Nikon NIS Elements 5.2 (Nikon) and intensity measurements were quantified using FIJI (ImageJ) Time Series Analyzer plugin.

2.11 Animals

Camk2d$^{flox/flox}$/*Camk2g*$^{flox/flox}$ mice were generously provided by the Oslon group[91]. These double-floxed mice were crossed with osteocalcin-cre mice (RRID:IMSR_JAX:019509) to produce Camk2delta/gamma double conditional knockout (double cKO) mice. Double-floxed mice were also bred with C57BL/6J mice (RRID:IMSR_JAX:000) to produce separate *Camk2d*$^{flox/flox}$ or *Camk2g*$^{flox/flox}$ strains. *Camk2d*$^{flox/flox}$ or *Camk2g*$^{flox/flox}$ mice were crossed with osteocalcin-cre mice to produce independent Camk2delta or Camk2gamma conditional knockout (cKO) mice. Cre negative *Camk2d*$^{flox/flox}$ or *Camk2g*$^{flox/flox}$ mice were used as littermate controls. Mice were maintained with ad libitum access to water and standard rodent chow under Animal Care and Use Committee-approved protocols at the University of Maryland Baltimore, protocol# 00000134.

2.12 Micro-computed Tomography

Micro-computed Tomography (μCt) was performed as described[94]. Briefly, 8-week-old mice were euthanized and femurs and spines (S1-L1 region) were isolated. Bones were fixed at 4% PFA for 24 hours before transfer to 100% ethanol. Bones were scanned on a SkyScan μCt at 55kV, 2k resolution, 0.5mm Al filter, 10μm voxel size, with flat-field correction 55-60%, 0.5 rotation step, 4 frame averaging, 5 random movement. NRecon reconstruction settings were 20% beam hardening, 5-5 ring artefact, 1 smoothing and 0-0.11 threshold. The growth plate in the distal femur was found and an ROI 100 slices thick with an offset of 25 was used for femoral trabecular measurement (70-255 threshold). The femoral notch was found and the halfway point between the growth plate and femoral notch

was determined. An ROI was drawn of 61 slices with no offset towards the femoral head for the cortical measurement (95-255 threshold). For the spine, the growth plate of the L5 vertebra was found and the ROI was defined within the vertebral body for 100 slices with no offset (85-255 threshold). We followed the guidance of the ASBMR for standardized reporting of bone histomorphometry[95].

2.13 4-point Bending

Briefly[94], soft tissue was removed from the left femurs from 8-week-old mice, which were wrapped in a saline-soaked kimwipe and flash frozen in liquid nitrogen. Once all femurs were collected, femurs were processively thawed in water and the kimwipes were removed. Femurs were loaded into the four-point bending rig (TA ElectroForce 5500) with condyles down and samples resting firmly in the holder. Settings (Win-Test software) were displacement (-3.0 to 4mm), load (-80 to 80N), dir cmd (-10 to 10), axial dr (-100 to 100). Bones were cyclically trained to 2N 2 times each, then 0.25N load was applied. Measurements were taken every 0.1 seconds as load was applied at 5μm/sec, until failure or -2.5mm displacement. Analysis was performed using a template adapted from Sergey Leikin (National Institute of Childhood Health and Human Development) with values normalized to body weight to determine parameters as described[96].

2.14 Analysis

Analysis and graphing were performed using GraphPad 10 (Prism). Normal distribution was determined via GraphPad. Multigroup comparisons performed via two-

way ANOVA with Holm-Sidak's post hoc correction. Graphs show mean with ±standard deviation. Asterisks represent p values: *=$p<0.05$, **=$p<0.01$, ***=$p<0.001$, ****=$p<0.0001$.

Chapter 3. Osteocyte-Mediated Mechanical Response Controls Osteoblast Differentiation and Function

3.1 Introduction

In the healthy skeleton, bone must respond to environmental cues to accommodate the organism's needs. This is easily demonstrated in athletes, where the results of repetitive high-intensity loading are clear. Both male and female collegiate tennis players, for example, develop significantly increased bone mineral density in the dominant arm, as compared to the contralateral arm[97]. Significant differences between an athlete's dominant and non-dominant arm can also be observed in a range of sports, like baseball, golf, and volleyball. Through training and competition, athletes expose their skeletons to repeated and intense strain; their bones respond to increased strain by upregulating anabolic bone processes, like osteoblast differentiation, extracellular matrix deposition, and mineralization to strengthen the bone and resist fracture. This increase in bone mass is accomplished through the close interplay of various bone-resident cells, namely osteoblasts, osteocytes, and osteoclasts. Generally, osteoblasts deposit and mineralize the collagen-rich extracellular matrix that will become new bone. Osteocytes receive mechanical and hormonal signals and transduce these cues among themselves and to osteoblasts and osteoclasts to coordinate bone deposition and resorption. Osteoclasts resorb mineralized bone and digest the collagenous extracellular matrix. Osteoclasts and osteoblasts are on-demand cells that form when they are needed and later become quiescent or undergo apoptosis. In contrast, osteocytes are long-lived cells that mediate the activation of osteoblast and osteoclasts. This review will discuss the bone anabolic response to

mechanical load, with a focus on how osteocytes sense and respond to loading to affect osteoblast differentiation.

3.1.1 Osteoblasts

Osteoblasts are cuboidal cells found on bony surfaces, where they are the primary producer and depositor of the extracellular matrix that will become mineralized bone[98]. They arise from mesenchymal progenitor cells, which can differentiate into a range of cells such as adipocytes, chondrocytes, and myocytes. They express mechanoresponsive calcium channels, like Piezo1, and have been shown *in vitro* to respond to tensile load with increased alkaline phosphatase expression and mineralization[99].

Following local bone resorption by osteoclasts, osteoblasts are recruited to the newly exposed bone surface where they begin to secrete collagen and other extracellular matrix proteins at their apical face[100]. This newly formed extracellular matrix, termed osteoid, is an arrangement of primarily type I collagen trimers, which are highly interlinked, along with other extracellular matrix proteins like osteopontin, osteocalcin, bone sialoprotein, and osteonectin[101]. Osteoid also contains other organic components, like embedded latent growth factors, and provides the lattice into which mineralization will occur[102].

The inorganic component of bone, hydroxyapatite, is comprised of phosphate and calcium, vital minerals found in circulation. Following matrix deposition, osteoblasts support hydroxyapatite crystal nucleation by expressing proteins such as alkaline phosphatase, which provide the appropriate inorganic phosphate and hydrolyze the mineralization inhibitor, pyrophosphate[103], and bone sialoprotein, which stimulates

hydroxyapatite nucleation[104]. The presence of fibrillar collagen, alkaline phosphatase, and the absence of endogenous inhibitors of mineralization seem to be the key combination that permits this tissue to mineralize[105]. After mineralization, osteoblasts either become entrapped into the accumulating bone matrix and differentiate into osteocytes, become quiescent bone lining cells, or undergo apoptosis[106].

3.1.2 Osteocytes

Osteocytes, which are found throughout mineralized bone in most vertebrates[107], are the primary integrator of mechanical signaling[108], utilizing their distinctive location encased in mineralized bone and their neuron-like morphology to detect mechanical load in the surrounding bone. Osteocytic cell bodies are located within ovular chambers, called lacunae, and their long, thin processes reside in a geometrically complex, three-dimensional series of tunnels, called canaliculi. This series of chambers and tunnels, the lacunar-canalicular network, is highly interconnected and provides a conduit for direct cell-to-cell communication amongst osteocytes and between osteocytes and other bone resident cells, mediated by gap junctions[92]. Surrounding the osteocytes, the fluid-filled space within the lacunar-canalicular system contains extracellular matrix elements like collagen, glycocalyx[109], and perlecan[110], which is believed to be a primary tethering protein, critical for load response[111].

When mechanically stimulated, osteocytes express many bone anabolic effectors, like WNT, nitric oxide, and PGE2, which act to upregulate the β-catenin pathway; unloaded osteocytes express catabolic signals like RANKL and the β-catenin pathway inhibitor sclerostin. Osteocytes are terminally differentiated osteoblasts[112], and while the

mechanism of their encapsulation within bone matrix has not been fully clarified[113,114], they are often distinguished from osteoblasts by their expression of markers such as DMP1, FGF23, podoplanin, and sclerostin[115].

3.1.3 Osteoclasts

Osteoclasts are large, multinucleated cells derived from macrophages and are the primary facilitator of bone resorption. They originate from hematopoietic stem cells and their differentiation is promoted by the binding of RANKL (receptor activator of NFκB ligand)[116] to its cognate receptor (RANK) on the surface of osteoclast progenitors. Osteocytic RANKL expression is increased during unloading, supporting increased osteoclastogenesis and bone resorption during disuse[117]. Emerging data suggest that osteoclasts may also directly respond to mechanical stimulation[118], but the way in which this response may participate in anabolic processes is not settled.

To remove mineralized bone, osteoclasts adhere to the bone surface, form an actin ring, and vectorially secrete acidic vesicles into the bone-facing extracellular milieu[119]. The accumulation of hydrogen protons and proteolytic enzymes on the bone-facing surface dissolve mineralized bone and extracellular matrix, liberating calcium and phosphate ions and forming a resorption pit[120].

3.1.4 Osteoprogenitors and the osteoblast cell lineage

A broad group of mesenchymal progenitor cells, commonly found in the bone marrow cavity, around vasculature, or in the fibrous periosteal and endocortical membrane surfaces that line cortical bone, give rise to skeletally associated cells including

chondrocytes, adipocytes, and osteoblasts[121,122]. Lineage allocation of these progenitor cells is mediated by specific cues and activators. Canonically, the transcription factor Sox9 is required for the differentiation of chondrocytes[123], cells necessary for growth, limb development, and cartilage maintenance. Differentiation into adipocytes, cells that support metabolism and lipid storage, is supported by the transcription factor PPARγ[124], while osteoblast differentiation requires the transcription factors RUNX2[125] and Osterix[126].

There are several influences that can bias mesenchymal progenitor cells towards osteoblast or adipocyte differentiation. For example, consistent administration of a high-fat diet increases the relative differentiation of progenitor cells into adipocytes over osteoblasts[127], while osteoblastogenesis is favored after mechanical load[128]. The stiffness of the extracellular matrix surrounding bone-resident cells is also believed to influence differentiation and anabolic response. It has been demonstrated *in vitro* that mesenchymal progenitor cells are more likely to differentiate into the osteogenic lineage[129] and that expression of osteoblastic deposition markers[130] increase in the presence of a relatively stiff extracellular matrix.

Even within the osteoblast lineage, varied cues can activate distinct progenitor populations to differentiate into bone-depositing osteoblasts. For example, discrete groups of skeletal progenitor cells may be recruited from the periosteal or endosteal compartments in response to fracture or mechanical loading[131], though this is still an area of emerging research.

3.1.5 Mechanical load: tissue and cellular responses

Like many other physiological systems, bone mass is regulated around a homeostatic set point. Mechanical loading, such as from customary physical activity to which an organism is acclimated, will be within the homeostatic range and insufficient to induce a net change in bone mass[132]. This broad range of mechanical loading is referred to as the "adapted window" in Harold Frost's mechano-stat theory[133] and is also known as the lazy zone. This level of load will be different for every organism and will adapt to the organism's activity level and peak loading forces. For example, an individual who regularly strength trains will accumulate more skeletal mass to adapt to increased load, but may not receive additional anabolic benefit from exercising with a weight to which they have habituated, even if that weight would be sufficient to drive deposition in a novice weightlifter.

The mechanical stimulation experienced by a population of osteocytes (known as strain) is in part controlled by the strength and resistance of their surrounding bone. Relatively high load cause shape changes in the bone, which shifts fluid within the lacunar-canalicular system, stimulating osteocytes[134]. These osteocytes locally induce osteoblastogenesis and increased bone mass. After mineralization, the same level of load may no longer be sufficient to cause deflection of the thicker, more resistant bone, resulting in reduced strain perceived by osteocytes. Consistent lack strain leads to resorption and thinner, more easily deflectable bones that will become more responsive to a given load. This process of continual readjustment tunes bone to the changing needs of the organism[135].

Load above the homeostatic range activates osteoblastogenesis[136] and leads to the deposition of new bone; this range is known as the bone overload zone. Deposition does

not occur globally, however, and is generally proportional to the amount of experienced strain[137]. In contrast to mechanical loading, unloading or disuse refers to a significant loss of mechanical stimuli and may be the result of local immobilization after fracture[138] or paralysis[139], or may affect the total organism, as during bedrest[140] or microgravity[141]. Sustained unloading leads to an increase in osteoclast number and activity[142] and decreased osteoblastogenesis and deposition[143], resulting in resorption and a net loss of bone mass. For either strenuous activity or disuse, bone adapts to the loading environment to which it is routinely exposed.

When sufficient force is applied to bone it flexes, causing fluid within the lacunar-canalicular system to be displaced[144]. The passage of fluid over the surface of the osteocyte creates shear stress against the cell, while movement of the tethering proteins that link to the osteocyte to the bone extracellular matrix is thought to amplify the mechanical stimulation of the osteocyte[145]. Mechanical signals are transmitted into the osteocyte through factors such as force-gated ion channels like Piezo1[146] and TRPV4[31,32], which allow for rapid calcium influx, cytoskeletal deformation[31,147], and primary cilia[148], which engage a range of anabolic signaling elements in the local area, including nitric oxide[149], reactive oxygen[31], PGE2[150], IGF1[151], BMP-2[152] and WNTs[153]. Additionally, loading causes osteocytes to reduce expression of proteins, like sclerostin and DKK1. Ultimately, many of these signaling factors participate in the β-catenin pathway.

In response to mechanical loading, osteocytes seem to respond in a binary manner with respect to calcium influx[154], with each osteocyte in either a ‘loaded’ or ‘non-loaded’ state. One loading event does not stimulate every osteocyte, however; osteocytes in regions of bone experiencing the highest mechanical strain are more likely to be stimulated, and

osteocytes in low strain areas are less likely to be stimulated. The magnitude of the loading event can increase the percentage of osteocytes in a given anatomic region that go into the 'loaded' state, with strain frequency being the largest determinant of successful stimulation[155]. The type of force applied, like tensile, compressive, or stretch, can also influence the molecular response[156]. The overall distribution and number of these 'loaded' and 'non-loaded' osteocytes contributes to the tuning of local bone mass.

3.2 Molecular signals mediate the cellular effects of mechanical loading

3.2.1 Sclerostin

Sclerostin is a glycoprotein secreted by mature osteocytes that can signal to a variety of cells and tissues[157] and also control deposition and resorption through regulation of bone-resident cells. Disruptive variants or genetic knockout of the *Sost* gene that encodes sclerostin are sufficient to produce a phenotype characterized by excessive skeletal deposition in both humans[158] and mice[159].

An osteocyte in the lazy zone, or one experiencing disuse, will constitutively secrete sclerostin, signaling that bone formation is not needed. In response to mechanical loading and other bone anabolic cues, sclerostin protein is reduced and bone formation is unleashed.

When secreted by osteocytes, sclerostin suppresses osteoblast differentiation and promotes osteoclast number and activity[160]. Additionally, sclerostin may bind to osteoblasts, preventing their differentiation into osteocytes[161]. Sclerostin also functions as an endocrine signal, perhaps facilitating glucose and fatty acid availability for new bone

formation when sclerostin expression is low[162], but the direct effect of these processes on bone mass have yet to be fully clarified[163,164].

Sclerostin suppresses the ability of mesenchymal progenitor cells, pre-osteoblasts, and bone lining cells to differentiate into osteoblasts via inhibition of the β-catenin pathway[165]. Sclerostin binds to LRP5/6, where it acts as a competitive inhibitor of WNT family members[166], like WNT3 and WNT10[167]. Once sclerostin binds to LRP5/6, LRP5/6 cannot form a complex with Frizzled, and β-catenin becomes ubiquitinated and is degraded by the proteosome[168]. Other mechanically regulated inhibitors of WNT binding, like DKK1, have been shown to suppress osteoblast differentiation in a similar way[169].

In contrast, a decrease in sclerotin abundance allows WNT to bind with LRP5/6, disrupting the β-catenin destruction complex[170]. Stabilized β-catenin translocates to the nucleus where it acts to support Runx2 and Osx (osterix) expression, leading to osteoblast differentiation and the expression of osteoid-associated genes[171]. Thus, β-catenin signaling is fundamentally important to increased osteoblast number and subsequent matrix deposition.

In addition to bone formation, sclerostin may also regulate bone resorption. *In vitro*, treatment of osteocyte-like cells with exogenous sclerostin leads to increased RANKL expression[172]. Overall, when sclerostin levels are high, osteoblast differentiation and bone formation are inhibited, while osteoclast formation and bone resorption are elevated. High levels of sclerostin, as is typically seen with disuse, is net catabolic to bone.

Loss of sclerostin abundance following mechanical load supports a powerful switch from catabolic to anabolic signaling. Short bouts of axial loading within the high-physiological range *in vivo* are sufficient to cause a temporary loss of sclerostin and induce

osteoprotegerin (OPG) expression and an increase in bone mass in regions of high strain[30]. Sclerostin protein undergoes tight, spatial regulation in regions of greatest mechanical strain, depressing bone formation where load is highest and bone is most likely to fail if appropriate adaptation does not occur. (Figure 16). This strain-dependent loss of sclerostin has been demonstrated following fluid shear stress *in vitro* as well[88].

3.2.2 Nitric oxide

Along with many other anabolic signaling molecules, osteocytes release nitric oxide in response to fluid shear stimulation[149]. Nitric oxide is produced by three isoforms (*Nos1*, *Nos2*, and *Nos3*), which are expressed in a wide range of cell types[173], and is sufficient to drive the loss of sclerostin protein *in vitro*[29]. Global knockouts of the *Nos3* gene have been shown to result in decreased trabecular bone volume basally in adult mice, while *Nos2* knockout reduces bone mass recovery after tail suspension and reloading[174]. Interestingly, *Nos1* knockout produces increased murine bone mineral density in cortical and trabecular compartments[175] . While these isoforms convert the same substrates, they have diverse expression profiles, activators, and repressors, leading to disparate functions in bone. Nitric oxide has long been understood to play an intrinsic role in bone homeostasis, but the translational potential of nitric oxide for bone mass has not been clarified[176].

3.2.3 PGE2

Like nitric oxide, prostaglandin E2 (PGE2) is also widely expressed across diverse tissues[177], is produced by osteocytes in response to stimulation via pulsatile fluid flow[178],

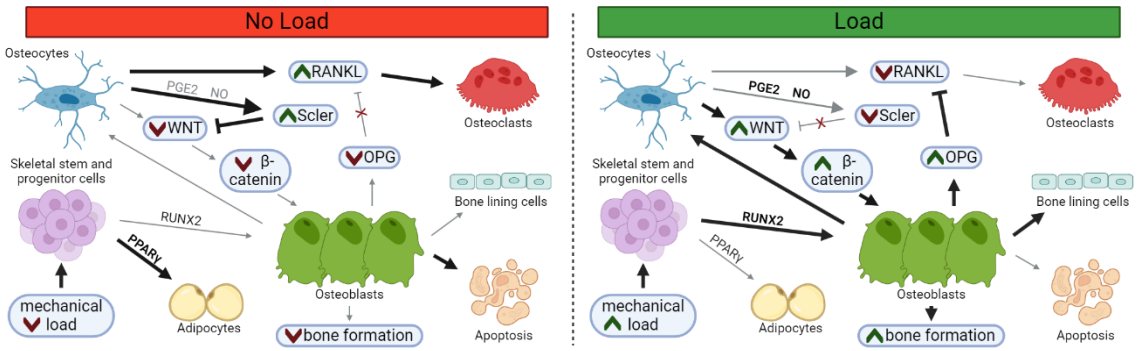

Figure 16. Loading Supports Osteoblast Differentiation and Suppresses Osteoclast Differentiation

In unloaded bone, sclerostin and RANKL expression is upregulated, supporting osteoclastogenesis and resorption. Following load, osteoblast and osteocyte differentiation increases, while osteoblast apoptosis and osteoclast differentiation decreases, leading to bone matrix deposition. Osteoblasts may embed and mature into osteocytes within the newly formed bone or may transition to quiescent bone lining cells on the newly formed bone surface. Bolded arrows and green chevrons indicate upregulated pathways, red chevrons indicate downregulated pathways.

Taken from: Buck HV, Stains JP. Osteocyte-mediated mechanical response controls osteoblast differentiation and function. *Front Physiol.* 2024;15:1364694.

and is sufficient to reduce sclerostin protein abundance *in vitro*[179]. PGE2 has been shown to support fracture healing[180] and bone formation[177], and to also support osteoclastogenesis *in vitro*[181]. Despite increasing both resorption and deposition, treatment with PGE2 appears to result in a net increase in bone mass, though persistent, systemic side effects have prevented it from being utilized as a clinical therapy for low bone mass[182].

3.2.4 WNT

Removal of β-catenin pathway inhibitors (e.g., sclerostin, DKK1) is insufficient to stimulate the pathway unless the cognate ligands are also present during anabolic signaling[183]. WNTs are canonical anabolic activators of the β-catenin pathway[184] and osteoblastic expression of WNT family genes increases after load[185]. Through WNT expression, additional osteoblasts may be recruited to support deposition following relatively high strain. WNT1 specifically has been demonstrated to be necessary for local anabolic bone response following axial loading[186].

3.2.5 OPG

In addition to stimulating new bone formation, mechanical loading can also inhibit bone resorption. One mechanism of bone mass control is the regulation of osteoprotegerin following anabolic stimuli. Osteoprotegerin (OPG) is a cytokine receptor that is expressed by osteoblasts that can locally moderate osteoclastogenesis[187]. It is not membrane-bound, but rather secreted into extracellular space[188] where it acts as a decoy RANKL receptor, preventing RANKL from stimulating osteoclastogenesis and resorption[189]. OPG

production increases following mechanical strain[190] and is typically detectable in circulation as well as within the bone environment[191].

Conceptually, OPG expression could spatially restrain demineralization in loaded bone and prevent loss of bone mass in specific high-strain regions where new bone is being formed, even during periods of calcium deficit. Biologically active OPG is kept close to the osteoblast membrane, rather than diffused away, through association with osteoblastic surface proteins[192], supporting OPG's role in local control. (Figure 17). OPG has also been shown to support osteoblastic differentiation *in vitro*, increasing both osteoblast number and upregulation of markers associated with osteoblast maturity, like ALP[193]

3.2.6 Embedded growth factors

The majority of organic bone matrix is comprised of type I collagen[194], but other components are embedded during deposition, including growth factors such as BMPs, TGF-β and IGF-I[195]. Injury to bone can accumulate in the form of microscopic cracks due to intense, repetitive loading[196], or can occur acutely, as in fracture. Disruption of the bone results in osteoclastic dissolution of mineralized tissue, releasing these latent osteoid-embedded growth factors into the local environment. These factors may now stimulate osteoprogenitor recruitment and proliferation, osteoblast differentiation, and local bone deposition[197] in order to restore and strengthen the bone.

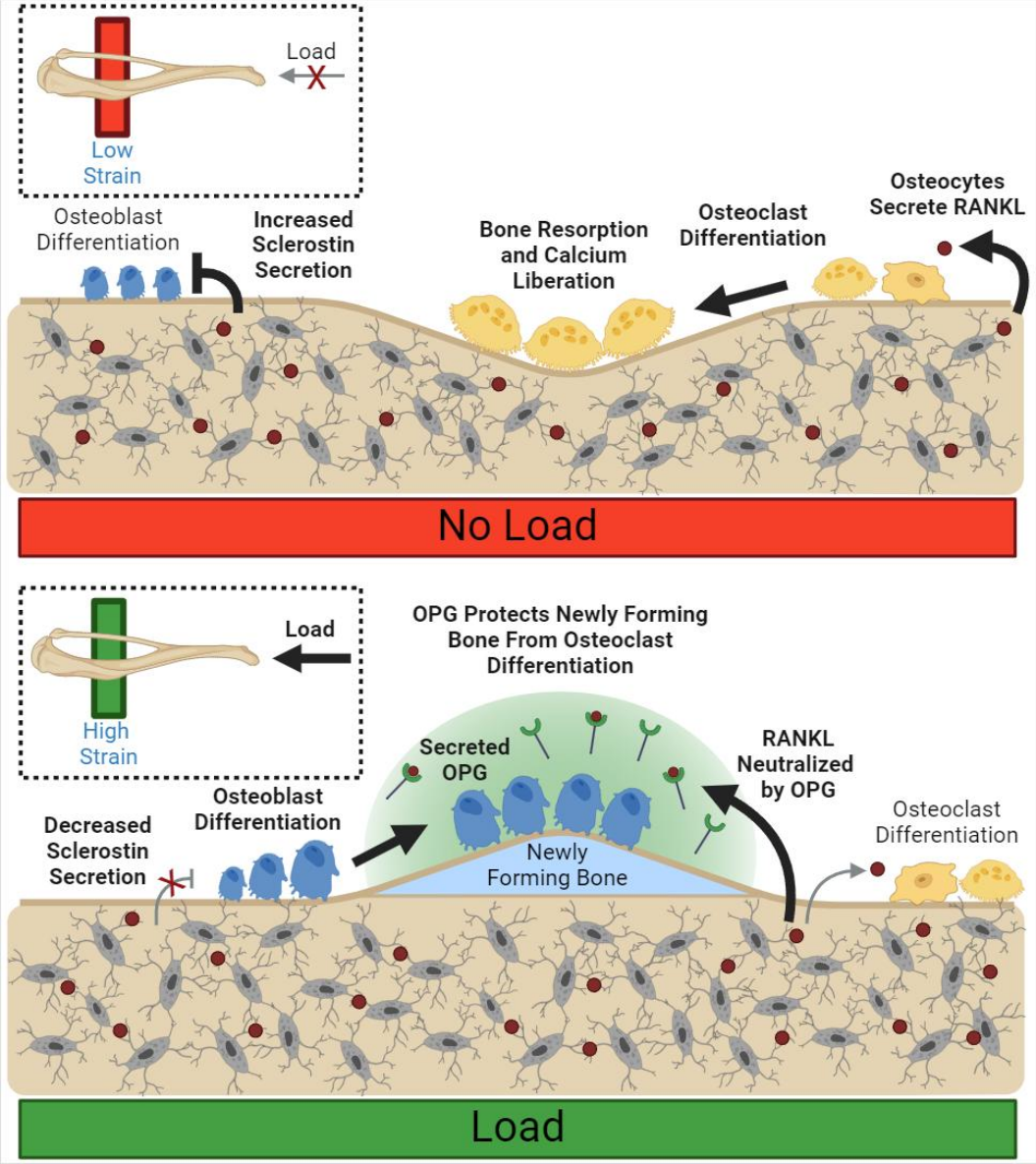

Figure 17. Load Spatially Controls Resorption and Deposition

Unloaded osteocytes secrete sclerostin, preventing osteoblast differentiation. Disinhibited RANKL expression allows for increased osteoclast differentiation and resorption. Load suppresses local sclerostin expression, allowing osteoblast differentiation. Local osteoclastic resorption and differentiation are downregulated through reduced RANKL availability. Bolded arrows indicate upregulated pathways for given conditions.

Taken from: Buck HV, Stains JP. Osteocyte-mediated mechanical response controls osteoblast differentiation and function. *Front Physiol*. 2024;15:1364694.

3.3 Discussion

Osteoporosis, a clinical designation of severe bone loss with greatly increased fracture risk, can result in hospitalization or death, especially in the elderly and frail[198]. There are several classes of clinically available treatments for low bone mass and osteoporosis, some of which effectively increase BMD by targeting the molecular mediators of mechanical loading. Anti-RANKL (denosumab), acts like an OPG mimetic to suppress osteoclastogenesis, and anti-sclerostin (romosozumab) antibody treatments reduce osteoclastogenesis and increase osteoblastogenesis.

Another class of treatment, teriparatide (PTH1-34) and abaloparatide (PTHrP) are synthetic analogs of parathyroid hormone, which has been shown to suppress sclerostin expression at the RNA[199,200] and protein[29,201] level. Parathyroid hormone-analog treatments are highly effective at preserving and restoring bone mass through an increase in osteoblast number and matrix deposition, due in part to β-catenin pathway upregulation[202].

The balance of deposition and resorption is necessary for skeletal health, but can be altered in individuals with mineral deficiency, leading to low bone mineral density (BMD) and associated disorders. For example, prolonged vitamin D deficiency can contribute to low bone mass and relatively high proportions of unmineralized osteoid[203], ultimately leading to rickets or osteomalacia if left untreated. Exercise, as well as dietary vitamin supplementation, have been shown to improve BMD in these patients[204].

Like many other tissues, the skeleton follows a ‘use it or lose it’ model, wherein continued disuse leads to a cycle of wasting, decreased capacity, and fragility, especially in aging[205], when the balance of deposition and resorption shifts towards net loss of

mineralized bone. Bone mass and osteoblast number decrease with age[206], but study after study[207–210] report the protective benefits of mechanical loading and exercise. Load increases expression of osteoblastogenesis-related signals, like WNTs and OPG, while suppressing availability of osteoclastogenesis-related signals like RANKL and high sclerostin expression, and continues to be the best defense against bone loss.

Chapter 4. Nitric Oxide Contributes to Rapid Sclerostin Protein Loss Following Mechanical Load

4.1 Introduction

Bone is an adaptable, mechano-responsive tissue, able to accommodate changes in load by removing, repairing, and accumulating bone according to mechanical strain[211]. This remodeling occurs through the coordination of bone resorption by osteoclasts and the deposition of new bone matrix by osteoblasts[212]. Control of these two processes is moderated by osteocytes, which receive mechanical input from experienced mechanical strain and covert it to the chemical signals that coordinate bone anabolism and catabolism[213] in a process termed 'mechano-transduction'. One of the primary effectors of osteocyte mechano-transduction is a secreted glycoprotein, sclerostin (gene name *Sost*). Sclerostin is a WNT/β-catenin antagonist[214] that suppresses osteoblastogenesis and matrix deposition[215]. In response to mechanical loading, sclerostin protein abundance is reduced via transcriptional[30] and post-translational[29,31,32] control, de-inhibiting Wnt/β-catenin signaling and unleashing osteoblast differentiation and new bone formation.

Nitric oxide (NO•) is a free radical signaling molecule that is produced by osteocytes in response to mechanical loading cues[149], which has a long-studied role in bone physiology[176]. NO• is produced by three synthases, neuronal (nNOS/*Nos1*), inducible (iNOS/*Nos2*), and endothelial (eNOS/*Nos3*), which are widely expressed throughout a variety of tissues, including bone[216,217]. Genetic deletion of two of the nitric oxide synthase genes (*Nos2* and *Nos3*) in bone cells reveals a role consistent with bone anabolism. *Nos3* knockout mice have low bone mass and decreased osteoblast activity[218,219]. Basally, the skeletal phenotype of adult *Nos2* knockout mice is no different than control mice. However,

reloading of *Nos2*$^{-/-}$ mice after tail suspension exposes a less robust response to reloading relative to control, with decreased bone mass and osteoblast activity[174]. Additionally, there are defects in the mineralization capacity of primary osteoblasts isolated from these *Nos2* deleted mice after unloading[174]. In contrast to *Nos2* and *Nos3*, *Nos1* knockout mice have increased bone mass, suggesting a distinct role in bone physiology[175].

The molecular basis for NO•'s influence on bone-resident cells is not entirely clear, although its effects on osteoblast proliferation or differentiation[173], cell survival effects in osteocytes[220], and osteoblast glycolysis[221] have been reported. Previously, we described a signal transduction pathway regulating the post-translational control of sclerostin[29,31,32]. Among the findings of this paper was evidence that NO• also may influence sclerostin protein abundance. Here, we investigate the role that NO• plays within this pathway in osteocytes and tie NO• to the post-translational control of a fundamentally important effector of bone formation, sclerostin.

4.2 Results

4.2.1 Nitric oxide is necessary for sclerostin protein control

We recently described a mechanical transduction pathway that controls lysosomal degradation of sclerostin protein following mechanical stimulation, thereby coordinating later bone anabolism[29,31,32]. We demonstrated that mechanical stimulation of osteocytes *in vivo* or *in vitro* caused NOX2-dependent generation of reactive oxygen species, resulting in the activation of TRPV4 Ca^{2+} channels and an increase in intracellular calcium. This increase in calcium stimulates activation of CaMKII, leading to the minute-scale degradation of sclerostin by the lysosome.

NO• is a signaling compound capable of supporting multiple protein modifications and is rapidly produced by osteocytes following mechanical stimulation[149]. NO• production and its interaction with CaMKII is commonly studied in cardiac and neuronal systems but less is known about the relationship of NOS and CaMKII in bone.

To determine the potential role of NO• in the control of sclerostin protein abundance, Ocy454 osteocyte-like cells were transfected with myc-tagged *Sost* plasmid (mycSost) and treated with vehicle or the non-specific NOS inhibitor LNAME prior to mechanical stimulation. Following exposure to FSS via pulsatile flow, vehicle treated cells exhibited an ~40% reduction in sclerostin protein abundance (Figure 18A). In contrast, treatment with LNAME fully blocked the effects of FSS on sclerostin protein abundance. These data indicate that NO• production is required for the loss of sclerostin protein following mechanical stimulation.

Osteocytes have been shown to express eNOS[222,223], but the relative abundance of nNOS (gene: *Nos1*), iNOS (*Nos2),* or eNOS (*Nos3)* isoforms in Ocy454 cells has not been reported. Consistent with primary osteocytes, *Nos3* was found to have higher expression than *Nos1* or *Nos2*, as indicated via RT-qPCR (Figure 18B).

Next, Ocy454 cells were transfected with scramble or isoform-specific siRNA before exposure to FSS. Western blots of Ocy454 cell homogenates confirmed reduced expression of respective NOS isoform protein after isoform-specific siRNA transfection (Figure 18C). Following mechanical stimulation, scramble siRNA transfected cells exhibited the expected fluid shear stress-dependent decrease in sclerostin protein abundance (Figure 18D). Knockdown of eNOS inhibited the loss of sclerostin protein.

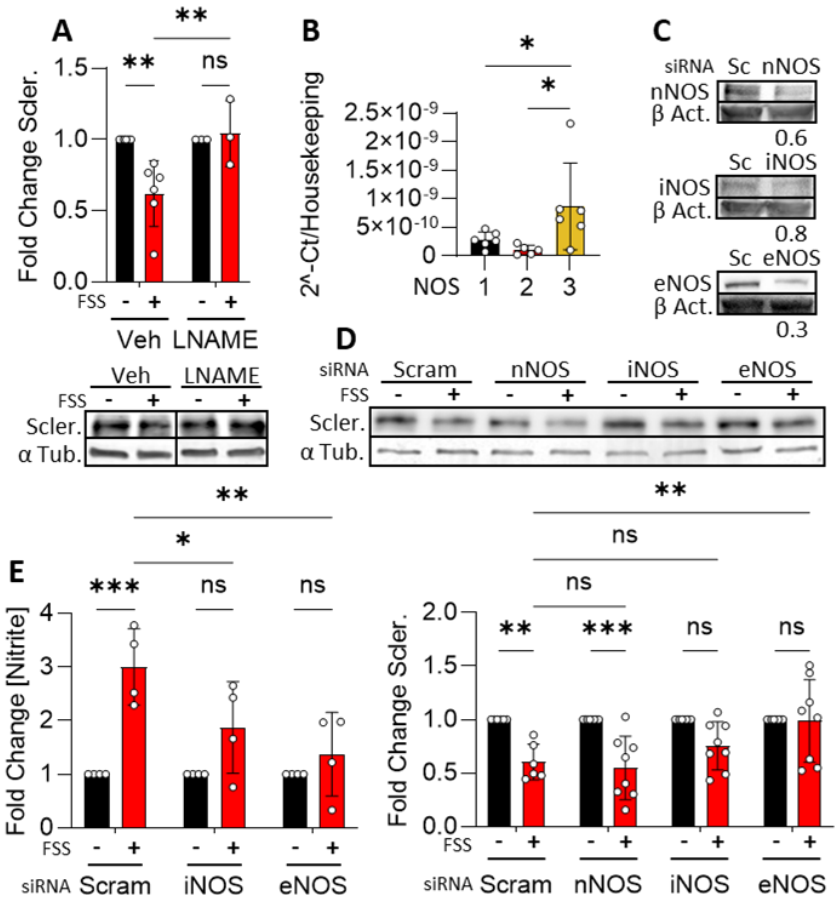

Figure 18. Nitric Oxide is Necessary for Sclerostin Protein Control

(A) Fold change in relative sclerostin protein abundance in mycSost-transfected Ocy454 cells following pretreatment with vehicle or L-NAME (1mM, 30min), and no-flow control or fluid shear stress (FSS) at 38ml/min (7 dynes/cm^2, 5min), samples collected 10m after FSS, with representative blots for sclerostin and alpha tubulin. **(B)** Relative gene expression of individual nitric oxide synthase (NOS) isoforms in Ocy454 cells. **(C)** Relative abundance of individual NOS isoform protein in Ocy454 cells transfected with scramble (Sc) or specified isoform siRNA. Number represents fold change in protein abundance of knockdown relative to control, as normalized to beta actin. **(D)** Fold change in relative sclerostin protein abundance in Ocy454 cells with mycSost and specified siRNA transfections following respective no-flow control or FSS, collected 5m after FSS, with representative blots for sclerostin and alpha tubulin. **(E)** Fold change in relative nitrite production in Ocy454 cells with mycSost and specified siRNA transfections following respective no-flow control or FSS, collected immediately after FSS.

Taken from: Buck HV, Torre OM, Leser JM, Gould NR, Ward CW, Stains JP. Nitric oxide contributes to rapid sclerostin protein loss following mechanical load. *Biochem Biophys Res Commun.* 2024;727:150315.

siRNA knockdown of iNOS appears to blunt the loss of sclerostin after FSS. This partial inhibition could be due to the lower efficacy of the iNOS knockdown relative to eNOS knockdown (Figure 18C), or potentially due to lesser participation of iNOS-derived NO• in anabolic sclerostin control. In contrast, knockdown of nNOS had no effect on sclerostin protein loss after FSS (Figure 18D), despite robust knockdown of nNOS protein (Figure 18C). Neither plasmid nor siRNA transfection significantly altered cell viability (Figure 19).

As nNOS knockdown did not prevent the loss of sclerostin after FSS (Figure 18D) and because global knockout of nNOS is mice results in increased bone mass, we chose to focus on the role of eNOS- and iNOS-derived NO•. eNOS or iNOS knockdown cells were exposed to FSS, with samples collected at a timepoint suitable for nitrite analysis as a proxy for NO• production. After exposure to FSS, scramble siRNA transfected cells demonstrated a significant increase in nitrite concentration, while eNOS and iNOS siRNA transfected cells did not (Figure 18E). In total, these data support that NO• production in response to fluid shear stress occurs via eNOS and iNOS, and the resultant NO• is required for loss of sclerostin protein abundance.

4.2.1 NO• production is downstream of CaMKII

To determine whether NO• production falls within this previously reported mechanical response pathway that regulates sclerostin degradation (Figure 20A), various components of this pathway were inhibited prior to mechanical stimulation. Following pre-treatment with apocynin (NOX inhibitor), or GSK219 (TRPV4 channel inhibitor), nitrite production was not increased by mechanical stimulation, as compared to vehicle treated

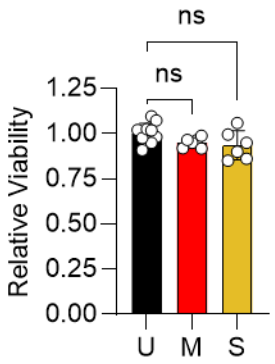

Figure 19. Cell Viability Was Not Significantly Altered by Transfection

Relative viability of mycSOST plasmid (M) (0.125µg/40,000 cells) or scramble siRNA (S) (10pmol/40,000 cells) transfected cells, normalized to untransfected cells (U).

Taken from: Buck HV, Torre OM, Leser JM, Gould NR, Ward CW, Stains JP. Nitric oxide contributes to rapid sclerostin protein loss following mechanical load. *Biochem Biophys Res Commun.* 2024;727:150315.

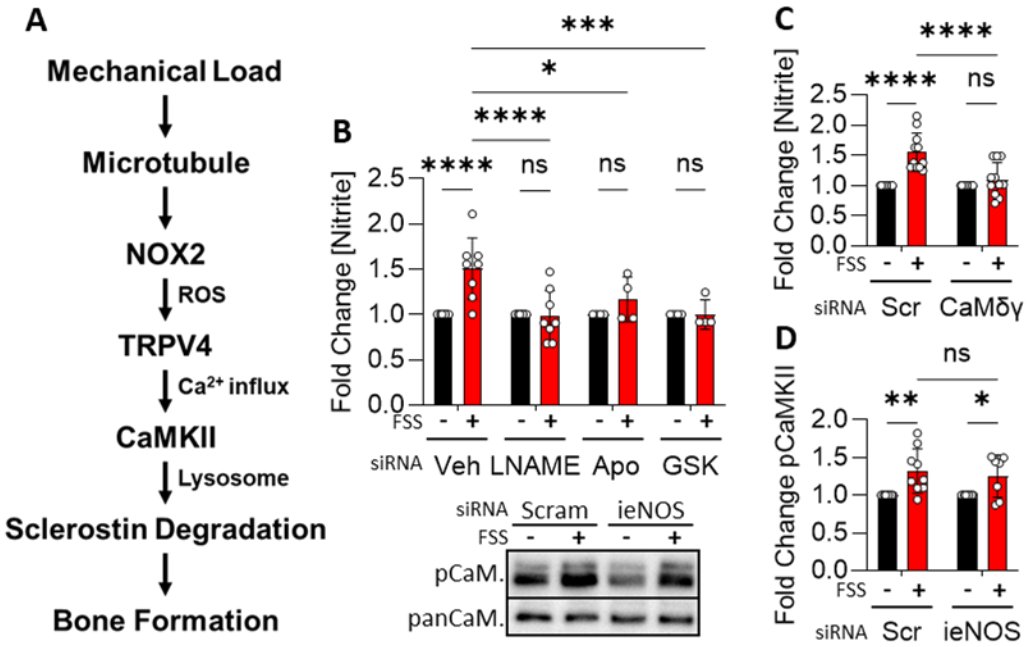

Figure 20. NO Production is Downstream of CaMKII

(A) Representation of 'Mechano-Pathway,' a mechanical-response pathway in osteocytes. **(B)** Fold change in nitrite production in Ocy454 cells treated with vehicle, LNAME (1mM, 30min), Apocynin (500µM, 1hr), or GSK219 (15µM, 10min) following no-flow control or fluid-shear stress (FSS) at 35ml/min (4 dynes/cm^2, 5min), collected immediately after FSS. **(C)** Fold change in nitrite production in Ocy454 cells with scrambled (Scr) or CaMKIIδ/γ (CaMδγ) siRNA transfection following respective no-flow control or FSS, collected immediately after FSS. **(D)** Fold change in relative CaMKII activation (phosphorylation at T286) in Ocy454 cells with scrambled (Scr) or i/eNOS (ieNOS) siRNA transfection following no-flow control or FSS, collected within 1m of FSS, with representative blots for phospho-CaMKII and panCaMKII.

Taken from: Buck HV, Torre OM, Leser JM, Gould NR, Ward CW, Stains JP. Nitric oxide contributes to rapid sclerostin protein loss following mechanical load. *Biochem Biophys Res Commun.* 2024;727:150315.

samples (Figure 20B). Apocynin is not fully specific to NOX2 (NADPH oxidase enzyme) inhibition, but inhibition of TRPV4 channels, which allow Ca^{2+} influx after NOX2 activation[87], also prevented significant NO• production. FSS of vehicle treated cells or LNAME (non-specific NOS inhibitor) served as positive and negative controls, respectively. These data suggest NO• production in response to fluid shear stress occurs downstream of TRPV4-dependent Ca^{2+} influx.

Next, we examined the calcium signaling integrator CaMKII as it relates to NO• production. CaMKII activation is required for the loss of sclerostin protein following multiple bone anabolic signals, including fluid shear stress[29,31,32] and parathyroid hormone[29]. Of the four CaMKII isoforms, CaMKIIδ and CaMKIIγ are primarily expressed in osteocytes[94]. These isoforms function redundantly[91], so Ocy454 cells were co-transfected with CaMKIIδ- (*Camk2d*) and CaMKIIγ- (*Camk2g*) targeted siRNA prior to mechanical stimulation. Scramble transfected samples demonstrated a significant increase in nitrite production following FSS, but co-knockdown of CaMKIIδ/γ in siRNA-transfected cells inhibited the production of NO• (Figure 20C); further indicating that NO• production falls within this pathway, subsequent to CaMKII. As siRNA transfection against both eNOS and iNOS prevented nitrite production following FSS (Figure 19E), we co-transfected Ocy454 cells with siRNA against eNOS and iNOS to maximally suppress NO• production. Co-transfection with eNOS and iNOS siRNA (ieNOS) prior to FSS did not blunt the activation of CaMKII, as measured via phosphorylation of site T286 (Figure 20D), further supporting that NO• production occurs downstream of CaMKII activation.

4.2.2 Nitric oxide donation alters protein abundance within minutes

We have demonstrated above the physiological role that NO• plays in sclerostin-mediated anabolic signaling following FSS, but wanted to further investigate the ability of NO• to effect elements of this signaling pathway independent of mechanical stimulation. Thus, we exposed cells to NONOate, a pharmacological NO• donor. Activation of CaMKII, as determined by phosphorylation at site T286, was increased following one minute of treatment with NONOate, compared to samples collected immediately after treatment (Figure 21A). Sclerostin protein abundance was also significantly decreased after 5min of NONOate treatment (Figure 21B). This effect was also observed in *ex vivo* bone samples. Isolated and flushed control murine long bones exhibited a ~47% reduction in sclerostin protein abundance following 15min of NONOate treatment (Figure 21C). In contrast, the response to NONOate was fully abrogated in CaMKIIδ/γ double conditional knockout (dCKO) murine long bones, although a lower abundance of sclerostin is found in CaMKIIδ/γ dCKO long bones in the untreated state. These data suggest that while CaMKII is required for NO• production, NO• may also modulate CaMKII to direct sclerostin protein loss in response to FSS.

As short-term, minute-scale changes to sclerostin protein abundance were observed, changes to *Sost* gene expression were also quantified. Two, four, or 24 hours after NONOate treatment, no significant changes in *Sost* gene expression were detectable via RT-qPCR, relative to vehicle treated controls (Figure 21D). These data suggest that protein expression changes following NO• exposure occur post-translationally, rather than at the level of gene expression, consistent with our prior observations[29,31,32].

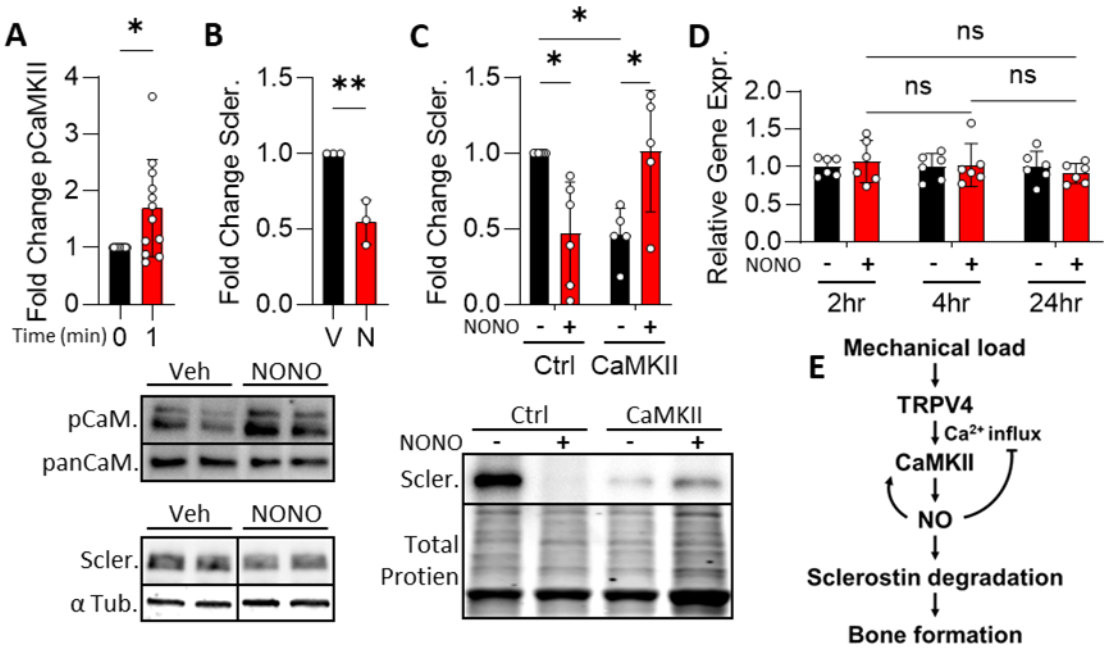

Figure 21. Nitric Oxide Donation Alters Protein Abundance Within Minutes

(A) Fold change in relative CaMKII activation (phosphorylation at T286) in mycSost transfected Ocy454 cells with NONOate (10µM), sample collection immediately (0) or 1 minute (1) after treatment, with representative blots for phospho-CaMKII and panCaMKII. **(B)** Fold change in relative sclerostin protein abundance in mycSost transfected Ocy454 cells following treatment with vehicle or NONOate (10µM, 5min), with representative blots for sclerostin and alpha tubulin. **C)** Fold change in relative sclerostin protein abundance following treatment with vehicle or NONOate (NONO) (10µM, 15min) in *ex vivo* CaMKIIδ/γ double conditional knockout (CaMKII) or littermate control (Ctrl) long bone homogenate, with representative blots for sclerostin and total protein. Bones were flushed of marrow and flash frozen before homogenization. **(D)** Fold change in relative *Sost* gene expression in Ocy454 cells following vehicle or NONOate treatment. Samples were collected post treatment at indicated time points. **(E)** Representation of NO's role with mechano-response pathway.

Taken from: Buck HV, Torre OM, Leser JM, Gould NR, Ward CW, Stains JP. Nitric oxide contributes to rapid sclerostin protein loss following mechanical load. *Biochem Biophys Res Commun.* 2024;727:150315.

Previously published data[29], in conjunction with the data presented here, suggest that NO• production does indeed fall within this mechanical response pathway, and that NO• has the ability to support the modulation of calcium influx (Figure 22) and CaMKII activation to regulate sclerostin degradation and, ultimately, bone formation (Figure 21E).

4.2.3 Inhibition of nitric oxide alters calcium response with FSS

To further clarify the interaction between calcium and NO production, live-cell calcium imaging was used. Ocy454 cells were pretreated with vehicle or LNAME (non-specific NOS inhibitor), and the calcium dye Fluo-4. Imaging was performed and average fluorescent intensity was measured before, during, and after mechanical stimulation. (Figure 21A-D). Vehicle and LNAME treated samples showed no difference in the average percent of cells that responded to FSS, as indicated by a $\Delta F/F > 1.5$ (Figure 21B) and no difference in the average maximum $\Delta F/F$ fold change in signal intensity (Figure 21C). The time required for samples to achieve 80% of their average maximal $\Delta F/F$ was different however, with LNAME-treated cells reaching their upper range of response an average of 19.75s earlier than vehicle treated samples (Figure 21D). The lack of difference in average magnitude or responding cells, coupled with the difference in response speed, indicate that NO may assist in the tuning of the mechano-induced calcium response, perhaps as negative feedback, but is not obligated for the calcium response following FSS.

NO donation was also used during live calcium imaging with Fluo-4. There was no difference in the average calcium response in vehicle or NONOate treated samples (Figure 21E), indicating that NO alone is not sufficient to initiate an influx of calcium.

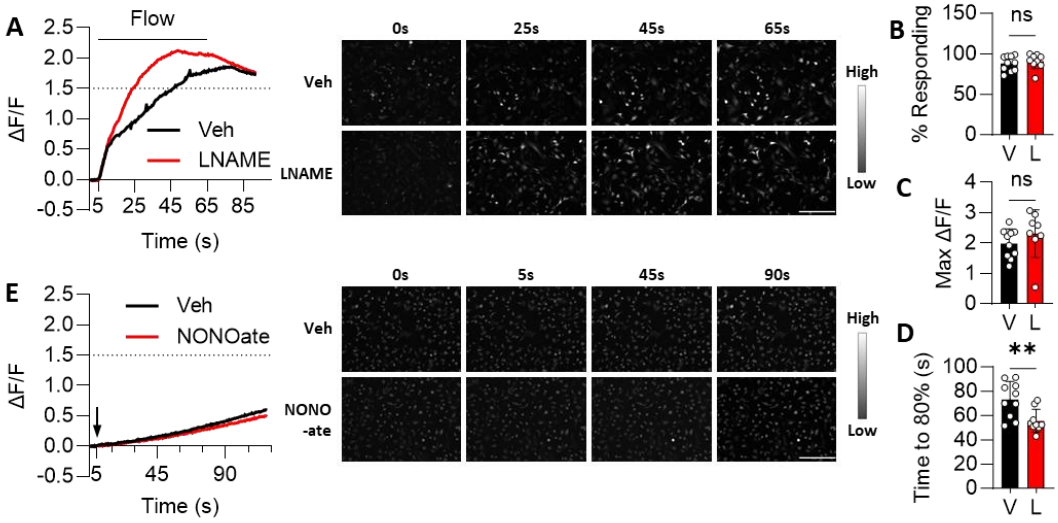

Figure 22. Inhibition of Nitric Oxide Alters Calcium Response with FSS

(A) Ca^{2+} responses (Fluo-4, 5µM, 30min) of Ocy454 cells treated with vehicle (V) or LNAME (L) (1mM, 45min) and fluid-shear stress at 35ml/min (4 dynes/cm^2, 1min). Fold change in signal intensity normalized to baseline (pre-FSS). FSS initiated at 5s. Average traces represent 3 independent experiments of >200 cells each. Images taken every 500ms. Dashed line represents threshold ΔF/F for responding cells. Representative images, scale bar=200µm. **(B)** Percent of cells with ΔF/F greater than 1.5-fold, normalized to baseline. **(C)** Average maximum ΔF/F, normalized to baseline. **(D)** Average elapsed time (s) for samples to reach 80% of respective maximum intensity. Figures A-D were generated from the same experiment. Data points represent samples of 50-100 cells each (B-D). **(E)** Ca^{2+} responses (Fluo-4, 5µM, 30min) of Ocy454 cells treated with vehicle or NONOate (10µM). Fold change in signal intensity normalized to baseline (pre-treatment). Treatments dispensed at 5s. Average traces represent N=3 of 100 cells each. Images taken every 500ms. Dashed line represents threshold ΔF/F for responding cells. Representative images, scale bar=200µm.

Taken from: Buck HV, Torre OM, Leser JM, Gould NR, Ward CW, Stains JP. Nitric oxide contributes to rapid sclerostin protein loss following mechanical load. *Biochem Biophys Res Commun.* 2024;727:150315.

4.3 Discussion

Here, we demonstrated that NO• production participates in a mechano-transduction pathway controlling sclerostin protein abundance. Hierarchically, our data support that mechanical stimulation leads to calcium influx and activation of CaMKII[31,32] prior to the production of NO• by osteocytes, and that NO• is required for the minute-scale loss of sclerostin protein following fluid shear stress[29]. Exogenous NO•, via NONOate, was sufficient to rapidly decrease sclerostin protein. While we have shown that activated CaMKII is necessary for NO• production, NO• also appears to feedback to tune CaMKII activation. Regulation of CaMKII activity by NO• has been described in other cell systems[224–227], and can occur via nitrosylation at Cys280/289 or by increased auto-phosphorylation at Thr286[228]. NO•'s ability to suppress TRPV4-mediated calcium influx via negative feedback has been demonstrated in other tissues[229,230], consistent with our findings that NO• appears to tune calcium influx following mechanical stimulation (Figure 21).

We demonstrated that Ocy454 osteocyte-like cells express all three NOS isoforms, and that eNOS is the most relevant to sclerostin protein control, although iNOS also may contribute to NO• production and sclerostin protein loss. Our siRNA transfection knockdown of *NOS2*/iNOS was less effective than *NOS1*/nNOS or *NOS3*/eNOS knockdown, which could contribute to the downward trending, but not significant, loss of sclerostin expression with iNOS knockdown in Figure 17D. These findings are in concordance with previous *in vivo* studies, where eNOS isoform-specific knockout mice were deficient in bone volume and deposition[218,219], while adult iNOS knockout mice have no significant basal bone phenotype, but are resistant to bone deposition after re-loading[174].

Our *in vitro* data indicate that nNOS does not appear to be involved in the loss of sclerostin protein following FSS, which is distinct from the roles of iNOS and eNOS and consistent with *in vivo* data demonstrating that nNOS deletion leads to high bone mass in mice[175].

These data reveal an important mechanism through which NO• can influence bone formation, beyond control of osteoblast mineralization. While these data were generated primarily *in vitro* in Ocy454 osteocyte-like cells, they align with many other observations both *in vitro* and *in vivo*. As sclerostin is a β-catenin pathway inhibitor that suppresses osteoblast differentiation, our findings agree with previous research, which has demonstrated that NO• donation supports both increased β-catenin signaling[231] and osteoblast differentiation[221]. Additionally, Ocy454 cells have been shown to express many mature murine osteocyte markers and be broadly representative of primary osteocytes[89,232,233], but like any cell line, they are not identical to *in situ* primary cells.

These findings are significant because there are many clinically available treatments for osteoporosis, but very few that target osteoblast function[234]. *In vitro* and *ex vivo* NO• donation is sufficient to stimulate decreased sclerostin protein abundance, which supports osteoblastogenesis and matrix deposition. NO• donation may yet be a promising area of investigation into the prevention or adjuvant treatment of osteoporosis[176].

Chapter 5. Single-Gene CaMKIIγ or CaMKIIδ Conditional Deletion in Osteoblast-Lineage Cells Does Not Recapitulate Severe Skeletal Phenotype of CaMKIIγ/δ Double Conditional Deletion

5.1 Introduction

CaMKII, or calcium/calmodulin-dependent protein kinase II, is a calcium-responsive enzyme that acts to phosphorylate a range of proteins to modulate their activity[235]. CaMKII is expressed in most cell types and while it is commonly studied in neuronal[236] and cardiac[237] tissues, much less is known about its roll in osteocytes and bone anabolism.

CaMKII is inactive, with its catalytic site hidden, during periods of low intracellular calcium. An increased concentration of calcium allows calmodulin to bind to calcium. This calcium-bound calmodulin may now bind to CaMKII. Once bound to calcium and calmodulin, CaMKII auto-phosphorylates at site T286. While intracellular calcium remains high and CaMKII is phosphorylated it will maintain maximal activity. Decreasing calcium concentrations cause disassociation of calmodulin from CaMKII, leaving CaMKII with reduced kinase activity. CaMKII is returned to its inactive state through de-phosphorylation of site T286.

Following sufficient mechanical stimulation, osteocytes control their expression of sclerostin[29–31,33], a potent catabolic hormone that suppresses osteoblast differentiation and bone deposition. We have demonstrated that CaMKII is activated as part of the same mechano-response pathway that controls sclerostin expression[29,31,33] and that inhibition of CaMKII activation prevents osteocytes from appropriately controlling their sclerostin protein abundance[31].

There are four isoforms of CaMKII, CaMKIIα, CaMKIIβ, CaMKIIγ, and CaMKIIδ. These isoforms are produced by four distinct but highly-conserved genes, and vary in relative expression by cell type. We previously demonstrated that only CaMKIIγ and CaMKIIδ are detectably expressed in primary osteocytes[94]. It has been shown *in vivo* in cardiac tissues that CaMKIIγ or CaMKIIδ may serve overlapping functions[91]. Based on this knowledge, we produced a strain of mice utilizing the osteocalcin (OCN) Cre to conditionally delete CaMKIIγ and CaMKIIδ in osteocytes and mature osteoblasts to fully prevent CaMKII expression in these bone-resident cells and better understand the role that CaMKII plays in bone. These OCN Cre/*Camk2d*$^{flox/flox}$/*Camk2g*$^{flox/flox}$ mice, (referred to as Camk2delta/gamma double cKO), express a profound phenotype of low bone mass and extreme skeletal fragility[94], with FGF23 overexpression, hypophosphatemia, and deficient osteoid mineralization.

Due to the severity of the skeletal phenotype of the Camk2delta/gamma double cKO mice, we have since developed independent strains of mice with conditional deletion of Camk2delta or Camk2gamma to determine whether these isoforms might serve redundant or distinct functions in bone, and to determine whether loss of either isoform recapitulates the phenotype expressed through double conditional deletion.

5.2 Results

5.2.1 General body characteristics are not altered in cre-positive mice

Three strains of mice were generated using the Osteocalcin (*Bglap*) Cre driver (OCN), OCN Cre/*Camk2d*$^{flox/flox}$/*Camk2g*$^{flox/flox}$ (Camk2 double cKO), OCN

Cre/*Camk2d*$^{flox/flox}$ (Camk2 delta cKO), and OCN Cre/*Camk2g*$^{flox/flox}$ (Camk2gamma cKO). Cre negative pups were used as littermate controls for each strain.

We originally determined that the Camk2 double cKO phenotype was emerging by 3 weeks of age, and fully established by 8 weeks[94], so 8 weeks was utilized as the primary timepoint during this study. Body mass and nose-to-tail-base length were measured post-euthanasia, and while there were small differences between the floxed control groups of some of the strains, there were no differences between Cre positive and Cre negative groups of the same strain (Figure 23A-D).

5.2.2 Bone volume loss in single cKOs is not additive to loss in double cKO

Micro-computed tomography (μCt) was utilized to determine differences in bone microarchitecture in the L5 vertebrae (axial skeleton) and the distal femur (appendicular skeleton). We found that conditional deletion of either Camk2delta or Camk2gamma isoform alone did not result in any statistical decrease in trabecular bone volume fraction (BV/TV) of the L5 vertebrae and did not approximate the extreme decrease in L5 vertebral BV/TV observed in double cKO mice (Figure 24A, B). Additionally, the mean percent change of the two single cKOs, when added together, still did not reach the magnitude of the percent change in the double cKO. For example, there was a -75% mean change in BV/TV in female double cKO mice relative to their controls ($p=0.0007$), but only a -16% change in delta cKO ($p=0.2199$) and a -1% change in gamma cKO mice ($p=0.9945$), relative to their respective controls, which may indicate that the Camk2 delta and gamma isoforms serve redundant functions or that osteocytes may compensate for the loss of one isoform through increased expression of the other.

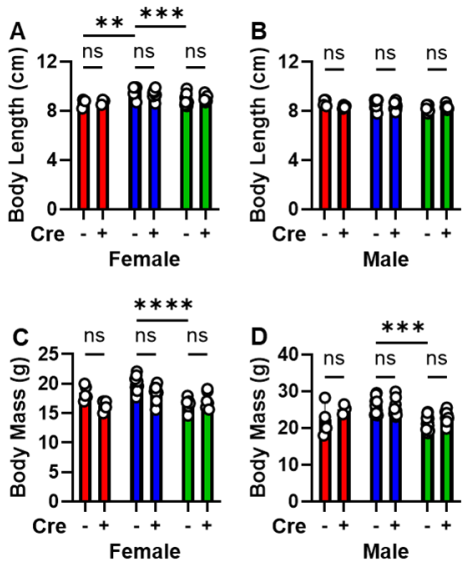

Figure 23. Conditional Knockout Does Not Alter Body Length or Mass

(A) Body length (nose to base of tail) and **(B)** mass are not altered within a given Cre+ conditional knockout strain, relative to their littermate controls, though there are significant differences between some colonies. Red = Camk2delta/gamma double cKO; blue = Camk2 delta cKO; green = Camk2gamma cKO.

Taken from: Taken from: Buck HV, Leser JM, Chatree S, Murray PM, Stains JP. Single-Gene CaMKIIγ or CaMKIIδ Conditional Deletion in Osteoblast-Lineage Cells Does Not Recapitulate Severe Skeletal Phenotype of CaMKIIγ/δ Double Conditional Deletion. [Manuscript in preparation].

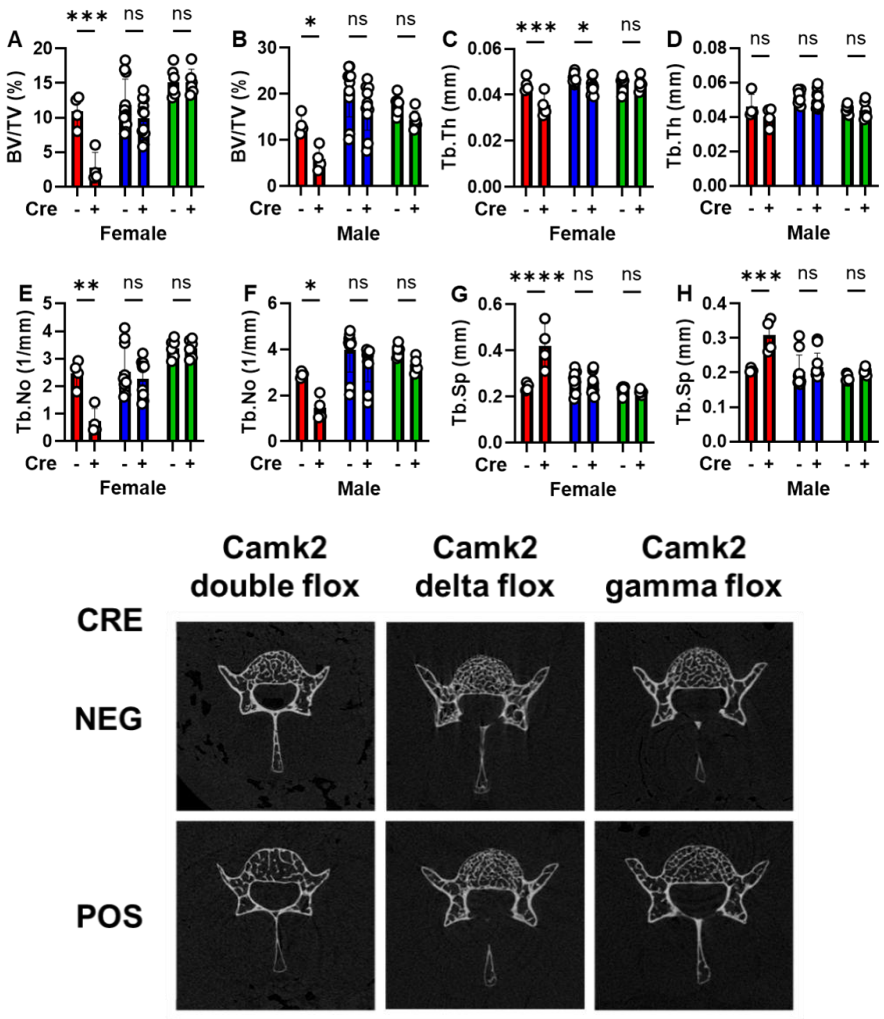

Figure 24. Bone Volume Reduction in the L5 Vertebra is Less Severe in Camk2delta or Camk2gamma cKO Mice

(A, B) Trabecular bone volume in the L5 vertebra is greatly reduced among Camk2delta/gamma double cKO mice (Camk2double cKO), relative to littermate controls, while no significant difference is seen in Camk2delta (Camk2d) or Camk2gamma (Camk2g) cKO mice, relative to respective littermate controls. **(C)** Trabecular thickness is decreased in female Camk2double and Camk2d cKO mice, **(D)** but not in males. **(E, F)** Trabecular number was decreased in Camk2double cKO mice, relative to controls, and **(G, H)** trabecular spacing was increased. Representative images from male mice. Male representative images shown. Red = Camk2double cKO; blue = Camk2delta cKO; green = Camk2gamma cKO.

Taken from: Taken from: Buck HV, Leser JM, Chatree S, Murray PM, Stains JP. Single-Gene CaMKIIγ or CaMKIIδ Conditional Deletion in Osteoblast-Lineage Cells Does Not Recapitulate Severe Skeletal Phenotype of CaMKIIγ/δ Double Conditional Deletion. [Manuscript in preparation].

Trabecular thickness was significantly decreased in the L5 vertebrae of female delta cKO mice relative to controls, but at a smaller percent change than double cKO females (Figure 24C), while no significant differences in the L5 vertebrae trabecular thickness were observed in female gamma cKO mice or any strain of male mice, relative to controls (Figure 24D). Trabecular thickness and spacing were decreased in both male and female double cKO mice, but not in delta or gamma cKO in the L5 vertebrae (Figure 24E-H).

Similar trends were observed in the trabecular compartment of the distal femur, where loss of bone volume among either single knockout mice again was neither statistically different from controls, nor did it approximate the magnitude of loss experienced by the double knockout mice. Indeed, BV/TV and trabecular number and spacing were all significantly decreased in both sexes in double cKO mice, but no significant differences were observed in delta or gamma cKO mice (Figure 25A-D, G, H). No differences in trabecular thickness amongst any group were detected (Figure 25E, F).

Micro-computed tomography of the cortical bone of the mid-diaphyseal femur revealed slight differences between the Camk2 delta and Camk2gamma cKO mice. While Camk2delta/gamma double cKO mice expressed relatively large reductions in cortical parameters (Figure 26A-C, E-G), no cortical phenotype was observed in Camk2gamma cKO mice (Figure 26A-H) and a only subtle loss of cortical bone in female Camk2delta cKO mice was observed (Figure 26A, C).

Estimated resistance to force (polar, maximum, and minimum moments of inertia) were also calculated based on cortical volume and geometry. No difference was observed in Camk2gamma cKO females, while female Camk2double cKO and female Camk2delta cKO mice were significantly decreased across all three parameters, though the magnitude

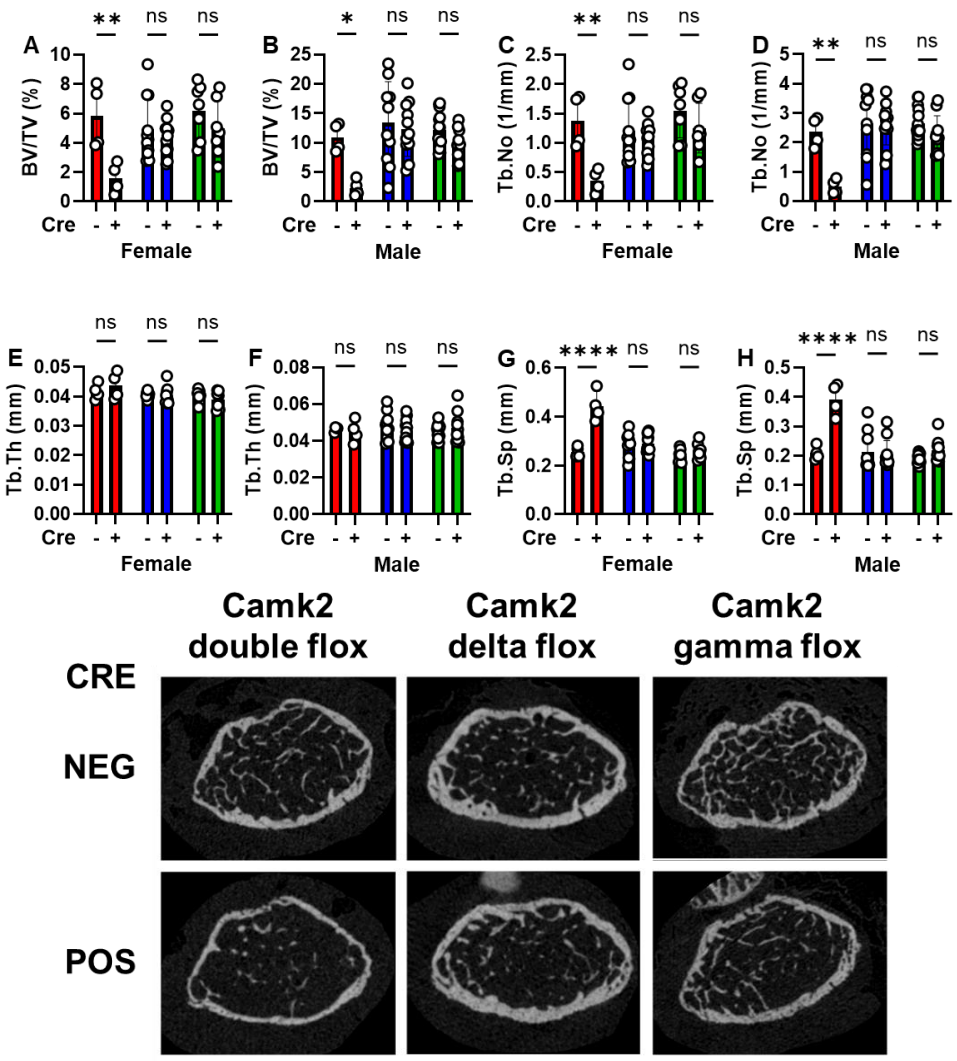

Figure 25. Bone Volume Reduction in the Distal Femur is Less Severe in Camk2delta or Camk2gamma cKO Mice

(A, B) Trabecular bone volume and **(C, D)** number are reduced, and **(G, H)** spacing is increased in the distal femur among Camk2delta/gamma double cKO mice (Camk2double cKO), relative to littermate controls, while no significant difference is seen in Camk2delta (Camk2d) or Camk2gamma (Camk2g) cKO mice, relative to respective littermate controls. **(E, F)** No differences were observed in trabecular thickness. Male representative images shown. Red = Camk2delta/gamma double cKO; blue = Camk2 delta cKO; green = Camk2gamma cKO.

Taken from: Taken from: Buck HV, Leser JM, Chatree S, Murray PM, Stains JP. Single-Gene CaMKIIγ or CaMKIIδ Conditional Deletion in Osteoblast-Lineage Cells Does Not Recapitulate Severe Skeletal Phenotype of CaMKIIγ/δ Double Conditional Deletion. [Manuscript in preparation].

Figure 26 continued on next page
(A, C) Cortical area and cross-sectional thickness were reduced in female Camk2double and Camk2delta cKO mice. **(B)** Cortical area was reduced in male Camk2double cKO mice, while **(D)** cross-sectional thickness was not altered in any strain of male mice. **(E, F)** Periosteal perimeter was reduced in both sexes, and **(G)** endocortical perimeter was reduced in female but **(H)** not male Camk2double cKO mice. **(I)** polarMMI, **(K)** iMAX, and **(M)** iMIN were reduced in females but not **(J, L, N)** males. Male representative images shown. Red = Camk2delta/gamma double cKO; blue = Camk2 delta cKO; green = Camk2gamma cKO.

Taken from: Taken from: Buck HV, Leser JM, Chatree S, Murray PM, Stains JP. Single-Gene CaMKIIγ or CaMKIIδ Conditional Deletion in Osteoblast-Lineage Cells Does Not Recapitulate Severe Skeletal Phenotype of CaMKIIγ/δ Double Conditional Deletion. [Manuscript in preparation].

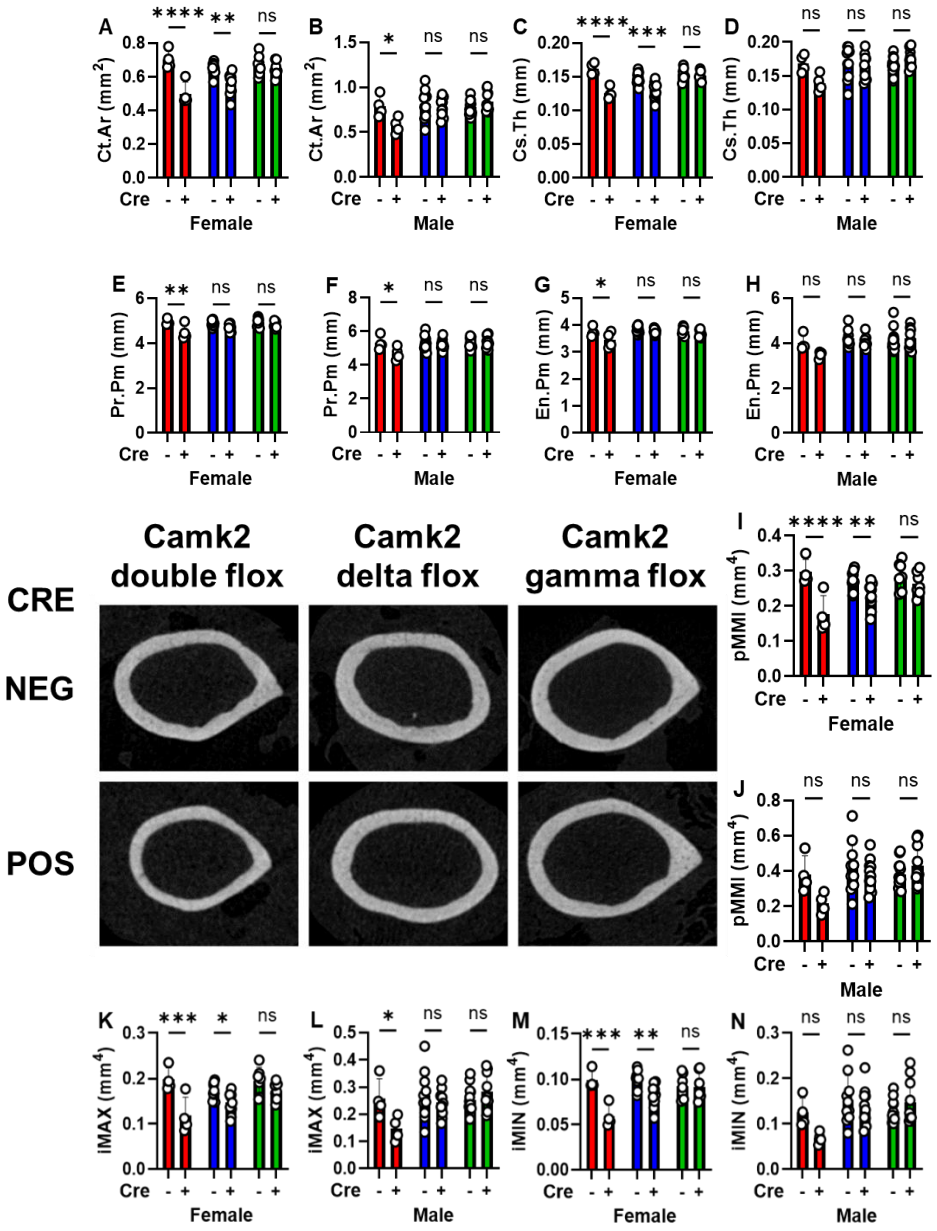

Figure 26. Bone Volume Reduction in the Mid-diaphyseal Femur is Less Severe in Camk2delta or Camk2gamma cKO Mice

of loss among the Camk2delta cKO mice never reached the fold-change difference among the Camk2double cKO mice (Figure 26I, K, M). iMAX values were significantly decreased among Camkdouble cKO males, but not either group of single knockout mice (Figure 26L). No difference in any group was observed in male mice for polarMMI or iMIN (Figure 26J, N). The average percent change between conditional knockouts and their respective controls, when added together, did not reach the magnitude of average percent change among the double cKO mice for any parameter.

5.2.3 The mechanical properties of the femur are altered in Camk2delta cKO mice

Four-point bending was utilized to reveal differences in the mechanical properties of femurs. Double cKO samples were not assayed for this study but were fully evaluated previously[94] and will be referenced here to provide context. Overall, the magnitude of the impact of Camk2delta or Camk2gamma deletion alone in the osteoblast lineage had little effect on the mechanical properties of bone, unlike co-deletion of both isoforms, with some limited exceptions. Stiffness, Yield Displacement, Total Displacement, and Total Work were not significantly altered among Camk2delta or gamma cKO mice of either sex (Figure 27A, D, F, H) while both sexes of double cKO mice expressed statistically significant decreases in these parameters[94]. Similar to double cKO mice[94], Post Yield Displacement was not altered among delta or gamma cKO mice (Figure 27E). Yield Load and Yield Work were significantly decreased among male delta cKO and female gamma cKO mice (Figure 27B, G). Interestingly, reductions in Yield Load and Yield Work among male delta cKO mice were the only mechanical parameters that approximate the phenotype observed in double cKO mice. Decreased resistance to force, as measured by Yield Load may

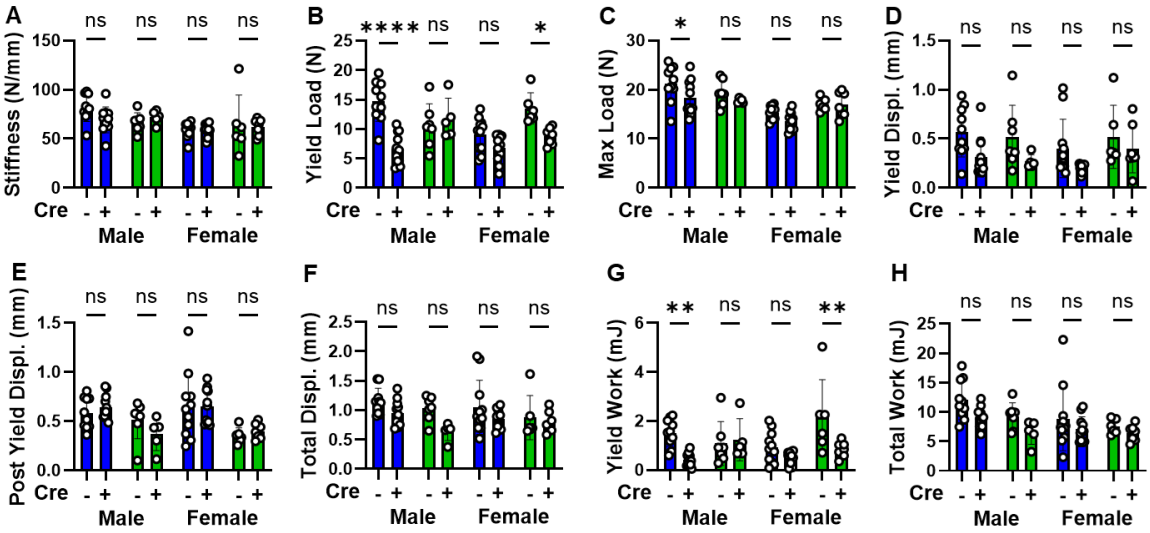

Figure 27. Mineralization may be somewhat altered in Camk2delta cKO mice

(A) Stiffness, **(D)** yield displacement, **(E)** post-yield displacement, **(F)** total displacement and **(H)** total work were not altered in either sex or genotype. **(B)** Yield load and **(G)** yield work was decreased in Camk2delta males and Camk2gamma females, while **(C)** max load was decreased only in Camk2delta cKO male mice. Blue = Camk2 delta cKO; green = Camk2gamma cKO.

Taken from: Taken from: Buck HV, Leser JM, Chatree S, Murray PM, Stains JP. Single-Gene CaMKIIγ or CaMKIIδ Conditional Deletion in Osteoblast-Lineage Cells Does Not Recapitulate Severe Skeletal Phenotype of CaMKIIγ/δ Double Conditional Deletion. [Manuscript in preparation].

indicate impaired structural properties[238] among male, and to a lesser extent, female gamma cKO mice. These findings may indicate that despite the lack of microarchitecture changes to the femurs of the Camk2delta cKO mice, mineralization defects, such as those observed in the Camk2double cKO mice[94], may be the driver of the reduced mechanical properties observed in Camk2delta cKO mice. Finally, only delta cKO males expressed a significant decrease in Max Load (Figure 27C), although the magnitude of this effect was trivial when compared to the observed differences in the Camk2double cKO mice. Notably, four-point bending of double cKO mice revealed robust decreases in resistance, with most parameters expressing an average 30-50% decrease in knockouts relative to control[94], while changes among delta or gamma cKO mice were not consistent across both sexes and were generally not as severe, again indicating the relative subtlety of the phenotype expressed by delta or gamma cKO mice, as compared to double cKO mice. Early data suggests that Camk2d may be a major driver of the changes in Yield Load and may serve a non-redundant role in the mineralization defects, like hypophosphatemia and hypomineralization, observed in the double cKO mice.

5.2.4 Expression of mineralization-associated markers is not altered in single cKOs

Whole-bone samples were enriched for osteocytes through the scraping of the periosteum and ejection of the contents of the bone marrow cavity before homogenization and western blotting. Membranes were probed for FGF23 and alkaline phosphatase (ALPL), normalized to total protein abundance. FGF23 and ALPL have a major role in bone mineralization by regulating phosphate homeostasis and contributing to hydroxyapatite crystal formation. In the Camk2double cKO mice, FGF23 both from bone

and in circulation were markedly increased, resulting in hypophosphatemia, and bone-derived, but not circulating ALPL was reduced. FGF23 expression was modestly increased but did not reach statistical significance among either sex of Camk2 delta or gamma cKO mice (Figure 28A), despite a roughly 50% mean increase in double cKO samples[94]. Conversely, ALPL abundance was decreased in double cKO mice[94], while there was again no significant change in Camk2 delta or gamma cKO mice (Figure 28B). The differences among double cKO mice that are not recapitulated by either single cKO may further indicate that the CaMKIIδ and CaMKIIγ isoforms may possess redundant function and/or compensatory expression.

5.3 Discussion

Our data show that conditional deletion of either Camk2delta or Camk2gamma produce only a subtle phenotype which does not recapitulate the profound skeletal differences expressed in Camk2delta/gamma double cKO mice, suggesting that Camk2delta and Camk2gamma serve redundant functions, as is seen in certain cardiac tissues[91]. This is consistent across our observed parameters, with the only exception being yield load in 4-point bending, where Camk2delta/gamma double cKO[94] and Camk2delta cKO males both experienced a roughly 50% decrease in required force- to-yield, relative to respective controls. Yield and pre-yield changes may suggest altered mineralization[239]; sectioning and staining is being completed to determine whether Camk2delta cKO mice express under-mineralized osteoid as observed in the Camk2delta/gamma double cKO mice.

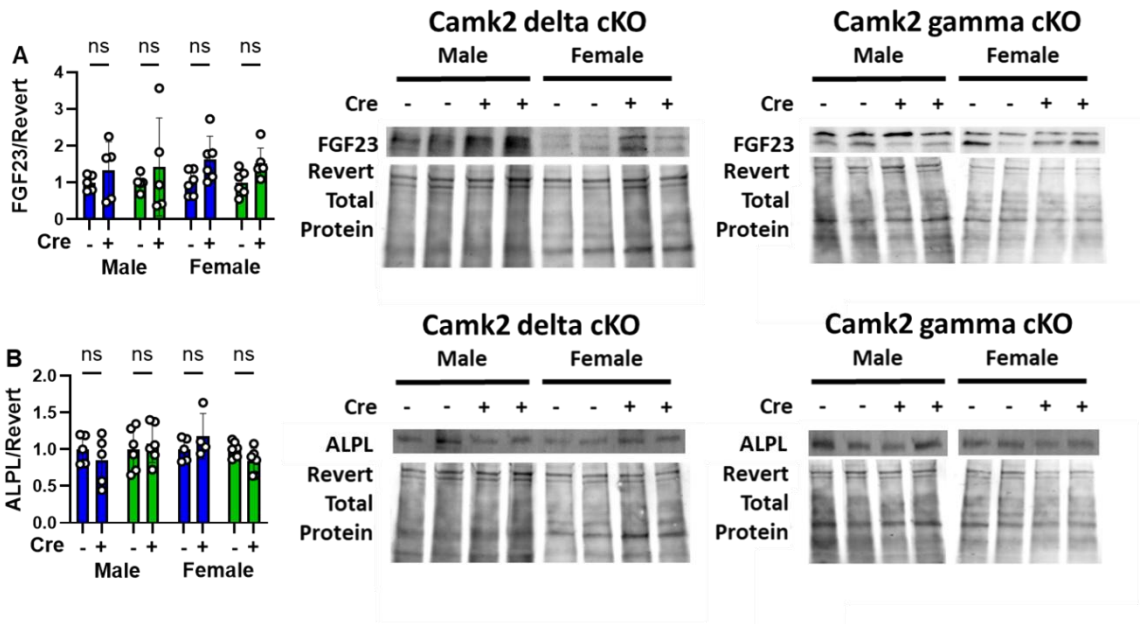

Figure 28. Expression of mineralization-associated markers is not altered in single cKOs

Western blotted tibial homogenates from Camk2delta or Camk2gamma cKO mice or littermate controls did not expresses altered normalized **(A)** FGF23 or **(B)** ALPL. With representative blots. Blue = Camk2 delta cKO; green = Camk2gamma cKO.

Taken from: Taken from: Buck HV, Leser JM, Chatree S, Murray PM, Stains JP. Single-Gene CaMKIIγ or CaMKIIδ Conditional Deletion in Osteoblast-Lineage Cells Does Not Recapitulate Severe Skeletal Phenotype of CaMKIIγ/δ Double Conditional Deletion. [Manuscript in preparation].

No sex-specific differences were observed among Camk2delta/gamma double cKO mice[94], which may be attributable to the fact that the observed deficits among knockout mice were so severe that differences between the sexes did not alter significance. This was not the case for the individual isoform knockouts, where we often observed slight, although significant changes in one sex but not the other, such as in several cortical parameters via microcomputed tomography data, where we saw changes in female Camk2delta cKO mice, but not males, or either sex of the Camk2gamma cKO mice. Similarly, we observed slight differences in yield load and yield work via 4-point bending among Camk2delta cKO males and Camk2gamma cKO females, but not in the corresponding groups, suggesting that loss of one isoform of Camk2 was not able to produce the same robust differences as the loss of both isoforms. Interestingly, Yield Load and Yield Work among Camk2delta cKO males were the only observed parameters that demonstrate an effect similar in magnitude to that of the Camk2double cKO mice. However, these male Camk2delta cKO did not also express a significant alteration in bone microarchitecture, suggesting that Camk2delta may play a role in mineralization that is distinct or dominant to the role played by Camk2gamma.

A trend that was observed repeatedly across techniques is that for a given parameter, the additive deficits of loss of both isoforms separately does not equal the deficit experienced when both isoforms are lost together. For example, average L5 BV/TV is reduced by around 75% for female Camk2delta/gamma double cKO mice, relative to littermate controls. However, the average percent change among female Camk2delta and Camk2gamma cKO mice is -16% and -1%, respectively. This is a more extreme example, but nonetheless, an effect that was observed repeatedly, where the combined effects of

individual knockout are not as severe as the effect of co-deletion, suggesting that these two isoforms do overlap in function.

No differences in body mass or length were observed within a given strain (i.e., cre-positive cKO mice vs cre-negative floxed littermate controls), but we did observe some small but statistically significant differences between strains which we attribute to normal variation between distinct breeding colonies.

While the phenotype expressed by mice lacking either Camk2delta or Camk2gamma in osteocytes and mature osteoblasts is not dramatic, especially when compared to Camk2delta/gamma double cKO mice (Table 4), the characterization of these models is a necessary step in understanding the functions and redundancy of these isoforms. Based on the subtly of the phenotypes observed thus far, we do not expect to find a severe difference in any of the outputs yet to be tested, but will continue to analyze

Table 4. Summary of Differences Between Camk2double, Camk2delta, and Camk2gamma cKO Mice

Parameter	Camk2 double cKO	Camk2 delta cKO	Camk2 gamma cKO
BV/TV (Femur)	↓↓↓	=	=
Cortical Area	↓↓↓	↓	=
BV/TV (Spine)	↓↓↓	=	=
Stiffness	↓↓↓	↓↓	↓
Yield Load	↓↓↓	↓↓	↓
Max Load	↓↓↓	↓	=
FGF23	↑	=	=
ALPL	↓	=	=

samples to determine whether this is the case. Mechanical differences between Camk2delta and gamma cKO mice beg investigation into mineralization differences. This project is still ongoing; future works are discussed in the next chapter.

Chapter 6. Conclusion and Future Directions

6.1 Summary

We have provided an overview of skeletal structure and function, and discussed the ways in which bone changes during various stages of life. We have broadly covered skeletal health, disease, and some of the clinically available therapeutics for the preservation of bone mass. We have also described pathways and molecular elements of cellular and mechanical response, which is central to bone health and maintenance.

We have discussed the factors and pathways through which mechanical stimulation of osteocytes supports the differentiation of mesenchymal stem cells into osteoblasts, rather than adipocytes, supporting new bone deposition.

We have provided an overview of nitric oxide and the three isoforms, neuronal (nNOS, *NOS1*), inducible (iNOS, *NOS2*), and endothelial (eNOS, *NOS3*) of the enzymes that produce nitric oxide. We have built on our earlier work[29] to demonstrate that nitric oxide donation is sufficient to control sclerostin protein abundance, and that when nitric oxide production is inhibited, osteocytes can no longer control their sclerostin abundance in response to mechanical stimulation. We have also shown that nitric oxide production appears to occur downstream of CaMKII activation in a previously described mechanical response pathway for the control of sclerostin protein abundance, and that nitric oxide production may feed back into CaMKII activation to tune calcium influx.

We have demonstrated that Camk2delta and Camk2gamma cKO mice express only some mild trabecular bone loss and some alterations in resistance to axial force, but that these differences do not reach the magnitude of the deficits expressed by Camk2delta/gamma double cKO mice. We have also demonstrated that the expression of

proteins such as FGF23 and alkaline phosphatase are not statistically altered in whole-bone homogenates from Camk2delta or Camk2gamma cKO mice. Examination of circulating markers such as FGF23, ALPL, calcium, and phosphate remain to be determined.

Our earlier work demonstrated the profound loss of bone mass that results from conditional deletion of Camk2 delta/gamma in osteocytes and mature osteoblasts[94], and our preliminary study of the Camk2 delta or Camk2 gamma cKO mice has found that neither group expresses a phenotype as severe as the Camk2 delta/gamma double cKO, nor do the differences within the individual knockout groups appear to be additive. This suggests that the Camk2 delta and gamma isoforms may serve redundant functions, and perhaps that either isoform may compensate for the loss of the other.

6.2 Future Directions

6.2.1 Nitric Oxide

While we demonstrated the *in vitro* role that nitric oxide plays in the control of sclerostin protein abundance after mechanical stimulation, there is still much more to be learned *in vivo*. We found that eNOS and iNOS both appear to meaningfully contribute to osteocytic mechanical response. Historically, nitric oxide synthases have been studied via global knockouts, which may result in serious cardiac defects[240]. eNOS[241] and iNOS[242] floxed mice have recently been developed for use as a tissue-specific deletion model. We would seek to cross eNOS and iNOS floxed mice with Osteocalcin Cre to target specific NOS deletion in osteocytes and mature osteoblasts. Adult knockout mice and Cre-negative litter mate controls would receive an injection of a red fluorescent calcium-labeling dye, alizarin. They would then receive strain-matched axial loading, followed by an injection of

the green fluorescent calcium-labeling dye, calcein. Following euthanasia, long bones would be sectioned, and the distance between the two dyes would be used to calculate the amount of new bone deposited during the interlabeling period. Based on our *in vitro* findings, we would expect eNOS flox / OCN Cre mice to deposit much less new bone than controls, with iNOS flox / OCN Cre mice expressing an intermediary phenotype. If no significant difference is observed, it may be necessary to suppress nitric oxide production even further by developing an eNOS / iNOS / OCN Cre double knockout model, in which both eNOS and iNOS are deleted in osteocytes and mature osteoblasts.

As osteocalcin Cre becomes active around day E17 of murine development[243], it may be desirable to allow mice to become skeletally mature before intervention to tease apart nitric oxide's ability to influence bone growth versus its ability to influence mechanical response. To do this, the OCN-Cre ERT2 driver could be utilized. In skeletally mature mice, tamoxifen injections would induce the Cre driver, resulting in the temporal loss of *NOS2* and *NOS3*. After NOS inhibition, mice would receive axial loading as above. Hopefully, we will see no significant difference between the loaded and unloaded limbs in these mice for mineral apposition rate or sclerostin expression, demonstrating that nitric oxide production is necessary for mechanical response.

Nitroglycerin may be prescribed acutely or as a maintenance treatment for the management of angina, or chest pain. Nitroglycerin, like many other nitric oxide donors, breaks down into nitric oxide in the body, where it relaxes blood vessels, and may also act on bone-resident cells. Clinical trials were performed to determine whether nitroglycerin administration can positively affect BMD or fracture risk, but after two important studies were retracted due to fraud[244,245] interest in this approach has waned. Nitroglycerin usage

studies usually focus on cardiovascular outcomes, but some secondary analyses of these studies have indicated that there may be improvements in BMD or fracture incidence, though dosage and frequency differences may be significant for positive skeletal outcomes[246,247].

6.2.2 Camk2delta and Camk2gamma cKO

While we have not yet observed large differences in the phenotypes expressed by Camk2delta and Camk2gamma cKO mice, we are continuing our analysis so that we may come to a definitive conclusion as to the roles that these isoforms play in osteocyte-mediated bone biology.

As there is no commercially available antibody that can differentiate between the four isoforms, we will use primary osteocytes isolated from Camk2delta or Camk2gamma cKO mice and their Cre-negative littermate controls to validate our knockouts. Cells will be lysed in TRIzol for RNA isolation. Once all samples are collected we will isolate RNA for RT-qPCR, and isolate protein for western blot. We will quantify relative gene expression to demonstrate the efficacy of our knockout models and to determine whether elimination of one Camk2 isoform results in a compensatory increase of the other isoform. Protein will also be harvested from the TRIzol lysates and western blots will be used to verify whether there are changes in the expression of targets associated with bone mass and mineralization, like sclerostin, FGF23, or alkaline phosphatase.

Histology was used to discover several types of defects in sections taken from Camk2delta/gamma double cKO mice. Samples have already been prepared for the production of plastic-embedded sections from both Camk2delta and Camk2gamma cKO

mice and their controls. Goldner's Trichrome staining will be used to determine whether Camk2delta or Camk2gamma cKO mice express under-mineralized seams to the same extent as Camk2delta/gamma double cKO mice. Changes in osteoblast number and mineralization rate and osteoclast number will also be quantified.

Hypophosphatemia appeared to be a major driver of the mineralization defect expressed by the Camk2delta/gamma double cKO mice. Blood was collected and serum was isolated from Camk2delta and Camk2gamma cKO mice and their controls. It will be commercially analyzed for phosphate concentration and other markers of kidney function. Blood samples will also be processed via ELISA to determine circulating concentrations of hormones like FGF23 and sclerostin as these proteins were significantly altered in Camk2delta/gamma double cKO mice.

Our initial observations of CaMKII implicated it in bone mechano-transduction following loading, however, axial loading could not be performed on the Camk2delta/gamma double cKO as strain matching was not possible due to their significant mineralization defect. OCN Cre-ERT2, a tamoxifen-inducible Cre, can be used to selectively delete Camk2delta and Camk2gamma in skeletally mature mice prior to loading. Loaded tibiae and their unloaded contralateral limbs will be analyzed via dynamic histomorphometry to determine whether mechanical response is altered in these mice. If we utilize a dosing protocol and timing sufficient to eliminate Camk2 in a significant number of osteocytes, then we believe that apposition will be reduced because Camk2 is a necessary element in the mechano-response pathway that controls sclerostin protein abundance[31].

The bone loss expressed by Camk2delta/gamma double cKO mice is profound. We would like to perform rescue experiments using clinically available treatments to determine whether our hypothesis that excess FGF23 and hypophosphatemia are in fact the cause of their bone phenotype. Burosumab is an anti-FGF23 antibody most commonly prescribed to persons with x-linked hypophosphatemia. We would treat 4-week-old Camk2delta/gamma double cKO mice with burosumab (anti-FGF23 antibody), asforase alfa (recombinant ALPL), or control for four weeks before euthanizing and comparing outcomes like bone volume and mineralization. If we are correct then the bone mass of burosumab-treated Camk2delta/gamma double cKO mice should be close to that of control-treated age-matched Cre-negative littermate controls. We would also expect bisphosphonate-treated Camk2delta/gamma double cKO mice to show preserved bone mass, though they may experience severe hypophosphatemia due to blocked resorption of phosphate from hydroxyapatite. If neither intervention preserves bone mass then the timing or duration of the study may need to be adjusted.

6.3 Conclusion

Bone is discounted by the public as a static and inert tissue that does not change outside of growth or fracture repair, but this could not be further from the truth. Bone is responsive, dynamic, and an important player in overall health and lifespan. Emerging technologies allow new discoveries every day, but much is still hidden. Bone loss and preservation are challenges of increasing importance. We must develop better therapeutics and techniques to prevent bone loss during spaceflight and to preserve bone health and functionality in an increasingly long-lived population. Almost all currently osteoporosis

therapeutics began in basic research and many promising new preventatives and treatments are still waiting to be discovered.

References

1. Olszta MJ, Cheng X, Jee SS, Kumar R, Kim YY, Kaufman MJ, et al. Bone structure and formation: A new perspective. Mater Sci Eng R Reports. 2007;58(3–5):77–116.

2. Fan J, Abedi-Dorcheh K, Sadat Vaziri A, Kazemi-Aghdam F, Rafieyan S, Sohrabinejad M, et al. A Review of Recent Advances in Natural Polymer-Based Scaffolds for Musculoskeletal Tissue Engineering. Polymers (Basel) [Internet]. 2022 May 20;14(10). Available from: http://www.ncbi.nlm.nih.gov/pubmed/35631979

3. Florencio-Silva R, Sasso GRDS, Sasso-Cerri E, Simões MJ, Cerri PS. Biology of Bone Tissue: Structure, Function, and Factors That Influence Bone Cells. Biomed Res Int [Internet]. 2015;2015. Available from: http://dx.doi.org/10.1155/2015/421746

4. Kazimierczak P, Wessely-Szponder J, Palka K, Barylyak A, Zinchenko V, Przekora A. Hydroxyapatite or Fluorapatite—Which Bioceramic Is Better as a Base for the Production of Bone Scaffold?—A Comprehensive Comparative Study. Int J Mol Sci. 2023;24(6).

5. Panda S, Biswas CK, Paul S. A comprehensive review on the preparation and application of calcium hydroxyapatite: A special focus on atomic doping methods for bone tissue engineering. Ceram Int [Internet]. 2021;47(20):28122–44. Available from: https://doi.org/10.1016/j.ceramint.2021.07.100

6. Šromová V, Sobola D, Kaspar P. A Brief Review of Bone Cell Function and Importance. Cells. 2023;12(21).

7. Surowiec RK, Allen MR, Wallace JM. Bone hydration: How we can evaluate it, what can it tell us, and is it an effective therapeutic target? Bone reports [Internet]. 2022 Jun;16:101161. Available from: https://doi.org/10.1016/j.bonr.2021.101161

8. Xiong J, Onal M, Jilka RL, Weinstein RS, Manolagas SC, O'Brien CA. Matrix-embedded cells control osteoclast formation. Nat Med [Internet]. 2011 Sep 11;17(10):1235–41. Available from: http://www.ncbi.nlm.nih.gov/pubmed/21909103

9. Atkins GJ, Kostakis P, Pan B, Farrugia A, Gronthos S, Evdokiou A, et al. RANKL expression is related to the differentiation state of human osteoblasts. J Bone Miner Res [Internet]. 2003 Jun;18(6):1088–98. Available from: http://www.ncbi.nlm.nih.gov/pubmed/12817763

10. Nakamura I, Duong LT, Rodan SB, Rodan GA. Involvement of αvβ3 integrins in osteoclast function. J Bone Miner Metab. 2007;25(6):337–44.

11. Madel MB, Ibáñez L, Wakkach A, De Vries TJ, Teti A, Apparailly F, et al. Immune function and diversity of osteoclasts in normal and pathological conditions. Front Immunol. 2019;10(JUN):1–18.

12. Lee CYS, Suzuki JB. CTX biochemical marker of bone metabolism. is it a reliable predictor of bisphosphonate-associated osteonecrosis of the jaws after surgery? Part II: A prospective clinical study. Implant Dent. 2010;19(1):29–38.

13. Liu Z, Wang Q, Zhang J, Qi S, Duan Y, Li C. The Mechanotransduction Signaling Pathways in the Regulation of Osteogenesis. Int J Mol Sci. 2023;24(18).

14. Komori T. Regulation of proliferation, differentiation and functions of osteoblasts by runx2. Int J Mol Sci. 2019;20(7).

15. Murshed M. Mechanism of bone mineralization. Cold Spring Harb Perspect Med. 2018;8(12):1–11.

16. Neve A, Corrado A, Cantatore FP. Osteoblast physiology in normal and pathological conditions. Cell Tissue Res. 2011;343(2):289–302.

17. Zurick KM, Qin C, Bernards MT. Mineralization induction effects of osteopontin, bone sialoprotein, and dentin phosphoprotein on a biomimetic collagen substrate. J Biomed Mater Res A [Internet]. 2013 Jun;101(6):1571–81. Available from: http://www.ncbi.nlm.nih.gov/pubmed/23161527

18. Matic I, Matthews BG, Wang X, Dyment NA, Worthley DL, Rowe DW, et al. Quiescent Bone Lining Cells Are a Major Source of Osteoblasts During Adulthood. Stem Cells [Internet]. 2016 Dec;34(12):2930–42. Available from: http://www.ncbi.nlm.nih.gov/pubmed/27507737

19. Choi JUA, Kijas AW, Lauko J, Rowan AE. The Mechanosensory Role of Osteocytes and Implications for Bone Health and Disease States. Front cell Dev Biol [Internet]. 2021;9(February):770143. Available from: http://www.ncbi.nlm.nih.gov/pubmed/35265628

20. Tiede-Lewis LAM, Dallas SL. Changes in the osteocyte lacunocanalicular network with aging. Bone. 2019;122:101–13.

21. Sugawara Y, Kamioka H, Honjo T, Tezuka KI, Takano-Yamamoto T. Three-dimensional reconstruction of chick calvarial osteocytes and their cell processes using confocal microscopy. Bone. 2005;36(5):877–83.

22. Manolagas SC. Choreography from the tomb: An emerging role of dying osteocytes in the purposeful, and perhaps not so purposeful, targeting of bone remodeling. BoneKEy-Osteovision. 2006;3(1):5–14.

23. Buenzli PR, Sims NA. Quantifying the osteocyte network in the human skeleton.

Bone [Internet]. 2015;75:144–50. Available from: http://dx.doi.org/10.1016/j.bone.2015.02.016

24. Qin L, Liu W, Cao H, Xiao G. Molecular mechanosensors in osteocytes. Bone Res [Internet]. 2020;8(1):23. Available from: https://doi.org/10.1038/s41413-020-0099-y

25. Gould NR, Torre OM, Leser JM, Stains JP. The cytoskeleton and connected elements in bone cell mechano-transduction. Bone [Internet]. 2021 Aug;149(5):115971. Available from: http://www.ncbi.nlm.nih.gov/pubmed/33892173

26. Chen CY, Caporizzo MA, Bedi K, Vite A, Bogush AI, Robison P, et al. Suppression of detyrosinated microtubules improves cardiomyocyte function in human heart failure. Nat Med [Internet]. 2018 Aug;24(8):1225–33. Available from: https://doi.org/10.1038/s41591-018-0046-2

27. Mohan N, Sorokina EM, Verdeny IV, Alvarez AS, Lakadamyali M. Detyrosinated microtubules spatially constrain lysosomes facilitating lysosome-autophagosome fusion. J Cell Biol. 2019;218(2):632–43.

28. Trivedi PC, Bartlett JJ, Pulinilkunnil T. Lysosomal Biology and Function: Modern View of Cellular Debris Bin. Cells. 2020;9(5):1–35.

29. Gould NR, Williams KM, Joca HC, Torre OM, Lyons JS, Leser JM, et al. Disparate bone anabolic cues activate bone formation by regulating the rapid lysosomal degradation of sclerostin protein. Elife. 2021;10:1–26.

30. Robling AG, Niziolek PJ, Baldridge LA, Condon KW, Allen MR, Alam I, et al. Mechanical stimulation of bone in vivo reduces osteocyte expression of Sost/sclerostin. J Biol Chem [Internet]. 2008;283(9):5866–75. Available from: http://dx.doi.org/10.1074/jbc.M705092200

31. Lyons JS, Joca HC, Law RA, Williams KM, Kerr JP, Shi G, et al. Microtubules tune mechanotransduction through NOX2 and TRPV4 to decrease sclerostin abundance in osteocytes. Sci Signal. 2017;10(506).

32. Williams KM, Leser JM, Gould NR, Joca HC, Lyons JS, Khairallah RJ, et al. TRPV4 calcium influx controls sclerostin protein loss independent of purinergic calcium oscillations. Bone [Internet]. 2020;136(April):115356. Available from: https://doi.org/10.1016/j.bone.2020.115356

33. Buck H V., Torre OM, Leser JM, Gould NR, Ward CW, Stains JP. Nitric oxide contributes to rapid sclerostin protein loss following mechanical load. Biochem Biophys Res Commun [Internet]. 2024;727(June):150315. Available from: https://doi.org/10.1016/j.bbrc.2024.150315

34. Robles-Linares JA, Ramírez-Cedillo E, Siller HR, Rodríguez CA, Martínez-López JI. Parametric Modeling of Biomimetic Cortical Bone Microstructure for Additive Manufacturing. Mater (Basel, Switzerland) [Internet]. 2019 Mar 19;12(6):1–16. Available from: http://www.ncbi.nlm.nih.gov/pubmed/30893894

35. Carmeliet P, Jain RK. Angiogenesis in cancer and other diseases. Nature [Internet]. 2000 Sep 14;407(6801):249–57. Available from: www.nature.com

36. Marinelli Busilacchi E, Morsia E, Poloni A. Bone Marrow Adipose Tissue. Cells. 2024;13(9):1–13.

37. Shen F, Huang X, He G, Shi Y. The emerging studies on mesenchymal progenitors in the long bone. Cell Biosci [Internet]. 2023 Jun 10;13(1):105. Available from: https://doi.org/10.1186/s13578-023-01039-x

38. Riddle RC, Clemens TL. Bone cell bioenergetics and skeletal energy homeostasis. Physiol Rev. 2017;97(2):667–98.

39. B. Frank C. Normal ligament structure and physiology. J Musculoskelet Neuronal Interact. 2004;4(2):199–201.

40. Kirkendall DT, Garrett WE. Function and biomechanics of tendons. Scand J Med Sci Sport. 1997;7(2):62–6.

41. Liu Y, Shah KM, Luo J. Strategies for Articular Cartilage Repair and Regeneration. Front Bioeng Biotechnol [Internet]. 2021;9(December):770655. Available from: http://www.ncbi.nlm.nih.gov/pubmed/34976967

42. Mackie EJ, Ahmed YA, Tatarczuch L, Chen KS, Mirams M. Endochondral ossification: How cartilage is converted into bone in the developing skeleton. Int J Biochem Cell Biol. 2008;40(1):46–62.

43. Berendsen AD, Olsen BR. Bone development. Bone [Internet]. 2015 Nov;80(1):14–8. Available from: http://www.ncbi.nlm.nih.gov/pubmed/26453494

44. Kruger MJ, Nell TA. Bone mineral density in people living with HIV: A narrative review of the literature. AIDS Res Ther. 2017;14(1):1–17.

45. Park-Min KH, Lorenzo J. Osteoclasts: Other functions. Bone [Internet]. 2022;165(July):116576. Available from: https://doi.org/10.1016/j.bone.2022.116576

46. Kovacs CS, Fuleihan GEH. Calcium and bone disorders during pregnancy and lactation. Endocrinol Metab Clin North Am [Internet]. 2006 Mar;35(1):21–51, v. Available from: http://www.ncbi.nlm.nih.gov/pubmed/16310641

47. Ryan BA, Kovacs CS. The puzzle of lactational bone physiology: Osteocytes

masquerade as osteoclasts and osteoblasts. J Clin Invest. 2019;129(8):3041–4.

48. Tsourdi E, Jähn K, Rauner M, Busse B, Bonewald LF. Physiological and pathological osteocytic osteolysis. J Musculoskelet Neuronal Interact. 2018;18(3):292–303.

49. Jähn K, Kelkar S, Zhao H, Xie Y, Tiede-Lewis LM, Dusevich V, et al. Osteocytes Acidify Their Microenvironment in Response to PTHrP In Vitro and in Lactating Mice In Vivo. J Bone Miner Res [Internet]. 2017 Aug;32(8):1761–72. Available from: http://www.ncbi.nlm.nih.gov/pubmed/28470757

50. Kameda T, Mano H, Yuasa T, Mori Y, Miyazawa K, Shiokawa M, et al. Estrogen inhibits bone resorption by directly inducing apoptosis of the bone-resorbing osteoclasts. J Exp Med. 1997;186(4):489–95.

51. Bi J, Zhang C, Lu C, Mo C, Zeng J, Yao M, et al. Age-related bone diseases: Role of inflammaging. J Autoimmun [Internet]. 2024;143(November 2023):103169. Available from: https://doi.org/10.1016/j.jaut.2024.103169

52. ElHawary H, Baradaran A, Abi-Rafeh J, Vorstenbosch J, Xu L, Efanov JI. Bone Healing and Inflammation: Principles of Fracture and Repair. Semin Plast Surg [Internet]. 2021 Aug;35(3):198–203. Available from: http://www.ncbi.nlm.nih.gov/pubmed/34526868

53. Gao H, Huang J, Wei Q, He C. Advances in Animal Models for Studying Bone Fracture Healing. Bioeng (Basel, Switzerland) [Internet]. 2023 Feb 3;10(2). Available from: http://www.ncbi.nlm.nih.gov/pubmed/36829695

54. Lane NE. Epidemiology, etiology, and diagnosis of osteoporosis. Am J Obstet Gynecol. 2006;194(2 SUPPL.).

55. Xiao PL, Cui AY, Hsu CJ, Peng R, Jiang N, Xu XH, et al. Global, regional prevalence, and risk factors of osteoporosis according to the World Health Organization diagnostic criteria: a systematic review and meta-analysis. Osteoporos Int. 2022;33(10):2137–53.

56. Coughlan T, Dockery F. Osteoporosis and fracture risk in older people. Clin Med J R Coll Physicians London. 2014;14(2):187–91.

57. Guzon-Illescas O, Perez Fernandez E, Crespí Villarias N, Quirós Donate FJ, Peña M, Alonso-Blas C, et al. Mortality after osteoporotic hip fracture: Incidence, trends, and associated factors. J Orthop Surg Res. 2019;14(1):1–9.

58. Uday S, Högler W. Nutritional rickets & osteomalacia : A practical approach to management. 2020;(October):356–67.

59. Elder CJ, Bishop NJ. Rickets. Lancet (London, England) [Internet]. 2014 May

10;383(9929):1665–76. Available from: http://www.ncbi.nlm.nih.gov/pubmed/24412049

60. Russell RGG. Bisphosphonates: Mode of Action and Pharmacology. Pediatrics. 2007;119(SUPPL. 2).

61. Shakeri A, Adanty C. Romosozumab (sclerostin monoclonal antibody) for the treatment of osteoporosis in postmenopausal women: A review. J Popul Ther Clin Pharmacol = J la Ther des Popul la Pharmacol Clin [Internet]. 2020 Jan 6;27(1):e25–31. Available from: http://www.ncbi.nlm.nih.gov/pubmed/31922699

62. Wu D, Li L, Wen Z, Wang G. Romosozumab in osteoporosis: yesterday, today and tomorrow. J Transl Med [Internet]. 2023;21(1):1–13. Available from: https://doi.org/10.1186/s12967-023-04563-z

63. Romosozumab [package insert]. Amgen Incorporated; 2019. /www.fda.gov/drugsatfda

64. Tsur A, Cahn A, Levy L, Pollack R. Cardiovascular outcomes of romosozumab treatment-real-world data analysis. JBMR plus [Internet]. 2025 Jan;9(1):ziae146. Available from: http://www.ncbi.nlm.nih.gov/pubmed/39687784

65. Hanley DA, Adachi JD, Bell A, Brown V. Denosumab: Mechanism of action and clinical outcomes. Int J Clin Pract. 2012;66(12):1139–46.

66. Denosumab [package insert]. Amgen Incorporated; 2010. Revised 2024. /www.fda.gov/drugsatfda

67. Kendler DL, Cosman F, Stad RK, Ferrari S. Denosumab in the Treatment of Osteoporosis: 10 Years Later: A Narrative Review. Adv Ther [Internet]. 2022;39(1):58–74. Available from: https://doi.org/10.1007/s12325-021-01936-y

68. Eknoyan G. A history of the parathyroid glands. Am J Kidney Dis [Internet]. 1995 Nov;26(5):801–7. Available from: http://www.ncbi.nlm.nih.gov/pubmed/26902094

69. Lindsay R, Krege JH, Marin F, Jin L, Stepan JJ. Teriparatide for osteoporosis: Importance of the full course. Osteoporos Int [Internet]. 2016;27(8):2395–410. Available from: http://dx.doi.org/10.1007/s00198-016-3534-6

70. Arlt H, Mullarkey T, Hu D, Baron R, Ominsky MS, Mitlak B, et al. Effects of abaloparatide and teriparatide on bone resorption and bone formation in female mice. Bone reports [Internet]. 2020 Dec;13(June):100291. Available from: https://doi.org/10.1016/j.bonr.2020.100291

71. Teriparatide [package insert]. Lilly USA; 1987. Revised 2020. /www.fda.gov/drugsatfda

72. Abaloparatide [package insert]. Radius Health Incorporated; 2017. www.fda.gov/drugsatfda

73. Bellido T, Saini V, Pajevic PD. Effects of PTH on osteocyte function. Bone. 2013;54(2):250–7.

74. Cormier C, Koumakis E. Bone and primary hyperparathyroidism. Jt Bone Spine. 2022;89(1).

75. Lerner UH, Ohlsson C. The WNT system: Background and its role in bone. J Intern Med. 2015;277(6):630–49.

76. Lawson LY, Migotsky N, Chermside-Scabbo CJ, Shuster JT, Joeng KS, Civitelli R, et al. Loading-induced bone formation is mediated by Wnt1 induction in osteoblast-lineage cells. FASEB J. 2022;36(9):1–21.

77. Robinson JA, Chatterjee-Kishore M, Yaworsky PJ, Cullen DM, Zhao W, Li C, et al. Wnt/beta-catenin signaling is a normal physiological response to mechanical loading in bone. J Biol Chem [Internet]. 2006 Oct 20;281(42):31720–8. Available from: http://dx.doi.org/10.1016/S0021-9258(19)84086-3

78. Ben-Ghedalia-Peled N, Vago R. Wnt Signaling in the Development of Bone Metastasis. Cells. 2022;11(23).

79. Holdsworth G, Roberts SJ, Ke HZ. Novel actions of sclerostin on bone. J Mol Endocrinol. 2019;62(2):R167–85.

80. Bonewald LF, Wacker MJ. FGF23 production by osteocytes. Pediatr Nephrol [Internet]. 2013 Apr;28(4):563–8. Available from: http://www.ncbi.nlm.nih.gov/pubmed/22983423

81. Agoro R, Ni P, Noonan ML, White KE. Osteocytic FGF23 and Its Kidney Function. Front Endocrinol (Lausanne) [Internet]. 2020;11(August):592. Available from: http://www.ncbi.nlm.nih.gov/pubmed/32982979

82. Razzaque MS. The FGF23-Klotho axis: endocrine regulation of phosphate homeostasis. Nat Rev Endocrinol [Internet]. 2009 Nov;5(11):611–9. Available from: https://www.ncbi.nlm.nih.gov/pmc/articles/PMC3624763/pdf/nihms412728.pdf

83. Frost HM. Perspectives: A proposed general model of the “Mechanostat” (Suggestions from a new skeletal-biologic paradigm). Anat Rec. 1996;244(2):139–47.

84. Su SC, Skedros JG, Bachus KN, Bloebaum RD. Loading conditions and cortical bone construction of an artiodactyl calcaneus. J Exp Biol [Internet]. 1999 Nov;202(Pt 22):3239–54. Available from:

http://www.ncbi.nlm.nih.gov/pubmed/10539972

85. McBride SH, Silva MJ. Adaptive and Injury Response of Bone to Mechanical Loading. Bonekey Osteovision [Internet]. 2012 Oct 10;1(OCTOBER):192. Available from: http://dx.doi.org/10.1038/bonekey.2012.192

86. Zhao D, Riquelme MA, Guda T, Tu C, Xu H, Gu S, et al. Connexin Hemichannels with Prostaglandin Release in Anabolic Function of Bone to Mechanical Loading. bioRxiv [Internet]. 2021;2021.10.15.464551. Available from: https://www.biorxiv.org/content/10.1101/2021.10.15.464551v1%0Ahttps://www.biorxiv.org/content/10.1101/2021.10.15.464551v1.abstract

87. Lyons JS, Joca HC, Law RA, Williams KM, Kerr JP, Shi G, et al. Microtubules tune mechanotransduction through NOX2 and TRPV4 to decrease sclerostin abundance in osteocytes. Sci Signal [Internet]. 2017 Nov 21;10(506):42–51. Available from: http://www.ncbi.nlm.nih.gov/pubmed/29162742

88. Gould NR, Leser JM, Torre OM, Khairallah RJ, Ward CW, Stains JP. In vitro Fluid Shear Stress Induced Sclerostin Degradation and CaMKII Activation in Osteocytes. Bio-protocol. 2021;11(23):1–15.

89. Spatz JM, Wein MN, Gooi JH, Qu Y, Garr JL, Liu S, et al. The Wnt Inhibitor Sclerostin Is Up-regulated by Mechanical Unloading in Osteocytes in Vitro. J Biol Chem [Internet]. 2015 Jul 3;290(27):16744–58. Available from: http://dx.doi.org/10.1074/jbc.M114.628313

90. Lyons, James S., Iyer, Shama R., Lovering, Richard M., Ward, Christopher W., Stains JP. Novel multi-functional fluid flow device for studying cellular mechanotransduction. J Biomech. 2016;

91. Kreusser MM, Lehmann LH, Keranov S, Hoting MO, Oehl U, Kohlhaas M, et al. Cardiac CaM kinase II genes δ and γ contribute to adverse remodeling but redundantly inhibit calcineurin-induced myocardial hypertrophy. Circulation. 2014;130(15):1262–73.

92. Moorer MC, Hebert C, Tomlinson RE, Iyer SR, Chason M, Stains JP. Defective signaling, osteoblastogenesis and bone remodeling in a mouse model of connexin 43 C-terminal truncation. J Cell Sci. 2017;130(3):531–40.

93. Buo AM, Tomlinson RE, Eidelman ER, Chason M, Stains JP. Connexin43 and Runx2 Interact to Affect Cortical Bone Geometry, Skeletal Development, and Osteoblast and Osteoclast Function. J Bone Miner Res. 2017;32(8):1727–38.

94. Leser JM, Torre OM, Gould NR, Guo Q, Buck H V, Kodama J, et al. Osteoblast-lineage calcium/calmodulin-dependent kinase 2 delta and gamma regulates bone mass and quality. Proc Natl Acad Sci U S A [Internet]. 2023 Nov

21;120(47):e2304492120. Available from: http://www.pnas.org/lookup/suppl/doi:10.1073/pnas.2216830120/-/DCSupplemental.https://doi.org/10.1073/pnas.2216830120

95. Dempster DW, Compston JE, Drezner MK, Kanis FHG, John A Malluche, Ott S, et al. Histomorphometry Nomenclature: A 2012 Update of the Report of the ASBMR Histomorphometry Nomenclature David. J Bone Miner Res [Internet]. 2014;28(1):2–17. Available from: http://www.ncbi.nlm.nih.gov/pubmed/23197339%0Ahttp://www.pubmedcentral.nih.gov/articlerender.fcgi?artid=PMC3672237

96. Jepsen KJ, Silva MJ, Vashishth D, Guo XE, van der Meulen MCH. Establishing biomechanical mechanisms in mouse models: practical guidelines for systematically evaluating phenotypic changes in the diaphyses of long bones. J Bone Miner Res [Internet]. 2015 Jun;30(6):951–66. Available from: https://www.ncbi.nlm.nih.gov/pmc/articles/PMC4794979/pdf/nihms765383.pdf

97. McClanahan BS, Harmon-Clayton K, Ward KD, Klesges RC, Vukadinovich CM, Cantler ED. Side-to-side comparisons of bone mineral density in upper and lower limbs of collegiate athletes. J strength Cond Res [Internet]. 2002 Nov;16(4):586–90. Available from: http://www.ncbi.nlm.nih.gov/pubmed/12423190

98. Mohamed AMFS. An overview of bone cells and their regulating factors of differentiation. Malaysian J Med Sci. 2008;15(1):4–12.

99. Liu P, Tu J, Wang W, Li Z, Li Y, Yu X, et al. Effects of Mechanical Stress Stimulation on Function and Expression Mechanism of Osteoblasts. Front Bioeng Biotechnol [Internet]. 2022;10(February):830722. Available from: http://www.ncbi.nlm.nih.gov/pubmed/35252138

100. Blair HC, Larrouture QC, Li Y, Lin H, Beer-Stoltz D, Liu L, et al. Osteoblast Differentiation and Bone Matrix Formation In Vivo and In Vitro. Tissue Eng Part B Rev [Internet]. 2017 Jun;23(3):268–80. Available from: http://www.ncbi.nlm.nih.gov/pubmed/27846781

101. Orgel JP, Miller A, Irving TC, Fischetti RF, Hammersley AP, Wess TJ. The in situ supermolecular structure of type I collagen. Structure [Internet]. 2001 Nov;9(11):1061–9. Available from: http://www.ncbi.nlm.nih.gov/pubmed/11709170

102. Linkhart TA, Mohan S, Baylink DJ. Growth factors for bone growth and repair: IGF, TGFβ and BMP. Bone. 1996;19(1 SUPPL.):S1–12.

103. Andrade MAR, Derradi R, Simão AMS, Millán JL, Ramos AP, Ciancaglini P, et al. Is alkaline phosphatase biomimeticaly immobilized on titanium able to propagate the biomineralization process? Arch Biochem Biophys [Internet].

2019;663(December 2018):192–8. Available from: https://doi.org/10.1016/j.abb.2019.01.014

104. Hunter GK, Hauschka P V, Poole AR, Rosenberg LC, Goldberg HA. Nucleation and inhibition of hydroxyapatite formation by mineralized tissue proteins. Biochem J [Internet]. 1996 Jul 1;317 (Pt 1(Pt 1):59–64. Available from: http://www.ncbi.nlm.nih.gov/pubmed/8694787

105. Murshed M, Harmey D, Millán JL, McKee MD, Karsenty G. Unique coexpression in osteoblasts of broadly expressed genes accounts for the spatial restriction of ECM mineralization to bone. Genes Dev. 2005;19(9):1093–104.

106. Dallas SL, Bonewald LF. Dynamics of the transition from osteoblast to osteocyte. Ann N Y Acad Sci [Internet]. 2010 Mar;1192(1):437–43. Available from: http://www.ncbi.nlm.nih.gov/pubmed/20392270

107. Shahar R, Dean MN. The enigmas of bone without osteocytes. Bonekey Rep [Internet]. 2013 May 1;2(January):343. Available from: http://dx.doi.org/10.1038/bonekey.2013.77

108. Schaffler MB, Cheung WY, Majeska R, Kennedy O. Osteocytes: master orchestrators of bone. Calcif Tissue Int [Internet]. 2014 Jan;94(1):5–24. Available from: http://www.ncbi.nlm.nih.gov/pubmed/24042263

109. Burra S, Nicolella DP, Jiang JX. Dark horse in osteocyte biology: Glycocalyx around the dendrites is critical for osteocyte mechanosensing. Commun Integr Biol [Internet]. 2011 Jan;4(1):48–50. Available from: http://www.ncbi.nlm.nih.gov/pubmed/21509177

110. Thompson WR, Modla S, Grindel BJ, Czymmek KJ, Kirn-Safran CB, Wang L, et al. Perlecan/Hspg2 deficiency alters the pericellular space of the lacunocanalicular system surrounding osteocytic processes in cortical bone. J Bone Miner Res. 2011;26(3):618–29.

111. Wang B, Lai X, Price C, Thompson WR, Li W, Quabili TR, et al. Perlecan-containing pericellular matrix regulates solute transport and mechanosensing within the osteocyte lacunar-canalicular system. J Bone Miner Res. 2014;29(4):878–91.

112. Mullen CA, Haugh MG, Schaffler MB, Majeska RJ, McNamara LM. Osteocyte differentiation is regulated by extracellular matrix stiffness and intercellular separation. J Mech Behav Biomed Mater [Internet]. 2013 Dec;28:183–94. Available from: http://www.ncbi.nlm.nih.gov/pubmed/23994943

113. Franz-Odendaal TA, Hall BK, Witten PE. Buried alive: How osteoblasts become osteocytes. Dev Dyn. 2006;235(1):176–90.

114. Robling AG, Bonewald LF. The Osteocyte: New Insights. Annu Rev Physiol. 2020;82:485–506.

115. Delgado-Calle J, Bellido T. The osteocyte as a signaling cell. Physiol Rev [Internet]. 2022 Jan 1;102(1):379–410. Available from: http://www.ncbi.nlm.nih.gov/pubmed/34337974

116. Yasuda H, Shima N, Nakagawa N, Yamaguchi K, Kinosaki M, Mochizuki SI, et al. Osteoclast differentiation factor is a ligand for osteoprotegerin/osteoclastogenesis-inhibitory factor and is identical to TRANCE/RANKL. Proc Natl Acad Sci U S A. 1998;95(7):3597–602.

117. Ono T, Hayashi M, Sasaki F, Nakashima T. RANKL biology: bone metabolism, the immune system, and beyond. Inflamm Regen [Internet]. 2020;40(1):2. Available from: http://www.ncbi.nlm.nih.gov/pubmed/32047573

118. Dsouza C, Komarova S V. Mechanosensitivity and mechanotransductive properties of osteoclasts. Am J Physiol Physiol. 2023;(November 2023):95–106.

119. Teitelbaum SL. The osteoclast and its unique cytoskeleton. Ann N Y Acad Sci. 2011;1240(1):14–7.

120. Han G, Zuo J, Holliday LS. Specialized roles for actin in osteoclasts: Unanswered questions and therapeutic opportunities. Vol. 9, Biomolecules. MDPI AG; 2019.

121. Kurenkova AD, Medvedeva E V., Newton PT, Chagin AS. Niches for Skeletal Stem Cells of Mesenchymal Origin. Front cell Dev Biol [Internet]. 2020;8(July):592. Available from: http://www.ncbi.nlm.nih.gov/pubmed/32754592

122. Matsushita Y, Ono W, Ono N. Skeletal Stem Cells for Bone Development and Repair: Diversity Matters. Curr Osteoporos Rep [Internet]. 2020 Jun;18(3):189–98. Available from: http://www.ncbi.nlm.nih.gov/pubmed/32172443

123. Wheatley S, Wright E, Jeske Y, MCCormack A, Bowles J, Koopman P. Aetiology of the skeletal dysmorphology syndrome campomelic dysplasia: expression of the Sox9 gene during chondrogenesis in mouse embryos. Ann N Y Acad Sci [Internet]. 1996 Jun 8;785:350–2. Available from: http://www.ncbi.nlm.nih.gov/pubmed/8702178

124. Lefterova MI, Zhang Y, Steger DJ, Schupp M, Schug J, Cristancho A, et al. PPARγ and C/EBP factors orchestrate adipocyte biology via adjacent binding on a genome-wide scale. Genes Dev. 2008;22(21):2941–52.

125. Drissi H, Luc Q, Shakoori R, De Sousa Lopes SC, Choi JY, Terry A, et al. Transcriptional autoregulation of the bone related CBFA1/RUNX2 gene. J Cell Physiol. 2000;184(3):341–50.

126. Nakashima K, Zhou X, Kunkel G, Zhang Z, Deng JM, Behringer RR, et al. The novel zinc finger-containing transcription factor osterix is required for osteoblast differentiation and bone formation. Cell [Internet]. 2002 Jan 11;108(1):17–29. Available from: http://www.ncbi.nlm.nih.gov/pubmed/11792318

127. Parhami F, Tintut Y, Beamer WG, Gharavi N, Goodman W, Demer LL. Atherogenic high-fat diet reduces bone mineralization in mice. J Bone Miner Res. 2001;16(1):182–8.

128. Sen B, Xie Z, Case N, Ma M, Rubin C, Rubin J. Mechanical strain inhibits adipogenesis in mesenchymal stem cells by stimulating a durable β-catenin signal. Endocrinology. 2008;149(12):6065–75.

129. Engler AJ, Sen S, Sweeney HL, Discher DE. Matrix Elasticity Directs Stem Cell Lineage Specification. Cell. 2006;126(4):677–89.

130. Zhang T, Lin S, Shao X, Zhang Q, Xue C, Zhang S, et al. Effect of matrix stiffness on osteoblast functionalization. Cell Prolif. 2017;50(3):1–9.

131. Atria PJ, Castillo AB. Skeletal adaptation to mechanical cues during homeostasis and repair: the niche, cells, and molecular signaling. Front Physiol [Internet]. 2023;14(October):1233920. Available from: http://www.ncbi.nlm.nih.gov/pubmed/37916223

132. Robling AG, Turner CH. Mechanical signaling for bone modeling and remodeling. Crit Rev Eukaryot Gene Expr. 2009;19(4):319–38.

133. Frost HM. Bone's Mechanostat: A 2003 Update. Anat Rec - Part A Discov Mol Cell Evol Biol. 2003;275(2):1081–101.

134. Price C, Zhou X, Li W, Wang L. Real-time measurement of solute transport within the lacunar-canalicular system of mechanically loaded bone: Direct evidence for load-induced fluid flow. J Bone Miner Res. 2011;26(2):277–85.

135. Christen P, Ito K, Ellouz R, Boutroy S, Sornay-Rendu E, Chapurlat RD, et al. Bone remodelling in humans is load-driven but not lazy. Nat Commun. 2014;5.

136. Turner CH, Owan I, Alvey T, Hulman J, Hock JM. Recruitment and proliferative responses of osteoblasts after mechanical loading in vivo determined using sustained-release bromodeoxyuridine. Bone. 1998;22(5):463–9.

137. Robling AG, Hinant FM, Burr DB, Turner CH. Improved bone structure and strength after long-term mechanical loading is greatest if loading is separated into short bouts. J Bone Miner Res. 2002;17(8):1545–54.

138. Ceroni D, Martin X, Delhumeau C, Rizzoli R, Kaelin A, Farpour-Lambert N. Effects of cast-mediated immobilization on bone mineral mass at various sites in

adolescents with lower-extremity fracture. J Bone Joint Surg Am [Internet]. 2012 Feb 1;94(3):208–16. Available from: http://www.ncbi.nlm.nih.gov/pubmed/22298052

139. Dionyssiotis Y, Trovas G, Galanos A, Raptou P, Papaioannou N, Papagelopoulos P, et al. Bone loss and mechanical properties of tibia in spinal cord injured men. J Musculoskelet Neuronal Interact. 2007;7(1):62–8.

140. Leblanc AD, Schneider VS, Evans HJ, Engelbretson DA, Krebs JM. Bone mineral loss and recovery after 17 weeks of bed rest. J Bone Miner Res. 1990;5(8):843–50.

141. LeBlanc A, Schneider V, Shackelford L, West S, Oganov V, Bakulin A, et al. Bone mineral and lean tissue loss after long duration space flight. J Musculoskelet Neuronal Interact [Internet]. 2000;1(2):157–60. Available from: http://www.ncbi.nlm.nih.gov/pubmed/15758512

142. Ishijima M, Rittling SR, Yamashita T, Tsuji K, Kurosawa H, Nifuji A, et al. Enhancement of osteoclastic bone resorption and suppression of osteoblastic bone formation in response to reduced mechanical stress do not occur in the absence of osteopontin. J Exp Med [Internet]. 2001 Feb 5;193(3):399–404. Available from: http://www.ncbi.nlm.nih.gov/pubmed/11157060

143. Dufour C, Holy X, Marie PJ. Transforming growth factor-β prevents osteoblast apoptosis induced by skeletal unloading via PI3K/Akt, Bcl-2, and phospho-Bad signaling. Am J Physiol - Endocrinol Metab. 2008;294(4):794–801.

144. Piekarski K, Munro M. Transport mechanism operating between blood supply and osteocytes in long bones. Nature [Internet]. 1977 Sep 1;269(5623):80–2. Available from: http://www.ncbi.nlm.nih.gov/pubmed/895891

145. You L, Cowin SC, Schaffler MB, Weinbaum S. A model for strain amplification in the actin cytoskeleton of osteocytes due to fluid drag on pericellular matrix. J Biomech. 2001;34(11):1375–86.

146. Li X, Han L, Nookaew I, Mannen E, Silva MJ, Almeida M, et al. Stimulation of piezo1 by mechanical signals promotes bone anabolism. Elife. 2019;8:1–22.

147. Han Y, Cowin SC, Schaffler MB, Weinbaum S. Mechanotransduction and strain amplification in osteocyte cell processes. Proc Natl Acad Sci U S A. 2004;101(47):16689–94.

148. Lee KL, Guevarra MD, Nguyen AM, Chua MC, Wang Y, Jacobs CR. The primary cilium functions as a mechanical and calcium signaling nexus. Cilia [Internet]. 2015;4(1):7. Available from: http://www.ncbi.nlm.nih.gov/pubmed/26029358

149. Klein-Nulend J, Semeins CM, Ajubi NE, Nijweide PJ, Burger EH. Pulsating Fluid Flow Increases Nitric Oxide (NO) Synthesis by Osteocytes but Not Periosteal

Fibroblasts - Correlation with Prostaglandin Upregulation. Biochem Biophys Res Commun. 1995 Dec 14;217(2):640–8.

150. Jiang JX, Cheng B. Mechanical stimulation of gap junctions in bone osteocytes is mediated by prostaglandin E2. Cell Commun Adhes. 2001;8(4–6):283–8.

151. Lean JM, Mackay AG, Chow JWM, Chambers TJ. Osteocytic expression of mRNA for c-fos and IGF-I: An immediate early gene response to an osteogenic stimulus. Am J Physiol - Endocrinol Metab. 1996;270(6 33-6):937–45.

152. da Silva Madaleno C, Jatzlau J, Knaus P. BMP signalling in a mechanical context – Implications for bone biology. Bone [Internet]. 2020;137(May):115416. Available from: https://doi.org/10.1016/j.bone.2020.115416

153. Du JH, Lin SX, Wu XL, Yang SM, Cao LY, Zheng A, et al. The Function of Wnt Ligands on Osteocyte and Bone Remodeling. J Dent Res. 2019;98(8):930–8.

154. Schaffler MB, Kennedy OD. Osteocyte signaling in bone. Curr Osteoporos Rep [Internet]. 2012 Jun;10(2):118–25. Available from: http://www.ncbi.nlm.nih.gov/pubmed/22552701

155. Lewis KJ, Frikha-Benayed D, Louie J, Stephen S, Spray DC, Thi MM, et al. Osteocyte calcium signals encode strain magnitude and loading frequency in vivo. Proc Natl Acad Sci U S A. 2017;114(44):11775–80.

156. Josephson TO, Morgan EF. Harnessing mechanical cues in the cellular microenvironment for bone regeneration. Front Physiol [Internet]. 2023;14(October):1232698. Available from: http://www.ncbi.nlm.nih.gov/pubmed/37877097

157. Weivoda MM, Youssef SJ, Oursler MJ. Sclerostin expression and functions beyond the osteocyte. Bone. 2017;96(507):45–50.

158. Brunkow ME, Gardner JC, Van Ness J, Paeper BW, Kovacevich BR, Proll S, et al. Bone dysplasia sclerosteosis results from loss of the SOST gene product, a novel cystine knot-containing protein. Am J Hum Genet [Internet]. 2001 Mar;68(3):577–89. Available from: http://www.ncbi.nlm.nih.gov/pubmed/11179006

159. Li X, Ominsky MS, Niu QT, Sun N, Daugherty B, D'Agostin D, et al. Targeted deletion of the sclerostin gene in mice results in increased bone formation and bone strength. J Bone Miner Res. 2008;23(6):860–9.

160. Suen PK, Qin L. Sclerostin, an emerging therapeutic target for treating osteoporosis and osteoporotic fracture: A general review. J Orthop Transl [Internet]. 2016 Jan;4:1–13. Available from: http://dx.doi.org/10.1016/j.jot.2015.08.004

161. Atkins GJ, Rowe PS, Lim HP, Welldon KJ, Ormsby R, Wijenayaka AR, et al. Sclerostin is a locally acting regulator of late-osteoblast/preosteocyte differentiation and regulates mineralization through a MEPE-ASARM-dependent mechanism. J Bone Miner Res. 2011;26(7):1425–36.

162. Riddle RC. Endocrine Functions of Sclerostin. Curr Opin Endocr Metab Res [Internet]. 2023 Feb;28. Available from: http://www.ncbi.nlm.nih.gov/pubmed/36713826

163. Gu P, Pu B, Xin Q, Yue D, Luo L, Tao J, et al. The metabolic score of insulin resistance is positively correlated with bone mineral density in postmenopausal patients with type 2 diabetes mellitus. Sci Rep [Internet]. 2023 May 31;13(1):8796. Available from: https://doi.org/10.1038/s41598-023-32931-8

164. Fu YH, Liu WJ, Lee CL, Wang JS. Associations of insulin resistance and insulin secretion with bone mineral density and osteoporosis in a general population. Front Endocrinol (Lausanne) [Internet]. 2022;13(September):971960. Available from: http://www.ncbi.nlm.nih.gov/pubmed/36204101

165. Rutkovskiy A, Stensløkken KO, Vaage IJ. Osteoblast Differentiation at a Glance. Med Sci Monit Basic Res. 2016;22:95–106.

166. Li X, Zhang Y, Kang H, Liu W, Liu P, Zhang J, et al. Sclerostin binds to LRP5/6 and antagonizes canonical Wnt signaling. J Biol Chem [Internet]. 2005;280(20):19883–7. Available from: http://dx.doi.org/10.1074/jbc.M413274200

167. Krishnan V, Bryant HU, MacDougald OA. Regulation of bone mass by Wnt signaling. J Clin Invest. 2006;116(5):1202–9.

168. Liao C, Liang S, Wang Y, Zhong T, Liu X. Sclerostin is a promising therapeutic target for oral inflammation and regenerative dentistry. J Transl Med [Internet]. 2022;20(1). Available from: https://doi.org/10.1186/s12967-022-03417-4

169. Ke HZ, Richards WG, Li X, Ominsky MS. Sclerostin and dickkopf-1 as therapeutic targets in bone diseases. Endocr Rev. 2012;33(5):747–83.

170. Stamos JL, Weis WI. The β-catenin destruction complex. Cold Spring Harb Perspect Biol. 2013;5(1):1–16.

171. Felber K, Elks PM, Lecca M, Roehl HH. Expression of osterix is regulated by FGF and Wnt/β-catenin signalling during osteoblast differentiation. PLoS One. 2015;10(12):1–17.

172. Wijenayaka AR, Kogawa M, Lim HP, Bonewald LF, Findlay DM, Atkins GJ. Sclerostin stimulates osteocyte support of osteoclast activity by a RANKL-dependent pathway. PLoS One. 2011;6(10).

173. Riancho JA, Zarrabeitia MT, Fernandez-Luna JL, Gonzalez-Macias J. Mechanisms controlling nitric oxide synthesis in osteoblasts. Mol Cell Endocrinol. 1995;107(1):87–92.

174. Watanuki M, Sakai A, Sakata T, Tsurukami H, Miwa M, Uchida Y, et al. Role of inducible nitric oxide synthase in skeletal adaptation to acute increases in mechanical loading. J Bone Miner Res. 2002;17(6):1015–25.

175. van't Hof RJ, Macphee J, Libouban H, Helfrich MH, Ralston SH. Regulation of bone mass and bone turnover by neuronal nitric oxide synthase. Endocrinology [Internet]. 2004 Nov;145(11):5068–74. Available from: http://www.ncbi.nlm.nih.gov/pubmed/15297441

176. Liu H, Rosen CJ. Nitric oxide and bone: The phoenix rises again. J Clin Invest. 2021;131(5).

177. Li M, Thompson DD, Paralkar VM. Prostaglandin E2 receptors in bone formation. Int Orthop. 2007;31(6):767–72.

178. Ajubi NE, Klein-Nulend J, Nijweide PJ, Vrijheid-Lammers T, Alblas MJ, Burger EH. Pulsating fluid flow increases prostaglandin production by cultured chicken osteocytes-A cytoskeleton-dependent process. Biochem Biophys Res Commun. 1996;225(1):62–8.

179. Koide M, Kobayashi Y, Yamashita T, Uehara S, Nakamura M, Hiraoka BY, et al. Bone Formation Is Coupled to Resorption Via Suppression of Sclerostin Expression by Osteoclasts. J Bone Miner Res. 2017;32(10):2074–86.

180. Wittenberg JM, Wittenberg RH. Release of prostaglandins from bone and muscle after femoral osteotomy in rats. Acta Orthop. 1991;62(6):577–81.

181. Li X, Okada Y, Pilbeam CC, Lorenzo JA, Kennedy CRJ, Breyer RM, et al. Knockout of the murine prostaglandin EP2 receptor impairs Osteoclastogenesis in vitro. Endocrinology. 2000;141(6):2054–61.

182. Hartke JR, Lundy MW. Bone anabolic therapy with selective prostaglandin analogs. J Musculoskelet Neuronal Interact [Internet]. 2001;2(1):25–31. Available from: http://www.ncbi.nlm.nih.gov/pubmed/15758474

183. Tu X, Rhee Y, Condon KW, Bivi N, Allen MR, Dwyer D, et al. Sost downregulation and local Wnt signaling are required for the osteogenic response to mechanical loading. Bone [Internet]. 2012 Jan;50(1):209–17. Available from: http://www.ncbi.nlm.nih.gov/pubmed/22075208

184. Kim JH, Liu X, Wang J, Chen X, Zhang H, Kim SH, et al. Wnt signaling in bone formation and its therapeutic potential for bone diseases. Ther Adv Musculoskelet Dis [Internet]. 2013 Feb;5(1):13–31. Available from:

http://www.ncbi.nlm.nih.gov/pubmed/23514963

185. Holguin N, Brodt MD, Silva MJ. Activation of Wnt Signaling by Mechanical Loading Is Impaired in the Bone of Old Mice. J Bone Miner Res [Internet]. 2016 Dec;31(12):2215–26. Available from: http://www.ncbi.nlm.nih.gov/pubmed/27357062

186. Lawson LY, Brodt MD, Migotsky N, Chermside-Scabbo CJ, Palaniappan R, Silva MJ. Osteoblast-Specific Wnt Secretion Is Required for Skeletal Homeostasis and Loading-Induced Bone Formation in Adult Mice. J Bone Miner Res. 2022;37(1):108–20.

187. Cawley KM, Bustamante-Gomez NC, Guha AG, MacLeod RS, Xiong J, Gubrij I, et al. Local Production of Osteoprotegerin by Osteoblasts Suppresses Bone Resorption. Cell Rep [Internet]. 2020;32(10):108052. Available from: https://doi.org/10.1016/j.celrep.2020.108052

188. Boyce BF, Xing L. The RANKL/RANK/OPG pathway. Curr Osteoporos Rep. 2007;5(3):98–104.

189. Udagawa N, Takahashi N, Yasuda H, Mizuno A, Itoh K, Ueno Y, et al. Osteoprotegerin produced by osteoblasts is an important regulator in osteoclast development and function. Endocrinology. 2000;141(9):3478–84.

190. Saunders MM, Taylor AF, Du C, Zhou Z, Pellegrini VD, Donahue HJ. Mechanical stimulation effects on functional end effectors in osteoblastic MG-63 cells. J Biomech. 2006;39(8):1419–27.

191. Tsukasaki M, Asano T, Muro R, Huynh NCN, Komatsu N, Okamoto K, et al. OPG Production Matters Where It Happened. Cell Rep [Internet]. 2020;32(10):108124. Available from: https://doi.org/10.1016/j.celrep.2020.108124

192. Li M, Xu D. Antiresorptive activity of osteoprotegerin requires an intact heparan sulfate-binding site. Proc Natl Acad Sci U S A. 2020;117(29):17187–94.

193. Yu H, de Vos P, Ren Y. Overexpression of osteoprotegerin promotes preosteoblast differentiation to mature osteoblasts. Angle Orthod. 2011;81(1):100–6.

194. Tzaphlidou M. Bone architecture: collagen structure and calcium/phosphorus maps. J Biol Phys [Internet]. 2008 Apr;34(1–2):39–49. Available from: http://www.ncbi.nlm.nih.gov/pubmed/19669491

195. Solheim E. Growth factors in bone. Int Orthop. 1998;22(6):410–6.

196. O'Brien FJ, Taylor D, Lee TC. Microcrack accumulation at different intervals during fatigue testing of compact bone. J Biomech. 2003;36(7):973–80.

197. Baylink DJ, Finkelman RD, Mohan S. Growth factors to stimulate bone formation. J Bone Miner Res. 1993;8(2 S):S565–72.

198. Li G, Thabane L, Papaioannou A, Ioannidis G, Levine MAH, Adachi JD. An overview of osteoporosis and frailty in the elderly. BMC Musculoskelet Disord [Internet]. 2017;18(1). Available from: http://dx.doi.org/10.1186/s12891-017-1403-x

199. Bellido T, Ali AA, Gubrij I, Plotkin LI, Fu Q, O'Brien CA, et al. Chronic elevation of parathyroid hormone in mice reduces expression of sclerostin by osteocytes: A novel mechanism for hormonal control of osteoblastogenesis. Endocrinology. 2005;146(11):4577–83.

200. Wein MN, Kronenberg HM. Regulation of bone remodeling by parathyroid hormone. Cold Spring Harb Perspect Med. 2018;8(8):1–20.

201. Drake MT, Srinivasan B, Mödder UI, Peterson JM, McCready LK, Riggs BL, et al. Effects of parathyroid hormone treatment on circulating sclerostin levels in postmenopausal women. J Clin Endocrinol Metab [Internet]. 2010 Nov;95(11):5056–62. Available from: http://www.ncbi.nlm.nih.gov/pubmed/20631014

202. Tian Y, Xu Y, Fu Q, He M. Parathyroid hormone regulates osteoblast differentiation in a Wnt/β-catenin-dependent manner. Mol Cell Biochem. 2011;355(1–2):211–6.

203. Francis RM, Selby PL. Osteomalacia. Baillieres Clin Endocrinol Metab [Internet]. 1997 Apr;11(1):145–63. Available from: http://www.ncbi.nlm.nih.gov/pubmed/9222490

204. Tønnesen R, Schwarz P, Hovind PH, Jensen LT. Physical exercise associated with improved BMD independently of sex and vitamin D levels in young adults. Eur J Appl Physiol. 2016;116(7):1297–304.

205. Leser JM, Harriot A, Buck H V., Ward CW, Stains JP. Aging, Osteo-Sarcopenia, and Musculoskeletal Mechano-Transduction. Front Rehabil Sci [Internet]. 2021;2(December):782848. Available from: http://www.ncbi.nlm.nih.gov/pubmed/36004321

206. Almeida M. Aging mechanisms in bone. Bonekey Rep [Internet]. 2012 Jul 1;1(7):1–7. Available from: http://dx.doi.org/10.1038/bonekey.2012.102

207. Layne JE, Nelson ME. The effects of progressive resistance training on bone density: a review. Med Sci Sports Exerc [Internet]. 1999 Jan;31(1):25–30. Available from: http://www.ncbi.nlm.nih.gov/pubmed/9927006

208. Holubiac I Ștefan, Leuciuc FV, Crăciun DM, Dobrescu T. Effect of Strength

Training Protocol on Bone Mineral Density for Postmenopausal Women with Osteopenia/Osteoporosis Assessed by Dual-Energy X-ray Absorptiometry (DEXA). Sensors (Basel) [Internet]. 2022 Feb 28;22(5):1904. Available from: http://www.ncbi.nlm.nih.gov/pubmed/35271050

209. Watson SL, Weeks BK, Weis LJ, Harding AT, Horan SA, Beck BR. High-Intensity Resistance and Impact Training Improves Bone Mineral Density and Physical Function in Postmenopausal Women With Osteopenia and Osteoporosis: The LIFTMOR Randomized Controlled Trial. J Bone Miner Res. 2018;33(2):211–20.

210. Mosti MP, Carlsen T, Aas E, Hoff J, Stunes AK, Syversen U. Maximal strength training improves bone mineral density and neuromuscular performance in young adult women. J strength Cond Res [Internet]. 2014 Oct;28(10):2935–45. Available from: http://www.ncbi.nlm.nih.gov/pubmed/24736773

211. Forwood MR, Turner CH. Skeletal adaptations to mechanical usage: results from tibial loading studies in rats. Bone. 1995;17(4 SUPPL.):197–205.

212. Sommerfeldt D, Rubin C. Biology of bone and how it orchestrates the form and function of the skeleton. Eur Spine J. 2001;10(SUPPL. 2):86–95.

213. Bonewald LF. The amazing osteocyte. J Bone Miner Res. 2011;26(2):229–38.

214. Van Bezooijen RL, Svensson JP, Eefting D, Visser A, Van Der Horst G, Karperien M, et al. Wnt but not BMP signaling is involved in the inhibitory action of sclerostin on BMP-stimulated bone formation. J Bone Miner Res. 2007;22(1):19–28.

215. Winkler DG, Sutherland MK, Geoghegan JC, Yu C, Hayes T, Skonier JE, et al. Osteocyte control of bone formation via sclerostin, a novel BMP antagonist. EMBO J. 2003;22(23):6267–76.

216. van't Hof RJ, Ralston SH. Nitric oxide and bone. Immunology [Internet]. 2001 Jul;103(3):255–61. Available from: http://www.ncbi.nlm.nih.gov/pubmed/11454054

217. Förstermann U, Closs EI, Pollock JS, Nakane M, Schwarz P, Gath I, et al. Nitric oxide synthase isozymes characterization, purification, molecular cloning, and functions. Hypertension. 1994;23(6):1121–31.

218. Aguirre J, Buttery LDK, O'Shaughnessy M, Afzal F, Fernandez de Marticorena I, Hukkanen M, et al. Endothelial nitric oxide synthase gene-deficient mice demonstrate marked retardation in postnatal bone formation, reduced bone volume, and defects in osteoblast maturation and activity. Am J Pathol. 2001;158(1):247–57.

219. Armour KE, Armour KJ, Gallagher ME, Gödecke A, Helfrich MH, Reid DM, et al. Defective bone formation and anabolic response to exogenous estrogen in mice with targeted disruption of endothelial nitric oxide synthase. Endocrinology. 2001;142(2):760–6.

220. Tan SD, Bakker AD, Semeins CM, Kuijpers-Jagtman AM, Klein-Nulend J. Inhibition of osteocyte apoptosis by fluid flow is mediated by nitric oxide. Biochem Biophys Res Commun. 2008;369(4):1150–4.

221. Jin Z, Kho J, Dawson B, Jiang MM, Chen Y, Ali S, et al. Nitric oxide modulates bone anabolism through regulation of osteoblast glycolysis and differentiation. J Clin Invest. 2021;131(5).

222. Fox SW, Chow JWM. Nitric oxide synthase expression in bone cells. Bone. 1998;23(1):1–6.

223. Zaman G, Pitsillides AA, Rawlinson SCF, Suswillo RFL, Mosley JR, Cheng MZ, et al. Mechanical strain stimulates nitric oxide production by rapid activation of endothelial nitric oxide synthase in osteocytes. J Bone Miner Res. 1999;14(7):1123–31.

224. Murthy S, Koval OM, Ramiro Diaz JM, Kumar S, Nuno D, Scott JA, et al. Endothelial CaMKII as a regulator of eNOS activity and NO-mediated vasoreactivity. PLoS One. 2017;12(10):1–23.

225. Araki S, Osuka K, Takata T, Tsuchiya Y, Watanabe Y. Coordination between calcium/calmodulin-dependent protein kinase II and neuronal nitric oxide synthase in neurons. Int J Mol Sci. 2020;21(21):1–17.

226. Song T, Hatano N, Kambe T, Miyamoto Y, Ihara H, Yamamoto H, et al. Nitric oxide-mediated modulation of calcium/calmodulin-dependent protein kinase II. Biochem J. 2008;412(2):223–31.

227. Gutierrez DA, Fernandez-Tenorio M, Ogrodnik J, Niggli E. NO-dependent Ca MKII activation during β-adrenergic stimulation of cardiac muscle. Cardiovasc Res. 2013;100(3):392–401.

228. Coultrap SJ, Bayer KU. Nitric oxide induces Ca2+-independent activity of the Ca 2+/calmodulin-dependent protein kinase II (CaMKII). J Biol Chem [Internet]. 2014;289(28):19458–65. Available from: http://dx.doi.org/10.1074/jbc.M114.558254

229. Marziano C, Hong K, Cope EL, Kotlikoff MI, Isakson BE, Sonkusare SK. Nitric Oxide–Dependent Feedback Loop Regulates Transient Receptor Potential Vanilloid 4 (TRPV4) Channel Cooperativity and Endothelial Function in Small Pulmonary Arteries. J Am Heart Assoc. 2017;6(12).

230. Yin J, Hoffmann J, Kaestle SM, Neye N, Wang L, Baeurle J, et al. Negative-feedback loop attenuates hydrostatic lung edema via a cGMP-dependent regulation of transient receptor potential vanilloid 4. Circ Res. 2008;102(8):966–74.

231. Kalyanaraman H, Ramdani G, Joshua J, Schall N, Boss GR, Cory E, et al. A Novel, Direct NO Donor Regulates Osteoblast and Osteoclast Functions and Increases Bone Mass in Ovariectomized Mice. J Bone Miner Res. 2017;32(1):46–59.

232. Wein MN, Spatz J, Nishimori S, Doench J, Root D, Babij P, et al. HDAC5 controls MEF2C-driven sclerostin expression in osteocytes. J Bone Miner Res [Internet]. 2015 Mar;30(3):400–11. Available from: http://www.ncbi.nlm.nih.gov/pubmed/25271055

233. Xu LH, Shao H, Ma YH V., You L. OCY454 Osteocytes as an in Vitro Cell Model for Bone Remodeling Under Mechanical Loading. J Orthop Res. 2019;37(8):1681–9.

234. Deal C. The use of intermittent human parathyroid hormone as a treatment for osteoporosis. Curr Rheumatol Rep. 2004;6(1):49–58.

235. Zhang T, Brown JH. Role of Ca2+/calmodulin-dependent protein kinase II in cardiac hypertrophy and heart failure. Cardiovasc Res. 2004;63(3):476–86.

236. Yasuda R, Hayashi Y, Hell JW. CaMKII: a central molecular organizer of synaptic plasticity, learning and memory. Nat Rev Neurosci. 2022;23(11):666–82.

237. Beckendorf J, van den Hoogenhof MMG, Backs J. Physiological and unappreciated roles of CaMKII in the heart. Basic Res Cardiol [Internet]. 2018;113(4):1–12. Available from: https://doi.org/10.1007/s00395-018-0688-8

238. Muszyński S, Świątkiewicz S, Arczewska-Włosek A, Dobrowolski P, Valverde Piedra JL, Arciszewski MB, et al. Analysis of mechanical properties of bones and tendons shows that modern hybrid rye can be introduced to corn-wheat based diet in broiler chickens as an alternative energy source irrespective of xylanase supplementation. Poult Sci. 2019;98(11):5613–21.

239. Granke M, Makowski AJ, Uppuganti S, Does MD, Nyman JS. Identifying Novel Clinical Surrogates to Assess Human Bone Fracture Toughness. J Bone Miner Res [Internet]. 2015 Jul;30(7):1290–300. Available from: http://www.ncbi.nlm.nih.gov/pubmed/25639628

240. Feng Q, Song W, Lu X, Hamilton JA, Lei M, Peng T, et al. Development of heart failure and congenital septal defects in mice lacking endothelial nitric oxide synthase. Circulation. 2002;106(7):873–9.

241. Jiang R, Wang S, Takahashi K, Fujita H, Fruci CR, Breyer MD, et al. Generation

of a conditional allele for the mouse endothelial nitric oxide synthase gene. Genesis. 2012;50(9):685–92.

242. Vilela VR, Samson N, Nachbar R, Perazza LR, Lachance G, Rokatoarivelo V, et al. Adipocyte-specific Nos2 deletion improves insulin resistance and dyslipidemia through brown fat activation in diet-induced obese mice. Mol Metab [Internet]. 2022;57(January):101437. Available from: https://doi.org/10.1016/j.molmet.2022.101437

243. Elefteriou F, Yang X. Genetic mouse models for bone studies-Strengths and limitations. Bone. 2011;49(6):1242–54.

244. Jamal SA, Goltzman D, Hanley DA, Papaioannou A, Prior JC, Josse RG. Retraction to: Nitrate use and changes in bone mineral density: the Canadian Multicentre Osteoporosis Study. Osteoporos Int [Internet]. 2017 Jan;28(1):421. Available from: http://www.ncbi.nlm.nih.gov/pubmed/27909783

245. Jamal SA, Hamilton CJ, Eastell R, Cummings SR. Effect of nitroglycerin ointment on bone density and strength in postmenopausal women: a randomized trial. JAMA [Internet]. 2011 Feb 23;305(8):800–7. Available from: http://www.ncbi.nlm.nih.gov/pubmed/21343579

246. Golchin N, Hohensee C, LaCroix A, Gray SL. Nitrate Medications, Fractures, and Change in Bone Mineral Density in Postmenopausal Women: Results from the Women's Health Initiative. J Bone Miner Res [Internet]. 2016 Sep;31(9):1760–6. Available from: http://www.ncbi.nlm.nih.gov/pubmed/26990305

247. Liu W, Meng Z, Wang G. The Efficacy of Nitrates for Bone Health: A Systematic Review and Meta-Analysis of Observational and Randomized Controlled Studies. Front Endocrinol (Lausanne) [Internet]. 2022;13(February):833932. Available from: http://www.ncbi.nlm.nih.gov/pubmed/35222289